Bioorganic Chemistry 90 (2019) 103080

Contents lists available at ScienceDirect

Bioorganic Chemistry

journal homepage: www.elsevier.com/locate/bioorg

Development of pyrazole and spiropyrazoline analogs as multifunctional agents for treatment of Alzheimer's disease

Gopichand Gutti, Devendra Kumar, Pankaj Paliwal, Ankit Ganeshpurkar, Khemraj Lahre, Ashok Kumar, Sairam Krishnamurthy, Sushil Kumar Singh*

Department of Pharmaceutical Engineering & Technology, Indian Institute of Technology (Banaras Hindu University), Varanasi 221005, India

ARTICLE INFO

Keywords:
Central nervous system
Alzheimer's disease
Acetylcholinesterase
Amyloid beta
De novo drug design
Spiropyrazoline

ABSTRACT

Cholinergic hypothesis of Alzheimer's disease has been advocated as an essential tool in the last couple of decades for the drug development. Here in, we report *de novo* fragment growing strategy for the design of novel 3,5-diarylpyrazoles and hit optimization of spiropyrazoline derivatives as acetyl cholinesterase inhibitors. Both type of scaffolds numbering forty compounds were synthesized and evaluated for their potencies against AChE, BuChE and PAMPA. Introduction of lipophilic cyclohexane ring in 3,5-diarylpyrazole analogs led to spiropyrazoline derivatives, which facilitated and improved the potencies. Compound **44** (AChE = 1.937 ± 0.066 μM; BuChE = 1.166 ± 0.088 μM; hAChE = 1.758 ± 0.095 μM; P_e = 9.491 ± 0.34 × 10^{-6} cm s^1) showed positive results, which on further optimization led to the development of compound **67** (AChE = 0.464 ± 0.166 μM; BuChE = 0.754 ± 0.121 μM; hAChE = 0.472 ± 0.042 μM; P_e = 13.92 ± 0.022 × 10^{-6} cm s^1). Compounds **44** and **67** produced significant displacement of propidium iodide from the peripheral anionic site (PAS) of AChE. They were found to be safer to MC65 cells and decreased metal induced $A\beta_{1\text{-}42}$ aggregation. Further, *in-vivo* behavioral studies, on scopolamine induced amnesia model, the compounds resulted in better percentage spontaneous alternation scores and were safe, had no influence on locomotion in tested animal groups at dose of 3 mg/kg. Early pharmacokinetic assessment of optimized hit molecules was supportive for further drug development.

1. Introduction

Alzheimer's disease (AD) is the most common cause of age-related dementia, which usually starts in the late middle age or in the old age. Major symptoms of the disease include progressive memory loss, impaired thinking, cognitive decline, disorientation, sudden fluctuations in personality and mood, and noticeable deterioration of brain neurons, particularly in cerebral cortex [1,2]. Inordinate symptoms of anxiety may, in fact, be an early cause of AD by enhancing the amyloid beta ($A\beta_{1\text{-}42}$) protein deposition [3–5]. Research endeavors in drug discovery strategies have yielded some exciting outcomes in the past two decades [6,7]. Donepezil (DNZ), galantamine, rivastigmine and memantine are the currently approved and marketed drugs for the treatment of AD-associated dementia. Out of these, first three act on central nervous system (CNS) cholinergic pathways, whereas memantine serves as *N*-methyl-D-aspartate (NMDA) receptor antagonist [2]. The cholinergic abnormalities and $A\beta_{1\text{-}42}$ aggregation have been observed in neurodegenerative conditions. The peripheral anionic site (PAS) of Acetylcholinesterase (AChE) catalyzes $A\beta_{1\text{-}42}$ aggregation and plays crucial role in senile plaques formation. A large number of potential therapeutic interventions have been developed to counteract the loss of presynaptic cholinergic functions [8–10].

AChE and butyrylcholinesterase (BuChE) are two major forms of cholinesterases present in mammalian brain. Both of these are diverse in genetic makeup, structure, and their kinetic activities. AChE is a serine hydrolase enzyme that catalyzes the breaking down of acetylcholine into choline and acetic acid and prevents neurotransmission at cholinergic synapses. In human brain, BuChE is present in neurons,

Abbreviations: Aβ, beta amyloid protein; AD, Alzheimer's disease; ANOVA, analysis of variance; AUC, area under curve; BBB, blood brain barrier; ChEs, cholinesterases; $CDCl_3$, deuterated chloroform; CNS, central nervous system; DMSO, dimethyl sulfoxide; DNZ, donepezil; EDG, electron donating group; ESI, electron spary ionisation; EWG, electron withdrawing group; HPLC, high performance liquid chromatography; MEM, minimum essential medium; MS, mass spectra; NaOH, sodium hydroxide; NMR, nuclear magnetic resonance; PAS, peripheral anionic site; PAMPA, parallel artificial membrane permeation assay; PBS, phosphate buffer saline; ppm, parts per million; ROS, reactive oxygen species; TC, tetracycline; TLC, thin layer chromatography; ThT, thioflavin T

* Corresponding author.
E-mail address: sksingh.phe@iitbhu.ac.in (S.K. Singh).

https://doi.org/10.1016/j.bioorg.2019.103080
Received 17 April 2019; Received in revised form 11 May 2019; Accepted 18 June 2019
Available online 24 June 2019

glial cells, as well as in amyloid plaques and neurofibrillary tangles in AD patients. AChE activity decreases progressively in the brain of AD patients, whereas, BuChE activity shows some increase [11]. An ideal drug candidate should inhibit the enzymes; produce potent activity against AD pathology and cross the blood brain barrier (BBB). Additionally, it should be non toxic to neuronal cells as well as normal cells. Further, good adsorption, distribution, metabolism, excretion and toxicity (ADMET) profiles form the major criteria for a clinical candidate to reach the patient from the laboratory. Chalcone, [12] flavonoid, [13] pyrazole, *N*-benzylpiperidine [10] and piperazinedione [14] derivatives are the major scaffolds involved in the preclinical studies acting through cholinesterase hypothesis. Pyrazole derivatives are progressively gaining immense significance in medicinal chemistry [15]. The therapeutic voyage of pyrazole derivatives and the presence of scaffold in various category of drugs viz. anti-Alzheimer's [16], anti-Parkinson's [17,18], anti-psychotic [19], neuroprotective [20], anti-inflammatory [21], anti-tumor [22], anti-tubercular [23] etc. have made it an indispensable anchor for the design and development of new druglike molecules.

Many of the traditional and *in-silico* drug discovery techniques have played a major role in picking out novel chemical entities at early stages. Among them, computational *de novo* drug design is the most viable method as it allows the target specific design and highly efficient drug like scaffolds with structural flexibility [24]. The present study includes, *de novo* drug design (fragment growing strategy) to develop cholinesterase inhibitors using AChE as a paradigm LigBuilder 2 was used to grow fragments from our in-house chemical library [25]. Fragments were developed into small molecule inhibitors through iterative cycles of generations using genetic algorithm. The designed compounds were selected for the synthesis based on their molecular interactions within the active site. The compounds were synthesized and evaluated for their inhibitory activities and other parameters. The obtained hit molecule was further optimized to improve lipophilicity and pharmacokinetic profiles. The hit (compound **44**) and hit optimized molecule (compound **67**) were further evaluated for neuro-protective property on MC65 (human neuroblastoma) cell line, $A\beta_{1\text{-}42}$ aggregation assay, *in-vivo* studies using scopolamine induced amnesia models to evaluate the working memory, learning response and brain pharmacokinetic profile in mice.

2. Results and discussion

2.1. Design and synthesis

2.1.1. De novo design and in-silico molecular docking studies

The overall designing strategy is shown in Fig. 1. In order to achieve successful de *novo* drug design, a fragment-growing strategy was utilized. For accomplishing this, LigBuilder 2.0 was employed (http://repharma.pku.edu.cn/ligbuilder/download.html). This package facilitates automatic build ligand molecules based on three dimensional structure of the target protein within the binding pocket and subsequently screen them. Human AChE (PDB ID: 4EY7) with DNZ as co-crystallized ligand was considered as a model target. Small fragments from known ligands of single target are usually well grounded to become lead structures. The in-house small fragment library was developed on the basis of following criteria: (1) the molecular weight should be less than 250 Da, (2) lipophilic groups, and (3) The number of aromatic rings should be equal or greater than one. In the initial stage, various in-house fragments were docked using Glide XP module of Schrödinger Maestro 2018.1. The first stage generation revealed three fragments with good binding interactions (S4, Fig. S3, supporting information). The fragment-1 (S4-Fig. S3A) showed hydrogen bonding interaction (TYR124) and hydrophobic interactions (TRP286, TYR341) at PAS of AChE. It also showed interaction with HIS447 residue of catalytic active site (CAS) of AChE through polar interaction. Consequently, fragment-1, which showed good docking poses was selected and used as a seed for the *de novo* designing of molecules.

As the fragments were small and their potencies were expected to be low, a second stage of seed growing was applied. Eventually, we obtained a virtual hit (compound **43**, 3,5-diarylpyrazole derivative) which had a better docking score and an improved interaction pose at the CAS and PAS of AChE (S4-Fig. S3E). The obtained virtual hit was successfully synthesized and chemically modified with various electron donating (EDG, methyl and methoxy etc.) and withdrawing groups (EWG, chloro, bromo, and trifluoromethyl etc.) to establish the potencies based on biological assays. The Glide score of compound **44** was found to be −9.5 Kcal/mole. The p-chlorophenylpyrazole part of the molecule was aligned towards PAS and benzamide group of compounds **44** was oriented towards CAS of AChE. The p-chlorophenyl ring interacted hydrophobically with TYR124 and formed π-π stacking interactions with TRP286 and TYR341 residues of PAS-AChE. At CAS, benzamide part formed polar interactions with HIS447 and SER203 residues. 3,5-Diarylpyrazole derivatives (**43–62**) showed satisfactory inhibitory activities and high BBB permeability (explained in Sections 2.3 and 2.5 respectively). Compound **44** was found to be a suitable hit molecule (Hit compound 1) for further investigation. Based on the findings of the protein-ligand interactions of compound **44** with AChE active sites, the following modifications (and combinations thereof) were explored in the next round of optimization step: (1) slight increase in total polar surface area (tPSA) and (2) increase in molecular weight and lipophilicity by incorporation of cyclohexane ring. The designed molecules retained the binding pose of previous hit molecules with characteristic interactions. Thus, a new series of spiropyrazoline derivatives (**66–85**) of the previous hit molecules, were designed and synthesized auspiciously. The docking study of compound **67** showed better Glide score of −11.5 Kcal/mole with improved binding pose at PAS-AChE compared to compound **44**. The benzamide functionality of compound **67** was oriented towards PAS and forming hydrophobic (TYR72, TYR124, TRP286), electrostatic (ASP72), and π-π stacking interactions (TYR341) with active site residues. Moreover, spiropyrazoline —NH of compound **67** formed hydrogen bonding interaction to HIS447 and polar interaction with SER203 at CAS-AChE. Additionally, compounds **44** and **67** interacted with anionic subsite (TRP86, GLU202, PHE338), oxyanion hole (GLY120, GLY121), and acyl binding pocket (PHE295, PHE297) residues. The effective binding modes of compounds **44** and **67** are depicted in Fig. 2. Hit compound (compound **44**) and potent optimized hit (compound **67**) were further subjected to biological evaluations.

2.1.2. Synthesis

The synthesis of 3,5-diaryl-1H-pyrazole derivatives **43–62** is illustrated in Scheme 1. Formation of N-(3-acetylphenyl)benzamide (**2**) from 3-aminoacetophenone (**1**), followed by Claisen-Schmidt condensation with various substituted aromatic aldehydes, afforded corresponding key α,β-unsaturated chalcone intermediates (**23–42**). Introduction of pyrazole ring (**43–62**) system was made feasible by refluxing **23–42** with 5.0 equivalent of hydrazine hydrate in methanol, which was followed by dehydrogenation by refluxing with catalytic molecular iodine in DMSO [26]. ^{1}H and ^{13}C NMR showed appearance of characteristic signals of 4^{th} position of the pyrazole ring (**43–62**) at δ 7.0 – 7.2 and 95 – 105 ppm respectively.

The synthetic route for spiropyrazoline derivatives **66–85** is delineated in Scheme 2. Compound **64** was prepared by reacting 1.5 equivalent of hydrazine hydrate with 4-methylbenzenesulfonyl chloride (**63**), which was refluxed with equivalent cyclohexanone to obtain cyclic ketone *N*-tosylhydrazone (**65**) in excellent yields. Stereoselective synthesis of spiropyrazolines was reported earlier [27–29]. Compound **65** underwent 1,3-cycloaddition with **23–42,** followed by a 1,3-hydrogen shift to afford spiropyrazolines (**66–85**) with high selectivity and excellent yields. In ^{1}H and ^{13}C NMR, appearance of the tertiary carbon and its corresponding proton signals at 4.0 – 4.5 and 50 – 57 ppm with other characteristic signal of derivatives confirmed formation of target compounds (**66–85**). Amidic –NH and pyrazole –NH

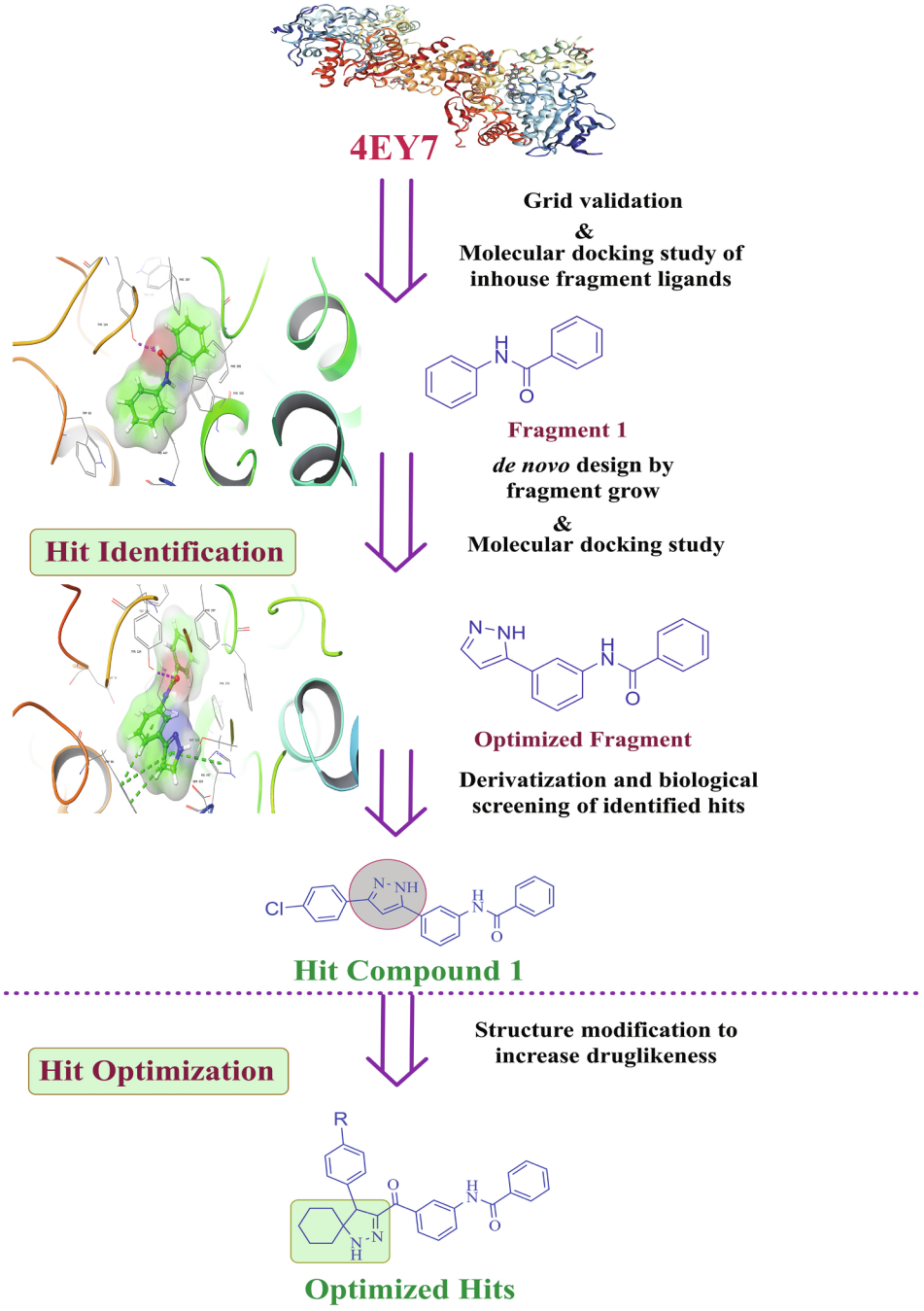

Fig. 1. Overview of drug design process for pyrazole and spiropyrazoline analogs.

were established by D_2O exchange analysis (Fig. S10). Cyclohexanone ring protons appeared as complex multiplet at aliphatic region in ^1H NMR and five distinct signals in aliphatic region of ^{13}C NMR spectra. Quaternary carbon atom at C-5 position of pyrazole ring was identified at 69.0 – 69.99 ppm for all derivatives. The above said signals were further reconfirmed with 2D NMR (Figs. S11 and S12) and DEPT 135° experiments (Fig. S13). To observe the configuration of the compound, specific rotation, differential scanning calorimetry and X-ray crystal structure analysis was performed for one representative compound **73** (3-Fluoro substituted). Specific rotation ($[\alpha]_{32.0}^{589}$) (Table 1) and melting temperature (Fig. S1) were observed as + 213.25° and 260.4 °C respectively. We were fortunate that compound **73** formed large crystals upon slow evaporative crystallization from ethylacetate and ethanol (1:1), allowing for structure determination through X-ray crystallography (Fig. 3).

2.2. In-vitro cholinesterase inhibitory activity and SAR studies

The pharmaceutical drug discovery and development efforts, at present, are focused on optimizing new chemical entities that act through specific enzyme inhibition. In AD, cholinergic hypothesis is an epitomized therapeutic strategy to produce effective agents [30]. The virtual hit (compound **43**) obtained from our *de novo* drug design was initially evaluated for preliminary enzyme inhibition on AChE and BuChE at concentrations of 50 and 100 µM. Our first goal was to ascertain the significance of phenyl ring at 3rd position of the pyrazole scaffold. Encouragingly, compound **43** showed better inhibition at these concentrations, this driving for further investigations. In the second stage, six different concentrations of (0.01 µM − 100 µM) the compounds were used to determine the IC_{50}. On AChE and BuChE, IC_{50} of the compound was determined as 4.048 ± 0.115 µM and

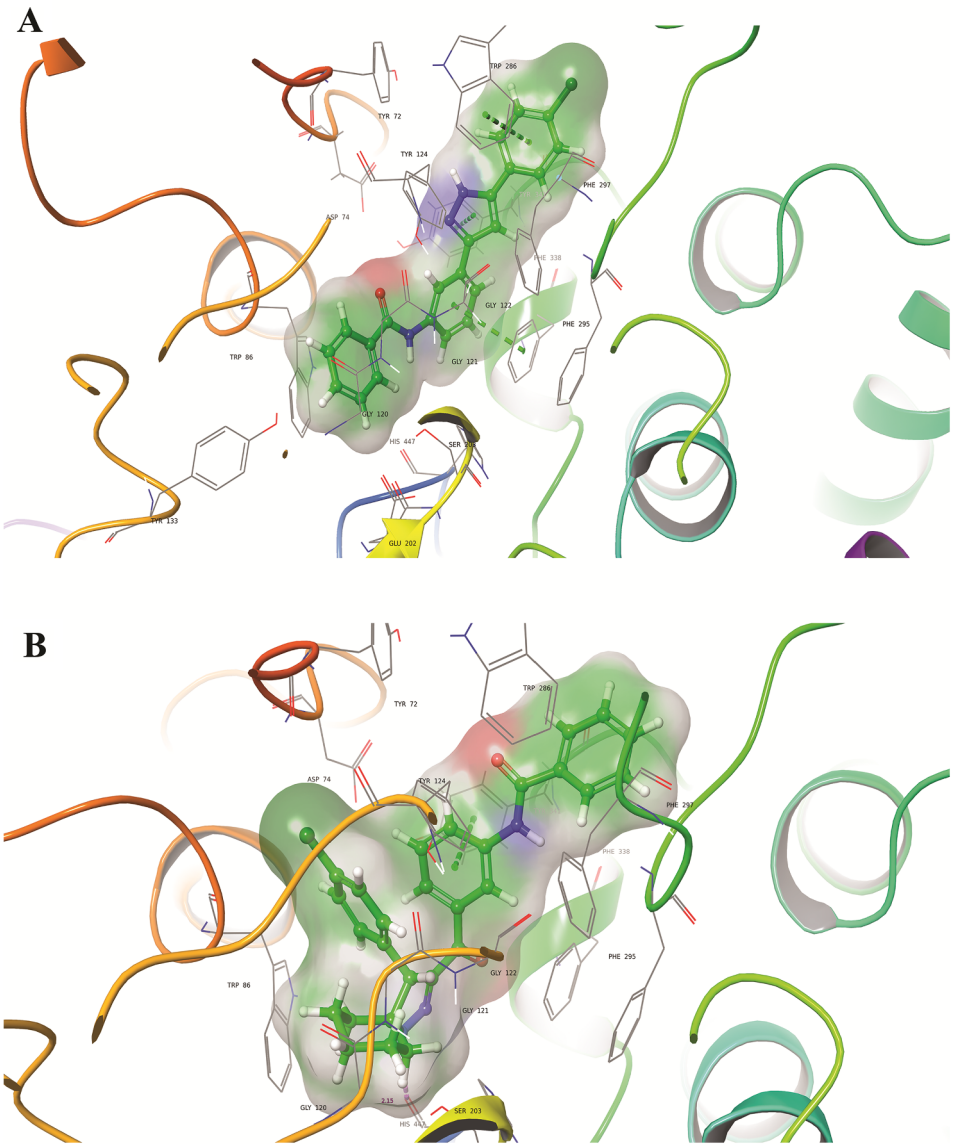

Fig. 2. Binding pattern of (A) compound **44** and (B) compound **67** in active site pocket of AChE (PDB: 4EY7).

8.633 ± 0.108 μM respectively. This may be due to the π-π interactions with PAS residue i.e TYR72. The phenyl ring attached to pyrazole was of interest for various structural modifications. Therefore, compound **43** was further explored with introduction of multiple EDG and EWG at phenyl ring. After successful synthetic assignment, compounds **43–62** were obtained and the role of substitutions in enzyme inhibition was evaluated. Fascinatingly, out of 20 derivatives, compound **44** (*para*-chloro) was found to be potent on both AChE and BuChE with two folds increase in IC_{50} (Table 2; AChE = 1.937 ± 0.066 μM; BuChE = 1.166 ± 0.087 μM). Among 3,5-diarylpyrazole series (**43–62**), halogen containing compounds (weak EWD groups; chloride, bromide, and fluoride) showed moderate to good IC_{50} values and remaining derivatives showed satisfactory activities (Table 2). However, increasing the bulkiness by adding another phenyl ring as in α-napthyl (**62**, AChE = 27.78 ± 0.107 μM; BuChE = 22.30 ± 0.068 μM) exhibited highest IC_{50} values. Interestingly, in all derivatives (**43–62**), *para* substituted analogs were slightly potent, when compared with other analogs. Bulky substituted analogs at *para* position (*para*-methoxy (**51**) AChE = 8.451 ± 0.069 μM; BuChE = 7.305 ± 0.087 μM; *para*-trifluoromethoxy (**56**) AChE = 6.092 ± 0.184 μM; BuChE = 6.755 ± 0.077 μM) of the phenyl ring showed moderate activities. Surprisingly, in spiropyrazoline series (**66–85**), same pattern of IC_{50} values were

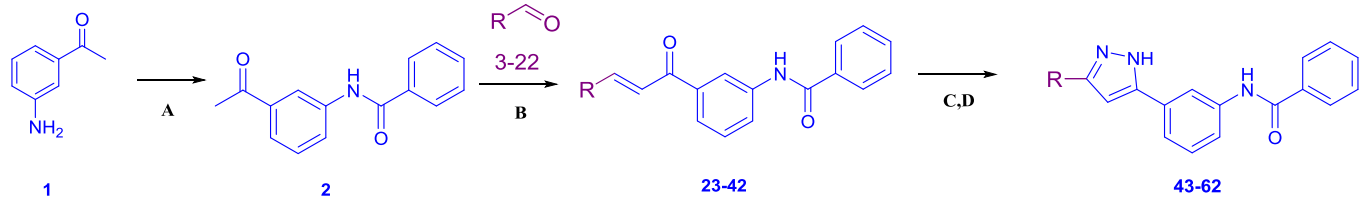

Scheme 1. Synthesis of 3,5-diaryl-1H-pyrazole derivatives[a]. [a]Reagents and conditions: (A) Benzoyl chloride 1.05 eq, triethylamine (1.05 eq), EtOAc, Rt, 6 h; (B) Aromatic aldehyde **3–22** (1.0 eq), 1 M NaOH 1 ml, EtOH, 25 °C, 6 h; (C,D) Hydrazine hydrate (5.0 eq), EtOH, reflux, 2 h, then catalytic I_2 , DMSO, 110 °C, 1.5 h.

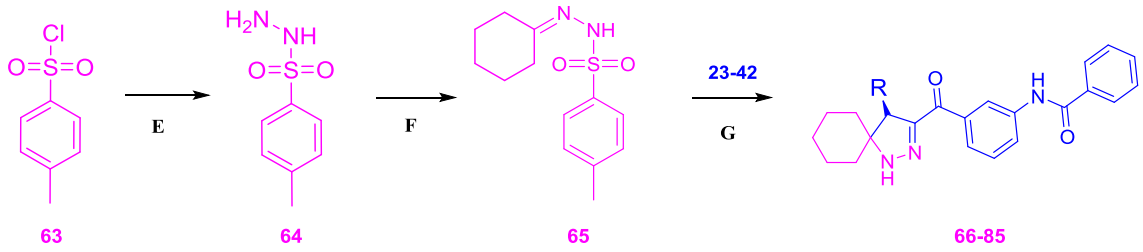

Comp. no	03,23 43,66	04,24 44,67	05,25 45,68	06,26 46,69	07,27 47,70	08,28 48,71	09,29 49,72	10,30 50,73	11,31 51,74	12,32 52,75
R		Cl	Cl	Cl Cl	Br	Br	F	F	O	O

Comp. no	13,33 53,76	14, 34 54,77	15,35 55,78	16,36 56,79	17,37 57,80	18,38 58,81	19,39 59,82	20,40 60,83	21,41 61,84	22,42 62,85
R	O O	CF_3	CF_3	O CF_3	CN	CN				

Scheme 2. Synthesis of spiropyrazolines derivatives[b]. [b]Reagents and conditions: (E) Hydrazine hydrate (1.5 eq), THF, 0 °C, 30 min; (F) Cyclohexanone (1.0 eq), MeOH, 60 °C, 1 h; (G) **23–42** (0.5 eq), CS_2CO_3 (1.0 eq), 1,4-dioxane, reflux, 2 h.

Table 1
Polarimetric data of compound **73**.

	Observed rotation $\alpha^{589}_{32.0}$	Specific rotation[a] $[\alpha]^{589}_{32.0}$
Compound **73**	+0.853	+213.25°

[a] Specific rotation of compound, 0.1 g in 25 ml CH_3OH.

observed in most of the analogs. Compound **67** (*para*-chloro) exhibited most potent inhibitory activities (AChE = 0.464 ± 0.166 μM; BuChE = 0.754 ± 0.121 μM). Compound **72** (*para*-fluoro) showed good inhibition at 0.948 ± 0.096 μM for AChE, where as in case of BuChE (IC_{50} = 1.959 ± 0.082 μM) it was more than double. Compound **74** (*para*-methoxy, AChE = 2.319 ± 0.147 μM; BuChE = 3.549 ± 0.116 μM) and **79** (*para*-trifluoromethoxy, AChE = 2.240 ± 0.122 μM; BuChE = 7.792 ± 0.066 μM) derivatives

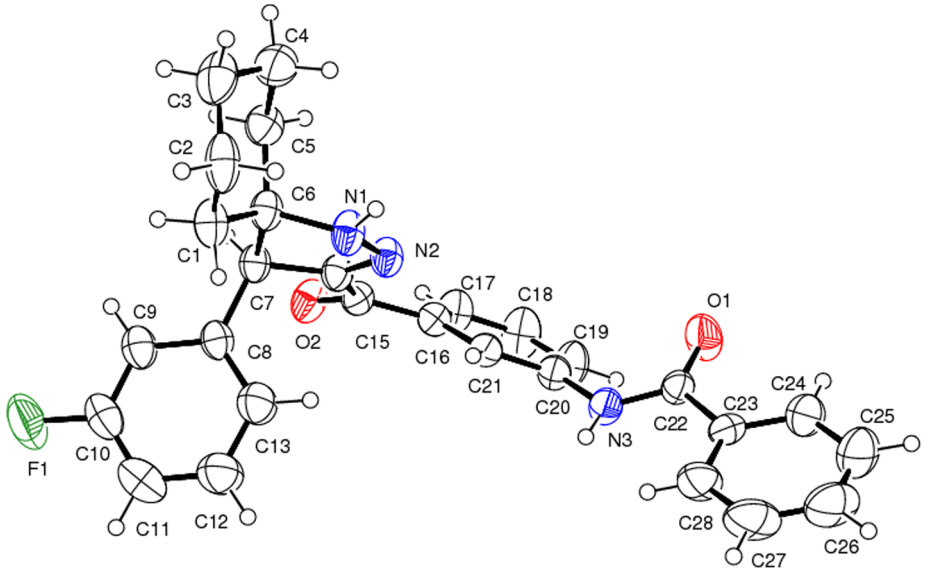

Fig. 3. ORTEP diagram of compound **73** (at 40% ellipsoid level).

Table 2
Inhibitory potencies and structures of 3,5-diaryl-1H-pyrazole **(43–62)** and spiropyrazolines **(66–85)** derivatives.

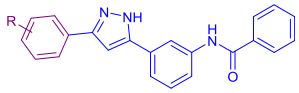

43-62

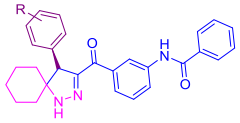

66-85

Comp. no	R	AChE IC_{50} ± SE (μM)	BuChE IC_{50} ± SE (μM)	selectivity ratio[a]	Comp. no	R	AChE IC_{50} ± SE (μM)	BuChE IC_{50} ± SE (μM)	selectivity ratio[a]
43	H	4.048 ± 0.115	8.633 ± 0.108	0.4	**66**	H	1.973 ± 0.143	1.626 ± 0.070	1.2
44	4-Cl	1.937 ± 0.066	1.166 ± 0.088	1.6	**67**	4-Cl	0.464 ± 0.166	0.754 ± 0.121	0.6
45	2-Cl	3.038 ± 0.128	3.821 ± 0.086	0.7	**68**	2-Cl	1.966 ± 0.104	2.753 ± 0.085	0.7
46	2,4-diCl	1.945 ± 0.107	2.572 ± 0.121	0.7	**69**	2,4-diCl	1.328 ± 0.107	2.041 ± 0.084	0.6
47	4-Br	2.164 ± 0.095	1.697 ± 0.073	1.2	**70**	4-Br	1.139 ± 0.105	1.533 ± 0.072	0.7
48	3-Br	3.011 ± 0.112	2.345 ± 0.072	1.2	**71**	3-Br	1.770 ± 0.110	2.116 ± 0.072	0.8
49	4-F	2.090 ± 0.090	2.648 ± 0.060	0.7	**72**	4-F	0.948 ± 0.096	1.959 ± 0.082	0.4
50	3-F	2.579 ± 0.121	2.102 ± 0.078	1.2	**73**	3-F	1.627 ± 0.097	1.811 ± 0.081	0.8
51	4-OMe	8.451 ± 0.069	7.305 ± 0.087	1.1	**74**	4-OMe	2.319 ± 0.147	3.549 ± 0.116	0.6
52	3-OMe	8.710 ± 0.182	5.863 ± 0.114	1.4	**75**	3-OMe	2.830 ± 0.172	3.872 ± 0.118	0.7
53	3,4-diOMe	15.22 ± 0.128	9.924 ± 0.119	1.5	**76**	3,4-diOMe	3.011 ± 0.112	7.279 ± 0.072	0.4
54	4-CF_3	2.360 ± 0.082	3.505 ± 0.115	0.6	**77**	4-CF_3	1.453 ± 0.137	2.385 ± 0.091	0.6
55	3-CF_3	3.196 ± 0.102	4.337 ± 0.059	0.7	**78**	3-CF_3	1.921 ± 0.178	3.670 ± 0.062	0.5
56	4-OCF_3	6.092 ± 0.184	6.755 ± 0.077	0.9	**79**	4-OCF_3	2.240 ± 0.122	7.792 ± 0.066	0.2
57	4-CN	3.829 ± 0.089	3.811 ± 0.067	1.0	**80**	4-CN	1.780 ± 0.090	2.697 ± 0.081	0.6
58	3-CN	3.936 ± 0.091	4.692 ± 0.052	0.8	**81**	3-CN	1.962 ± 0.122	3.694 ± 0.058	0.5
59	4-Me	14.86 ± 0.107	9.625 ± 0.098	1.5	**82**	4-Me	4.686 ± 0.096	8.775 ± 0.107	0.5
60	2-Me	16.94 ± 0.067	18.11 ± 0.112	0.9	**83**	2-Me	5.883 ± 0.134	9.460 ± 0.094	0.6
61	4-iPr	15.49 ± 0.10	16.57 ± 0.077	0.9	**84**	4-iPr	7.145 ± 0.114	12.74 ± 0.062	0.5
62	α-Napthyl	27.78 ± 0.107	22.30 ± 0.068	1.2	**85**	α-Napthyl	29.190 ± 0.117	35.49 ± 0.061	0.8
DNZ	———	0.019 ± 0.042	0.935 ± 0.026	–	**–**	——	——	——	–

[a] Selectivity ratio = (IC_{50} of AChE)/(IC_{50} of BuChE). DNZ = Donepezil.

of spiropyrazoline were potent in comparison to 3,5-diarylpyrazole derivatives (**51** and **56**) but not with *para*-chloro (**67**) of spiropyrazolines. Bulkiness was also not favored in spiropyrazoline analog (**85**, AChE = 29.190 ± 0.117 μM; BuChE = 35.49 ± 0.061 μM). The enzyme inhibition studies of both 3,5-diarylpyrazoles (**43–62**) and spiropyrazolines (**66–85**) on cholinesterase enzymes (AChE and BuChE) constructively developed the potency profiles of all the synthesized analogs. Weak EWD substituted derivatives showed good inhibitory activities. Compounds **44** and **67** showed significant IC_{50} values among them and were also evident from molecular docking studies. The SAR studies suggested that substitution at *para* position of phenyl ring will be beneficial for activity where as *ortho/meta* substitutions in the same analogs were found to be satisfactory. Further, bulkiness on the phenyl group led to decrease in activity.

To assess the selectivity towards human AChE (hAChE), four representative compounds (**44**, **46**, **67** and **69**) were selected and studied further. Compounds **44**, **46**, **67** and **69** exhibited IC_{50} 1.758 ± 0.095 μM, 1.027 ± 0.062 μM, 0.472 ± 0.042 μM and 0.693 ± 0.062 μM respectively (standard DNZ = 0.022 ± 0.031 μM). To demonstrate the worthiness of drug design approach, compounds **44** and **67** were additionally evaluated for enzyme kinetic assay on AChE.

2.3. AChE enzyme kinetic assay

To discover a potential analog, it is crucial that selective inhibitors be identified, which requires evaluation of candidate for binding pattern against selected target. The mechanistic role of AChE inhibition by compounds **44** and **67** was explored through enzyme kinetics parameters like maximal velocity (V_{max}), Michaelis–Menten/dissociation constant (K_m), and inhibitory concentration (ki). The reciprocal Lineweaver-Burk plot of compound **67** (Fig. 4) suggested decreased pattern of V_{max} and K_m with increase in inhibitor concentrations and the intersection point of trendlines fell in the second quardrant. This result demonstrated that compound **67** inhibited the AChE enzyme non-competitively. The Dixon plot showed that it has Ki = 2.65 μM (Fig. 5).

2.4. In-vitro blood-brain barrier permeation assay

BBB and its penetration by neurotherapeutics is the gate way towards CNS activity [31]. To screen the BBB permeability of all synthesized compounds (**43–62 & 66–85**), a parallel artificial membrane permeation assay (PAMPA) was employed as described in previous reports [14]. Nine representative commercially available drugs were selected and evaluated for BBB permeability (*Pe*, S3, Table S2). The *Pe* values of the tested compounds are listed in Table 3. As expected, the BBB penetration potential of spiropyrazoline series (compound **67** $Pe = 13.92 \pm 0.022 \times 10^{-6}\,cm\,s^{-1}$), was improved significantly as compared to 3,5-Diarylpyrazole series (Compound **44** $Pe = 9.491 \pm 0.34 \times 10^{-6}\,cm\,s^{-1}$). This could be explained by the introduction of lipophilic cyclohexane ring. Compound **82** (4-methyl substituted derivative) showed greater BBB permeability with *Pe* value of $14.745 \pm 0.01 \times 10^{-6}\,cm\,s^{-1}$. Moreover, all tested compounds could cross BBB *in vitro*, with excellent permeation potentials.

2.5. Propidium iodide displacement assay

Molecular docking studies suggested that compounds **44** and **67** demonstrated significant interactions with PAS residues. Further, enzyme inhibition and PAMPA assays manifest potent inhibition of AChE and BBB permeation. Therefore, PAS-binding affinity of compounds **44** and **67** was evaluated by propidium iodide displacement assay at 10 and 50 μM concentrations (Table 4). The binding of compounds **44** and **67** to PAS-AChE resulted into decreased fluorescence intensity. Compound **67** exhibited considerably equal displacement of propidium iodide at a concentration of 10 μM (21.24%) but higher in case of 50 μM (41.10%) compared to donepezil (10 μM = 21.30%; 50 μM = 38.23%). Compound **44** (10 μM = 15.68%; 50 μM = 28.04%) appeared to have lesser displacement of propidium iodide from PAS-AChE. The results of propidium iodide displacement assay are in concurrence with molecular docking studies of compounds **44** and **67**.

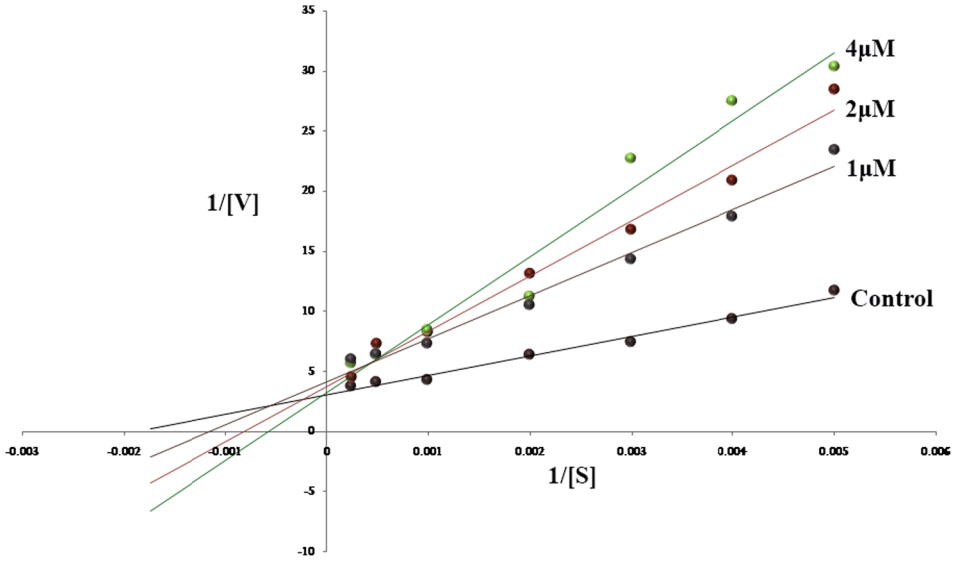

Fig. 4. Lineweaver-Burk plot on three different concentration of compound **67** for AChE: V_{max}, Km and V_{max}/K_m at 1 μM, 2 μM and 4 μM are found to be 3.145 ± 0.169 U/min, 0.4588 ± 0.156 U/min, 0.2305 ± 0.032 U/min and 0.0727 ± 0.415 μM, 0.0086 ± 0.003 μM, 0.0027 ± 0.0006 μM and 43.26, 57.35, 115.25 respectively.

2.6. $A\beta_{1-42}$ aggregation assay (Thioflavin T assay) and confocal fluorescence imaging

Compounds **44** and **67** were further evaluated by metal induced $A\beta_{1-42}$ aggregation assay to establish their potency. $A\beta_{1-42,}$ when incubated with the metal showed 100% aggregation. DNZ, at a dose of 20 μM, showed significant inhibition of metal induced $A\beta_{1-42}$ aggregation. Compound **44**, inhibited nearly 50% as of $A\beta_{1-42}$ aggregation, whereas in compound **67** it was more than 50% compared with Fe^{+2} + $A\beta_{1-42}$ and $A\beta_{1-42}$ groups (Fig. 7A). Recently, Avinash S. Kumbhar and coworkers demonstrated the use of Thioflavin T (ThT) based confocal imaging experiments to monitor conformational changes of $A\beta_{1-42}$ aggregation in presence of Ru(II) polypyridyl complexes [32]. Confocal imaging was carried out to understand the interaction of $A\beta_{1-42}$, Fe^{+2}, compound **44**, and **67** at molecular level after 10 days of incubation. Fluorescent background was obtained using ThT dye (Fig. 3B). $A\beta_{1-42}$ aggregates were obtained when incubated and treated with ThT (Fig. 7C), whereas no fluorescence was observed in $A\beta_{1-42}$ alone (Fig. 7D) and $A\beta_{1-42}$ along with the metal were incubated without ThT (Fig. 7E). These blank images explain that neither $A\beta_{1-42}$ and metal nor their combinations showed any background noises in absence of ThT. $A\beta_{1-42}$ incubated with metal showed vigorous plaques deposition (Fig. 7F), while the plaques were decreased upon treatment with compounds **44** and **67** (Fig. 7G and H). These results suggest that test compounds possibly inhibit or lessened the $A\beta_{1-42}$ aggregation at early stages of fibril formation.

2.7. Neuroprotection studies on MC65 cell lines

Cell line studies provide a system for ready and rapid evaluation [33]. The use of cell cytotoxicity analysis is a valuable tool to study issues of clinical relevance, especially those related to diseases, and cell toxicity mechanisms. MC65 is a versatile *in vitro* model in neurobiology and it conditionally expresses a C-terminal derivative of the amyloid β precursor protein (AβPP) termed SβC (a fusion protein composed of the amino-17 and carboxyl-99 residues of βPP), which further induces ROS generation. The cell line is accompanying with oxidative stress and Aβ induced cellular toxicity in tetracycline (TC) removal condition (TC-) [34]. Neurotherapeutic likeliness and toxicity profiles of the potent derivatives (compounds **44** and **67**) were ascertained by MTT (3-(4,5-

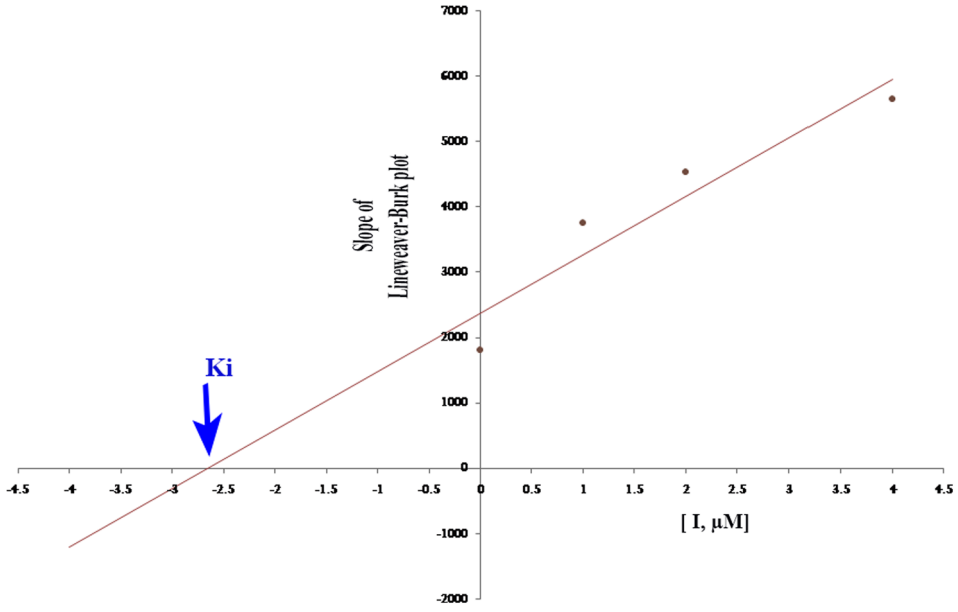

Fig. 5. Dixon plot of compound **67** showing the Ki value as negative intercept on X-axis of the Dixon plot for AChE.

Table 3
Permeability Pe (10^{-6} cm s^{-1}) results from the PAMPA-BBB assay of synthesized compounds and their prediction of BBB Penetration.

Comp.	Pe (10^{-6} cm s^{-1})[a,b]	Comp.	Pe (10^{-6} cm s^{-1}) [a,b]
43	9.655 ± 0.04	**66**	13.75 ± 0.01
44	9.491 ± 0.34	**67**	13.92 ± 0.022
45	9.513 ± 0.23	**68**	13.855 ± 0.60
46	9.9905 ± 0.01	**69**	14.175 ± 0.02
47	9.729 ± 0.007	**70**	13.579 ± 0.01
48	9.694 ± 0.05	**71**	13.654 ± 0.04
49	9.606 ± 0.008	**72**	13.764 ± 0.009
50	9.627 ± 0.009	**73**	13.698 ± 0.06
51	9.656 ± 0.06	**74**	13.83 ± 0.06
52	9.7485 ± 0.004	**75**	13.659 ± 0.035
53	9.925 ± 0.012	**76**	14.133 ± 0.012
54	9.964 ± 0.04	**77**	14.356 ± 0.04
55	9.748 ± 0.003	**78**	14.656 ± 0.025
56	9.367 ± 0.03	**79**	13.656 ± 0.02
57	9.369 ± 0.017	**80**	14.34 ± 0.02
58	9.664 ± 0.02	**81**	14.241 ± 0.005
59	9.731 ± 0.004	**82**	14.745 ± 0.01
60	9.627 ± 0.009	**83**	13.552 ± 0.03
61	9.76 ± 0.05	**84**	13.974 ± 0.004
62	9.631 ± 0.008	**85**	14.156 ± 0.04

[a] Data are expressed as the standard deviation (SD) of three independent experiments.

[b] Compounds with *Pe* greater than 4.324×10^{-6} cm s^{-1} could cross the BBB (CNS +). Compounds with *Pe* < 1.846×10^{-6} cm s^{-1} could not cross the BBB (CNS −), and compounds with 1.846×10^{-6} cm s^{-1} < *Pe* < $4.324 \times 10^{-}$ cm s^{-1}show uncertain BBB permeation (CNS ±); All compounds could cross the BBB.

Table 4
Propidium iodide displacement assay.

Comp.no	Displacement of Propidium iodide from AChE PAS (% inhibition)[a]	
	At 10 μM	At 50 μM
44	15.68 ± 1.96	28.04 ± 2.81
67	21.24 ± 2.18	41.10 ± 2.49
Donepezil	21.30 ± 1.69	38.23 ± 3.37

[a] Data are expressed as the standard deviation (SD) of three independent experiments.

dimethylthiazol-2-yl)-2,5-diphenyltetrazolium bromide) assay. Compounds **44** and **67** at concentrations of 50, 40, 30, 20, 10, and 1 μM were used in the experiment and compared to that of tetracycline (TC +). Significant decrease in the Aβ production was observed with respect to TC- cells (Fig. 6).

2.8. Behavioral studies by Y-maze test

The evaluation of a chemical molecule for potential *in-vivo* efficacy requires a robust approach, which screens for efficacy in appropriate cognitive domains and monitors behavior to appraise cognition. The spontaneous alternation behavior in Y-maze, as sign of short-term memory, is a fruitful method to screen new molecules against amnesic rodent model [35]. Effects of compounds **44** and **67** on scopolamine-induced impairment of spontaneous alternation behavior and number of arm entries were assessed by administering scopolamine hydrobromide (3 mg/kg) by intraperitoneal injection. Scopolamine hydrobromide showed markedly impaired spontaneous alternation behavior and significant difference ($p < 0.05$) with respect to control, vehicle and DNZ treated groups. (Fig. 8A). Compound **44** at a dose of 1.5 mg/kg, exhibited no significant difference with scopolamine hydrobromide treated group, whereas at doses of 3 mg/kg and 6 mg/kg showed significant difference. Notable differences were observed among compound **67** treated groups, relative to the Scopolamine hydrobromide 3 mg/kg group. There was a dose dependent increase in the percentage of spontaneous alternation among compound **44** treated groups. No significant difference in the percentage of spontaneous alternation was observed between DNZ treated group and compound **67** (at dose of 3 mg/kg and 6 mg/kg) treated groups. Neophobia and recognizing behaviors of all groups were assessed by monitoring their novel arm entries. Scopolamine hydrobromide (3 mg/kg) showed remarkable decrease in novel arm entries whereas, DNZ (3 mg/kg) exhibited no significant deference with respect to control and vehicle groups. Compound **44** at a dose of 1.5 mg/kg showed significant difference with respect to scopolamine and DNZ groups. Dose dependent increase in novel arm entries was observed until a dose of 3 mg/kg, before hitting a plateau at 6 mg/kg. Same pattern was observed with compound **67,** which at a dose of 3 mg/kg showed no significant difference compared to DNZ. Increase in novel arm entries by spiropyrazoline derivative (compound **67** at 3 mg/kg) was mainly because of greater availability of drug in the brain as compared to 3,5-diarylpyrazole analog (compound **44**). In case of % total arm entries, all groups are significantly different with respect to scopolamine group. This suggests that none of the compounds influenced the locomotor activity of the animals.

2.9. Neurochemical level estimation

The animals used in the behavioral study were further evaluated for neurochemical (AChE) level in brain by earlier described protocols [14]. High levels of AChE were observed in scopolamine treated animals (Fig. 9A), but was significantly lessened with DNZ treatment. Compounds **67** (3 mg/kg), **44** (3 mg/kg) showed slightly higher levels of AchE as compared to DNZ and compounds **67**. Catalase (CAT) is a

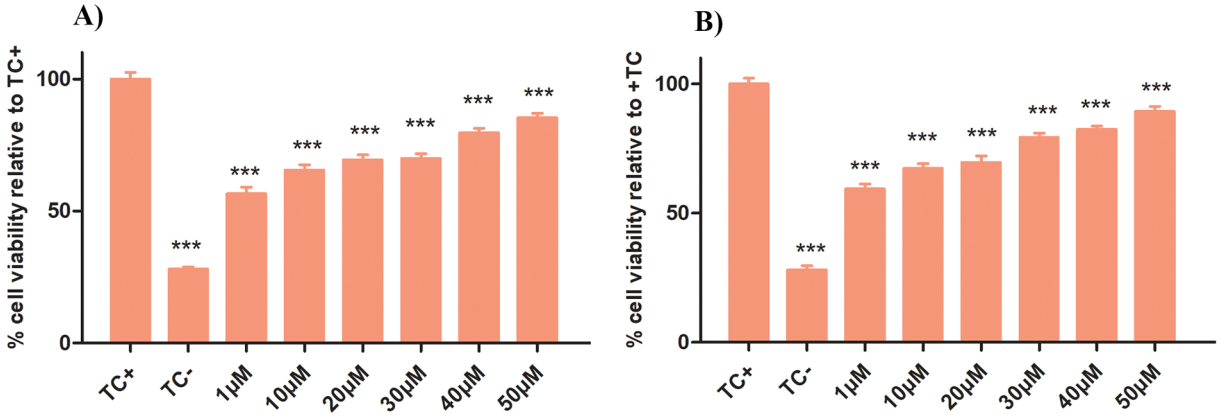

Fig. 6. Neuroprotection assay on MC65 cell lines with A) Compound **44** B) Compound **67**; MC65 cells were treated with Compound **44** and **67** at mentioned concentrations in the absence of Tetracycline (TC −). TC + was taken as control (One-way ANOVA followed by Newman-Keuls multiple comparison test compare all pair of columns *** $p < 0.0001$).

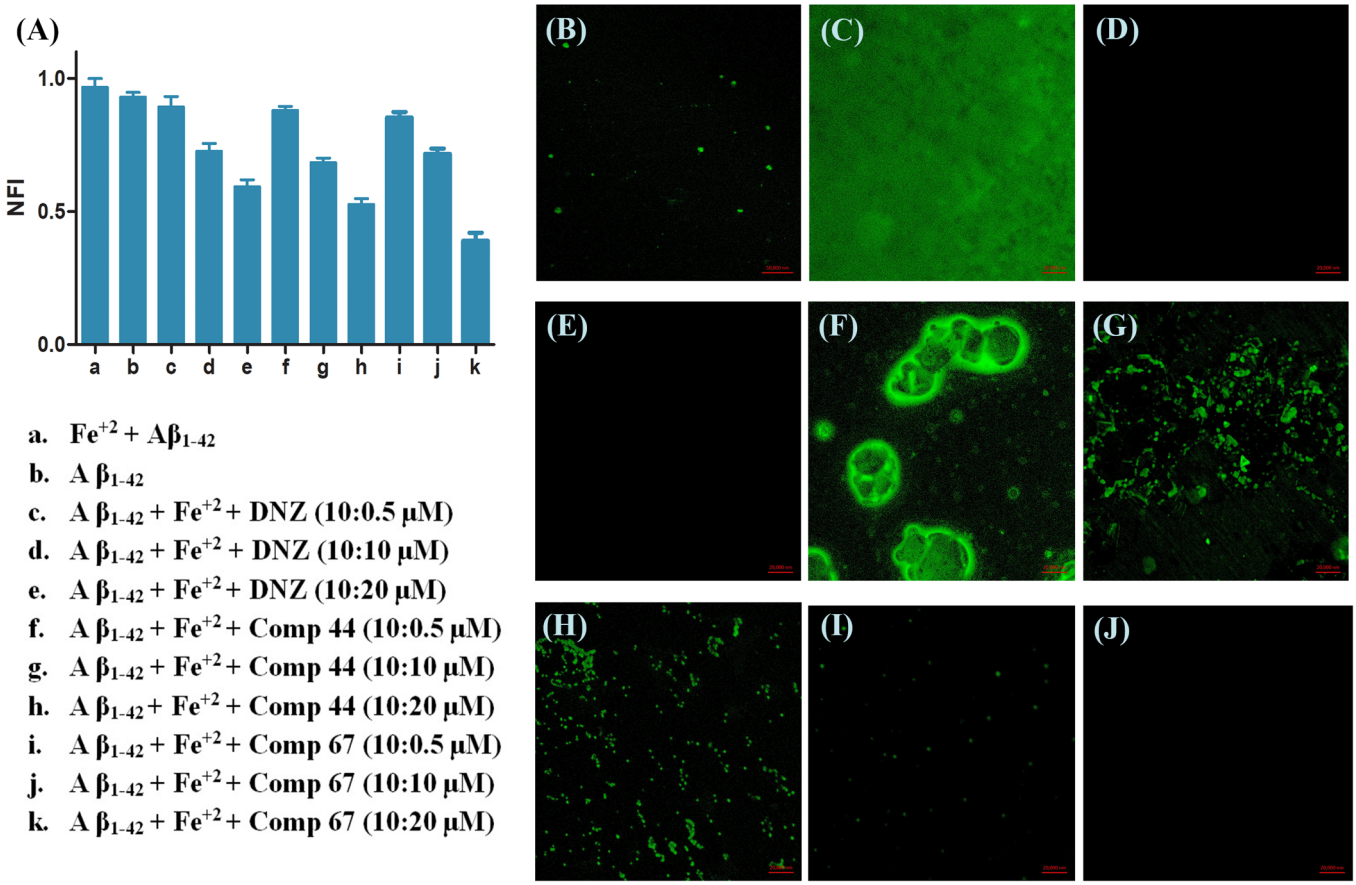

Fig. 7. $A\beta_{1\text{-}42}$ aggregation Inhibition assay and confocal imaging analysis: (A) metal induced $A\beta_{1\text{-}42}$ aggregation assay (One-way ANOVA followed by one-way analysis of variance*** $p < 0.0001$), error bars represent the standard deviation (SD) of the normalized fluorescence intensity (NFI), donepezil (DNZ)); Confocal image of (B) Thioflavin T (ThT) (C) $A\beta_{1\text{-}42}$ along with ThT (D) $A\beta_{1\text{-}42}$ without fluorescence dye ThT (E) $A\beta_{1\text{-}42}$ along with Fe^{+2} (F) $A\beta_{1\text{-}42}$ containing Fe^{+2} and ThT (G) $A\beta_{1\text{-}42}$ containing Fe^{+2}, compound **44** and ThT (H) $A\beta_{1\text{-}42}$ containing Fe^{+2}, compound **67** and ThT (I) compound **67** and ThT (J) containing only compound **67.** Scale size: 20000 nm.

very important enzyme in protecting the cells from oxidative damage by reactive oxygen species (ROS). CAT levels in the brain of animals were also determined after the behavioral studies (Fig. 9B) and compounds **44** and **67** maintained its normal level at a dose of 3 mg/kg (Fig. 9). The brain tissue pattern in the normal, toxic and treated groups was further evaluated by histopathological examination (Fig. 8E) of the brain samples. Some abnormal cell morphology was observed in the scopolamine treated animal, while the standard pattern of the brain tissues in control, compounds **44** and **67** treated animals evidently deduce that the test compounds were safer for brain tissues.

2.10. In-vivo mice brain pharmacokinetic profiles of compounds 44 and 67

For a potent CNS drug, it is necessary to understand the brain penetration and ratio of brain and plasma concentration [36]. In view of the appreciative potency in *in-vitro* BBB permeation and scopolamine induced amnesia models, compounds **44** and **67** were further evaluated for brain pharmacokinetic profile in mice. As shown in Table 5, compound **67** showed better brain penetration and it was increased by 2.05 times compared to compound **44**. Moreover, it showed acceptable terminal half-life ($t_{1/2}$ = 2.61 h) after oral administration.

3. Summary and conclusions

We described *de novo* drug design based on fragment growing strategy for the identification of potent chemical entities for AChE inhibition. The development of potent scaffolds and evaluation was the focus of present study by using tiny fragment molecules. Fragments which were having good binding interaction to AChE active site were selected and allowed to grow in LigBuilder 2. The obtained optimized hit was chemically modified to get improved binding interactions. Increase in potency from hit to optimized hit compound have proved the rationality of design strategy and inspired to search compounds with superior ChEs inhibitory profile. Using this approach, we designed, synthesized and evaluated 40 compounds through *in-vitro* assays and identified that compound **67** (AChE = 0.464 ± 0.166 μM; BuChE = 0.754 ± 0.121 μM; hAChE = 0.472 ± 0.042 μM; P_e = 13.92 ± 0.022 × 10^{-6} cm s^{1}) was most potent and showed displacement of propidium iodide from PAS-AChE. We also characterized all derivatives with sophisticated analytical techniques. The X-ray crystal structure of compound **73** established formation of spiropyrazoline derivatives. Hit (compound **44**) and optimized hit (compound **67**) were further assessed to support the design approach. At 50 μM, compounds **44** and **67** exhibited near 90% cell viability and diminished the metal induced $A\beta_{1\text{-}42}$ aggregation effectively at 20 μM. *In-vivo* behavioral analysis of compound **67** demonstrated better spontaneous alternation score and novel arm entries without influencing the locomotor activity. Rise in brain penetration of compound **67** by 2.05 times compared to compound **44,** reinforce the design strategy. Considering the ChE's inhibitory potency, BBB permeability, promising data from the MC65 cell line, propitious *in-vivo* behavioral and brain penetration analysis, compound **67** represents a beneficial hit for development of new chemical entities against Alzheimer's disease.

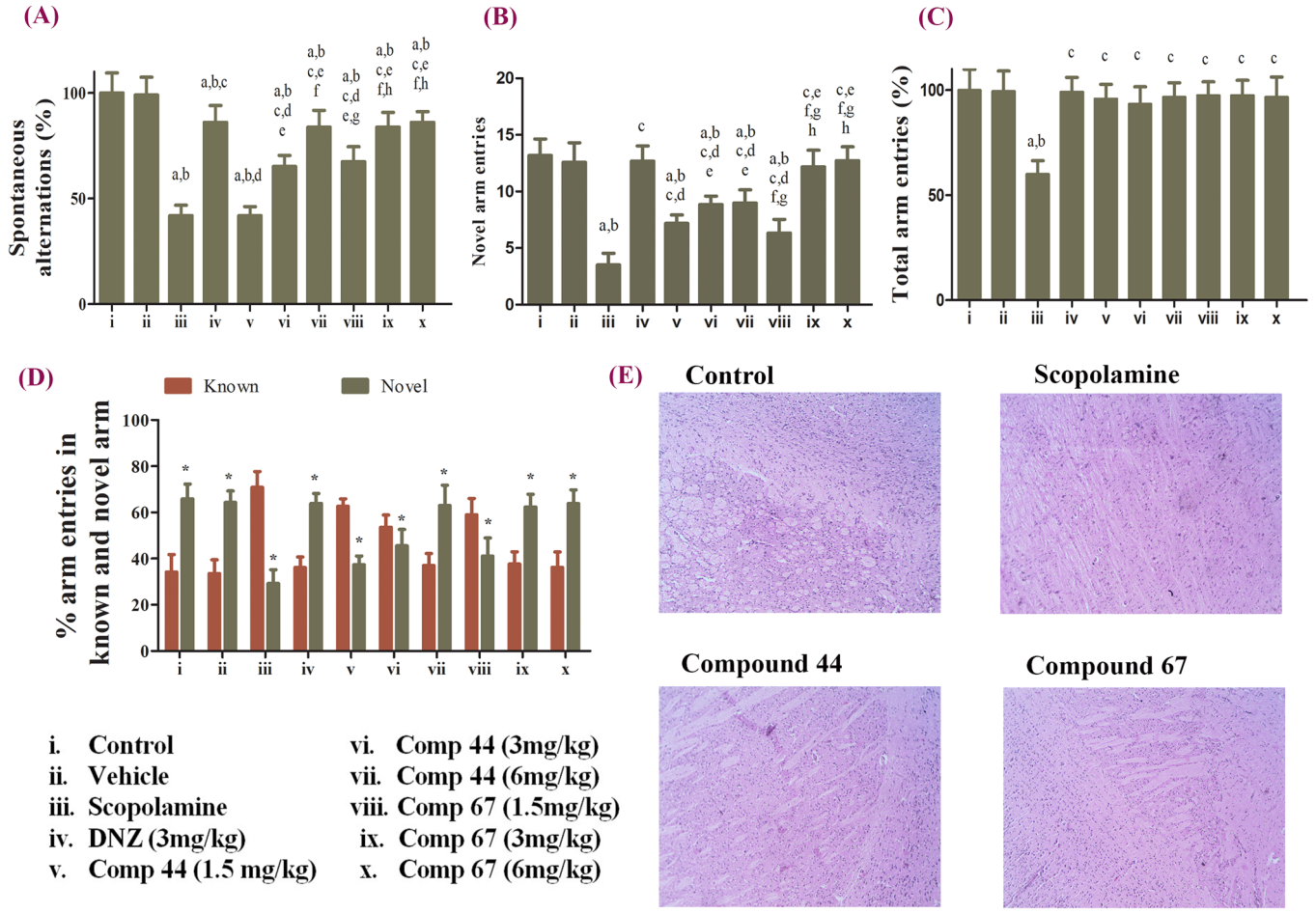

Fig. 8. Effect of compounds **44** and **67** on scopolamine-induced impairment of spontaneous alternation behavior (A) spontaneous alternation score (spontaneous alternation %); (B) Novel arm entries of the animals; (C) Total arm entries % in the Y-maze test. (D) % arm entries in known and novel arm in Y maze test (E) Histopathology of brain samples. Bars shows data as Mean ± SD, n = 6, $^{a}p < 0.05$ compared to control; $^{b}p < 0.05$ compared to vehicle; $^{c}p < 0.05$ compared to scopolamine; $^{d}p < 0.05$ compared to donepezil (DNZ) at dose of 3 mg/kg; $^{e}p < 0.05$ compared to compound **44** at dose of 1.5 mg/kg; $^{f}p < 0.05$ compared to compound **44** at dose of 3 mg/kg; $^{g}p < 0.05$ compared to compound **44** at dose of 6 mg/kg; $^{h}p < 0.05$ compared to compound **67** at dose of 1.5 mg/kg; $^{i}p < 0.05$ compared to compound **67** at dose of 3 mg/kg.

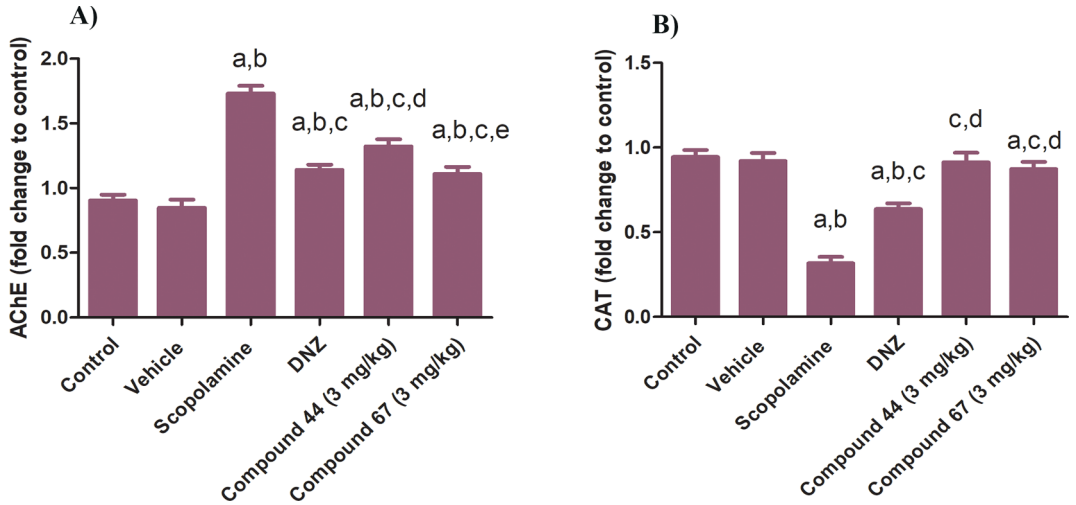

Fig. 9. Analysis of AChE and Catalase levels **(A)** Estimation of AChE level. **(B)** Estimation of CAT levels; (Mean ± SD, n = 6, $^{a}p < 0.05$ compared to control; $^{b}p < 0.05$ compared to vehicle; $^{c}p < 0.05$ compared to scopolamine; $^{d}p < 0.05$ compared to DNZ; $^{e}p < 0.05$ compared to compound 44 at dose of 3 mg/kg (One-way ANOVA followed by Newman - Keuls test).

Table 5
Pharmacokinetic and brain penetration parameters of compound **44** and **67** following oral administration (30 mg/kg) to mice.[a]

Parameter	Compound 44		Compound 67	
	Plasma	Brain	Plasma	Brain
C_{max} (μg/mL)	10.21 ± 2.24	4.12 ± 0.57	28.15 ± 3.45	40.12 ± 5.18
T_{max} (h)	0.25	1	0.25	1
AUC_{0-t} (μg min/mL)	6.77 ± 0.75	8.17 ± 0.97	57.11 ± 6.54	141.60 ± 19.78
$t_{1/2}$ (h)	0.60 ± 0.04	1.83 ± 0.09	1.68 ± 0.13	2.61 ± 0.34
MRT 0-inf_obs (h)	0.96 ± 0.08	3.10 ± 0.34	2.33 ± 0.16	3.75 ± 0.32
Cl/F (mL/kg/h)	383.2 ± 28.62	263.8 ± 14.47	49.9 ± 4.87	18.6 ± 2.45
Vz/F (mL/kg)	333.2 ± 42.95	695.7 ± 57.85	121.05 ± 16.45	70.2 ± 3.72
Brain penetration (AUC_{brain}/AUC_{Plasma})	1.21		2.48	

[a] Data are presented as mean ± S.D. (n = 5 per each time interval). Significant difference ($p < 0.05$); T_{max}, peak time; C_{max}, peak concentration; AUC, the extrapolated area under the plasma concentration-time curve; $t_{1/2}$, terminal half-life; MRT, mean resident time; CL, total plasma clearance; V_z volume of distribution.

4. Experimental section

4.1. Chemistry

4.1.1. General method

All commercially available chemicals were purchased from sigma Aldrich, TCI Co., ltd, and Avra synthesis pvt. Ltd. The solvents used for the study were dried by proper techniques and were used anhydrous unless otherwise stated. Experiments were carried out in oven-dried glassware under dry N_2 atmosphere and standard vacuum techniques were used. Purifications were carried out by using column chromatography on silica gel 60 (Avra), particle size = 0.140–0.25 mm (60–120 mesh), as the stationary phase. All reactions were monitored by silica gel F_{254} TLC aluminium sheets (Merck) and ultraviolet light (254 nm) or iodine vapors were used for visualization of spots. Melting points were determined by using automated melting point apparatus (Bamstead Electrothermal, UK). All intermediates and target compounds were characterized by ^{1}H NMR, ^{13}C NMR and mass spectrometry. NMR spectra were recorded in Bruker-500 (^{1}H 500 MHz, ^{13}C 125.8 MHz) instrument using $CDCl_3$ and DMSO-d_6 as solvents. Chemical shift was measured in the ppm (δ) and coupling constant (*J*) was measured in Hz. ^{1}H NMR spectra are represented as follows: chemical shift, multiplicity (s = singlet, d = doublet, t = triplet, q = quartet, m = multiplet, dd = doublet of doublet, td = triplet of doublet, bs = broad singlet), coupling constant (*J*) in Hertz (Hz), integration, and proton assignment. Massspectrometric analysis was performed using Waters Q-TOF premier-HAB213 instrument equipped with APCI and ESI multimode ionization source. Optical rotation was measured on a Fisher scientific, model ADP-45 automatic polarimeter using a light-emitting diode (LED) lamp, emitting light at a wavelength of 589 nm and a 1 dm polametric tube. Specific rotation $[\alpha]^{589}_{32.0}$, was calculated using the equation: α/lc, where α is the observed optical rotation $\alpha^{589}_{32.0}$, l is the path length of the cell in dm, and c is the concentration of test compound in g/ml. Differential scanning calotimetric analysis was performed by using heat flux type Shimadzu DSC-60 plus instrument with Chromel-Alumel thermocouple detector. X-ray data collection was performed with Bruker D8 VENTURE Kappa Apex III CMOS PHOTON 100 diffractometer equipped with graphite monochromated Mo (Kα) (λ = 0.71073 Å) radiation. The structures were solved by SHELXT-2014/5 (Sheldrick, 2014) and refined by full-matrix least squares techniques using SHELXL-2014, (Sheldrick, 2014) computer program. Molecular graphics were drawn using ORTEP3 (Farrugia, 1997).

Purity of the compounds was determined by high-performance liquid chromatography (HPLC-Agilent 1260 infinity II Quaternary LC). Isocratic mobile phase was delivered by quaternary pump with - flow rate of 1 ml/min. The mobile phase composition was phase A (Water) and phase B (methanol) in ratio of 1:9. 5 μL samples were injected into the HPLC column through auto sampler. Diode-array detectors (DAD HS G7115A) detector was used at 310 nm for the detection of the compounds. Agilent ZORBAX Eclipse plus C8 column (5 μm, 4.6 × 250 mm) was used. The purity of the compounds was found to be above 99%.

4.1.2. Synthesis of N-(3-acetylphenyl)benzamide (2)

Compound **2** was synthesized according to a previously described method [37] and obtained as off white solid. Yield − 94.6%, M.P.- 108–109 °C,^{1}H NMR (500 MHz, DMSO-d_6) δ 10.46 (s, 1H. amide), 8.38 (s, 1H, acetylphenyl C_2), 8.09 (d, *J* = 8 Hz, 1H, acetylphenyl C_6), 8.00 (d, *J* = 7.5 Hz, 2H, benzamide C_2, C_6), 7.73 (d, *J* = 8 Hz, 1H, acetylphenyl C_4), 7.63–7.60 (m, 1H, benzamide C_4), 7.57–7.50 (m, 3H, benzamide C_3, C_5 & acetylphenyl C_5), 2.59 (s, 3H, methyl). ^{13}C NMR (125 MHz, DMSO-d_6) δ 198.2 (-C═O, acetyl), 166.52 (-C═O, amide), 139.64 (acetylphenyl C_3), 138.26 (acetylphenyl C_1), 135.42 (benzamide C_1), 131.57 (acetylphenyl C_5), 129.62 (benzamide C_4), 128.76 (benzamide C_3, C_5), 127.23 (benzamide C_2, C_6), 125.53 (acetylphenyl C_6), 123.27 (acetylphenyl C_4), 119.53 (acetylphenyl C_2), 27.22 (-CH_3, methyl).

4.1.3. General procedure for the synthesis of 23–42

To a solution of compound **2** (1.0 eq) in ethanol (10 ml) were added aromatic aldehyde (**3**–**22**, 1.0 eq) and 1 M NaOH solution (1 ml) at below 25 °C. The reaction mixture was stirred at room temperature for 6 h. After completion of the reaction (monitored by TLC), reaction mixture was kept refrigeration. Then the precipitated compound was filtered off and washed with ice cold ethanol (8 to 10 ml) to afford titled compound.

*4.1.3.1. N-(3-cinnamoylphenyl)benzamide**(23)***. White solid, yield − 89%, M.P.- 115–116 °C, ^{1}H NMR (500 MHz, DMSO-d_6) δ 10.51 (s, 1H, amide NH), 8.48 (s, 1H, phenyl C_2), 8.16 (d, *J* = 7.5 Hz, 1H, β = CH), 8.03 (d, *J* = 7 Hz, 2H, benzamide C_2, C_6), 7.96 (d, *J* = 7.5 Hz, 1H, phenyl C_6), 7.89–7.87 (m, 3H, phenyl C_4, C_5, benzamide C_4), 7.80 (d, *J* = 16 Hz, 1H, α = CH), 7.63–7.54 (m, 4H, benzamide C_3, C_5, cinnamoyl C_2, C_6), 7.47 (s, 3H, cinnamoyl C_3, C_4, C_5). ^{13}C NMR (125 MHz, DMSO-d_6) δ 189.64 (-C═O, cinnamoyl), 166.24 (-C═O, amide), 144.64 (β = CH), 140.17 (phenyl C_3), 138.51 (phenyl C_1), 135.09 (cinnamoyl C_1), 132.25 (benzamide C_1), 131.18 (benzamide C_4), 129.64 (benzamide C_3, C_5), 129.45 (cinnamoyl C_3, C_5), 129.30 (Cinnamoyl C_2, C_6), 128.92 (benzamide C_2, C_6), 128.19 (phenyl C_6, cinnamoyl C_4), 125.36 (phenyl C_5), 124.47 (phenyl C_4), 122.63 (α = CH), 120.58 (Phenyl C_2); MS (ESI +): *m/z* calculated for $C_{22}H_{17}NO_2$: 327.38, found – 328.4 (M + 1).

*4.1.3.2. N-(3-(3-(4-chlorophenyl)acryloyl)phenyl)benzamide **(24)***. White solid, yield − 93%, M.P.- 105–106 °C, ^{1}H NMR (500 MHz, DMSO-d_6) δ 10.49 (s, 1H, amide NH), 8.47 (t, *J* = 2 Hz, 1H, phenyl C_2), 8.15 (d, *J* = 7 Hz, 1H, β = CH), 8.02–8.00 (d, *J* = 7 Hz, 2H, benzamide C_2, C_6), 7.97–7.90 (m, 4H, benzamide C_2, C_6, phenyl C_4, C_6), 7.78 (d, *J* = 15.5 Hz, 1H,α = CH), 7.64–7.53 (m, 6H, chlorophenyl C_2, C_6, C_3, C_5, benzamide C_4, phenyl C_5). ^{13}C NMR (125 MHz, DMSO-d_6) δ 189.50

(-C═O, acryloyl), 166.21 (-C═O, amide), 143.14 (β = CH), 140.18 (phenyl C_3), 138.40 (phenyl C_1), 135.64 (phenyl C_6), 135.07 (chlorophenyl C_4), 134.09 (chlorophenyl C_1), 132.25 (benzamide C_1), 131.01 (benzamide C_4), 129.63 (benzamide C_3, C_5), 129.47 (chlorophenyl C_2, C_6), 128.91 (chlorophenyl C_3, C_5), 128.18 (benzamide C_2, C_6), 125.46 (phenyl C_5), 124.56 (phenyl C_4), 123.34 (α = CH), 120.56 (Phenyl C_2); MS (ESI +): *m/z* calculated for $C_{22}H_{16}ClNO_2$: 361.83, found – 362.15 (M +), 364.12 (M + 2).

4.1.3.3. N-(3-(3-(2-chlorophenyl)acryloyl)phenyl)benzamide ***(25)***. Off white solid, yield − 92%, M.P.- 119–120 °C, ^{1}H NMR (500 MHz, DMSO-d_6) δ 10.50 (s, 1H, amide NH), 8.48 (s, 1H, phenyl C_2), 8.20 (d, *J* = 7.5 Hz, 1H, chlorophenyl C_3), 8.16 (d, *J* = 8 Hz, 1H, phenyl C_6), 8.08 (d, *J* = 15.5 Hz, 1H, β = CH), 8.02 (d, *J* = 7.5 Hz, 2H, benzamide C_2, C_6), 7.98 (d, *J* = 7.5 Hz, 1H, benzamide C_4), 7.95 (d, *J* = 15.5 Hz, 1H, α = CH), 7.63–7.54 (m, 5H, benzamide C_3, C_5, phenyl C_4, C_5, chlorophenyl C_6), 7.51–7.45 (m, 2H, chlorophenyl C_4, C_5). ^{13}C NMR (125 MHz, DMSO-d_6) δ 189.41 (-C═O, acryloyl), 166.24 (-C═O, amide), 140.23 (β = CH), 139.15 (phenyl C_3), 138.20 (phenyl C_1), 135.06 (chlorophenyl C_2), 134.83 (benzamide C_1), 132.75 (chlorophenyl C_1), 132.53 (phenyl C_6), 132.25 (benzamide C_4), 130.55 (chlorophenyl C_3), 129.68 (chlorophenyl C_4), 129.01 (chlorophenyl C_6), 128.91 (benzamide C_3, C_5), 128.22 (chlorophenyl C_5), 128.18 (benzamide C_2, C_6), 125.63 (phenyl C_5), 125.38 (phenyl C_4), 124.63 (α = CH), 120.60 (Phenyl C_2); MS (ESI +): *m/z* calculated for $C_{22}H_{16}ClNO_2$: 361.83, found – 362.05 (M +) 363.7 (M + 2).

4.1.3.4. N-(3-(3-(2,4-dichlorophenyl)acryloyl)phenyl)benzamide ***(26)***. Off white solid, yield − 94%, M.P.- 126–127 °C, ^{1}H NMR (500 MHz, DMSO-d_6) δ 10.49 (s, 1H, amide NH), 8.47 (t, *J* = 2 Hz, 1H, phenyl C_2), 8.22 (d, *J* = 8.5 Hz, 1H, β = CH), 8.15–8.13 (dd, *J* = 8 Hz, 1.5 Hz, 1H, phenyl C_6), 8.01–7.99 (m, 2H, benzamide C_2, C_6), 7.97–7.96 (m, 3H, phenyl C_4, benzamide C_4, α = CH), 7.74 (d, *J* = 2 Hz, 1H, dichlorophenyl C_5), 7.62–7.53 (m, 5H, benzamide C_3, C_5, phenyl C_5, dichlorophenyl C_3, C_6). ^{13}C NMR (125 MHz, DMSO-d_6) δ 188.77 (-C═O, acryloyl), 165.75 (-C═O, amide), 139.77 (β = CH), 137.62 (phenyl C_3), 137.40 (phenyl C_1), 135.67 (dichlorophenyl C_2), 135.15 (benzamide C_1), 134.57 (phenyl C_5), 131.77 (benzamide C_4), 131.35 (dichlorophenyl C_1), 129.78 (dichlorophenyl C_6), 129.53 (dichlorophenyl C_3), 129.18 (dichlorophenyl C_5), 128.43 (benzamide C_3, C_5), 127.97 (phenyl C_6), 127.70 (benzamide C_2, C_6), 125.41 (dichlorophenyl C_4), 125.24 (phenyl C4), 124.21(α = CH), 120.12 (phenyl C_2); MS (ESI +): *m/z* calculated for $C_{22}H_{15}Cl_2N_2O_2$: 396.27, found – 396.5 (M +), 398.6 (M + 2).

4.1.3.5. N-(3-(3-(4-bromophenyl)acryloyl)phenyl)benzamide ***(27)***. Whitish brown solid, yield − 92%, M.P.- 105–106 °C, ^{1}H NMR (500 MHz, DMSO-d_6) δ 10.49 (s, 1H, amide NH), 8.47 (t, *J* = 2 Hz, 1H, phenyl C_2), 8.15 (dd, *J* = 8 Hz, 1.5 Hz, 1H, phenyl C_6), 8.02 (s, 1H, benzamide C_2), 8.01 (s, 1H, benzamide C_6), 7.96 (d, *J* = 8 Hz, 1H, benzamide C_4), 7.93 (d, *J* = 15.5 Hz, 1H, β = CH), 7.86 (d, *J* = 8.5 Hz, 2H,bromophenyl C_3, C_5), 7.76 (d, *J* = 15.5 Hz, 1H, α = CH), 7.68 (d, *J* = 8.5 Hz, 2H, bromophenyl C_2, C_6), 7.64–7.54 (m, 4H, phenyl C_4, C_5, benzamide C_3, C_5). ^{13}C NMR (125 MHz, DMSO-d_6) δ 189.52 (-C═O, acryloyl), 166.21 (-C═O, amide), 143.22 (β = CH), 140.18 (phenyl C_3), 138.40 (phenyl C_1), 135.07 (benzamide C_1), 134.42 (beomophenyl C_1), 132.40 (bromophenyl C_3, C_5), 132.24 (phenyl C_5), 131.21 (benzamide C_3, C_6), 129.63 (benzamide C_4), 128.91 (bromophenyl C_2, C_6), 128.18 (benzamide C_2, C_6), 125.47 (phenyl C_6), 124.55 (phenyl C_4), 124.51 (bromophenyl C_4), 123.41 (α = CH), 120.58 (Phenyl C_2); MS (ESI +): *m/z* calculated for $C_{22}H_{16}NO_2$: 406.28, found – 405.9 (M +) 407.9 (M + 2).

4.1.3.6. N-(3-(3-(3-bromophenyl)acryloyl)phenyl)benzamide ***(28)***. Whitish brown solid, yield − 94%, M.P.- 109–110 °C, ^{1}H NMR (500 MHz, DMSO-d_6) δ 10.47 (s, 1H, amide NH), 8.46 (t, *J* = 2 Hz, 1H, phenyl C_2), 8.19 (s, 1H, bromophenyl C_2), 8.15–8.13 (dd, *J* = 8 Hz, 1.5 Hz, 1H, phenyl C_6), 8.01–7.94 (m, 4H, benzamide C_2, C_6, β = CH, benzamide C_4), 7.87 (d, *J* = 8 Hz, 1H, phenyl C_4), 7.75 (d, *J* = 15.5 Hz, 1H, α = CH), 7.65–7.54 (m, 5H, benzamide C_3, C_5, bromophenyl C_4, C_5, C_6), 7.44 (t, *J* = 8 Hz, 1H, bromophenyl C_5). ^{13}C NMR (125 MHz, DMSO-d_6) δ 189.00 (-C═O, acryloyl), 165.72 (-C═O, amide), 142.31 (β = CH), 139.68 (phenyl C_3), 137.83 (bromophenyl C_1), 137.16 (phenyl C_1), 134.58 (benzamide C_1), 133.07(phenyl C_5), 131.75 (bromophenyl C_2), 130.96 (benzamide C_4), 130.82 (bromophenyl C_4), 129.12 (bromophenyl C_5), 128.42 (benzamide C_3, C_5), 128.12 (bromophenyl C_6), 127.69 (benzamide C_2, C_6), 125.08 (phenyl C_6), 124.20 (phenyl C_4), 123.66 (bromophenyl C_3), 122.39 (α = CH), 120.13 (phenyl C_2); MS (ESI +): *m/z* calculated for $C_{22}H_{16}NO_2$: 406.28, found – 405.9 (M +) 407.9 (M + 2).

4.1.3.7. N-(3-(3-(4-fluorophenyl)acryloyl)phenyl)benzamide ***(29)***. White solid, yield- 96%, M.P.- 126–127 °C, ^{1}H NMR (500 MHz, DMSO-d_6) δ 10.50 (s, 1H, amide NH), 8.47 (s, 1H, phenyl C_2), 8.15 (d, *J* = 8 Hz, 1H, phenyl C_6), 8.02–7.95 (m, 5H, benzamide C_2, C_6, β = CH, fluorophenyl C_2, C_6), 7.87–7.76 (m, 2H, α = CH, benzamide C_4), 7.63–7.54 (m, 4H, benzamide C_3, C_5, phenyl C_4, C_5), 7.33 (t, *J* = 9 Hz, fluorophenyl C_3, C_5). ^{13}C NMR (125 MHz, DMSO-d_6) δ 189.52 (-C═O, acryloyl), 166.21 (-C═O, amide), 164.92 (fluorophenyl C_4), 143.39 (β = CH), 140.17 (phenyl C_3), 138.49 (phenyl C_1), 135.07 (benzamide C_1), 132.24 (phenyl C_5), 131.72 (benzamide C_4), 131.65(fluorophenyl C_1), 129.61 (fluorophenyl C_2, C_6), 128.91 (benzamide C_3, C_5), 128.18 (benzamide C_2, C_6), 125.38 (phenyl C_6), 124.51 (phenyl C_4), 122.51(α = CH), 120.56 (phenyl C_2), 116.54 (fluorophenyl C_3), 116.37 (fluorophenyl C_5); MS (ESI +): *m/z* calculated for $C_{22}H_{16}FNO_2$: 345.37, found – 346.52 (M + 1).

4.1.3.8. N-(3-(3-(3-fluorophenyl)acryloyl)phenyl)benzamide ***(30)***. White Solid, yield − 91%, M.P.- 128–129 °C, ^{1}H NMR (500 MHz, DMSO-d_6) δ 10.49 (s, 1H, amide NH), 8.47 (t, *J* = 2 Hz, 1H, phenyl C_2), 8.16–8.14 (m, *J* = 8, 2, 1 Hz, phenyl C_6), 8.02–7.95 (m, 4H, benzamide C_2, C_6, benzamide C_4,β = CH), 7.86–7.83 (dt, *J* = 10, 2 Hz, 1H, phenyl C_5), 7.79 (d, *J* = 15.5 Hz, 1H, α = CH), 7.72 (d, *J* = 7.5 Hz, phenyl C_4), 7.64–7.49 (m, 5H, benzamide C_3, C_5, fluorophenyl C_2, C_4, C_5), 7.32–7.29 (td, *J* = 8.5, 2 Hz, 1H, fluorophenyl C_5). ^{13}C NMR (125 MHz, DMSO-d_6) δ 189.54 (-C═O, acryloyl), 166.21 (-C═O, amide), 163.95 (fluorophenyl C_3), 143.13 (β = CH), 140.19 (phenyl C_3), 138.32 (fluorophenyl C_1), 137.73 (phenyl C_1), 135.06 (benzamide C_1), 132.25 (phenyl C_5), 131.41 (benzamide C_4), 131.34 (fluorophenyl C_5), 129.64 (phenyl C_6), 128.92 (benzamide C_3, C_5), 128.18 (benzamide C_2, C_6), 125.96 (fluorophenyl C_5), 125.55 (fluorophenyl C_6), 124.66 (phenyl C_4), 124.08 (α = CH), 120.60 (phenyl C_2), 117.88 (fluorophenyl C_4), 115.27 (fluorophenyl C_2); MS (ESI-): *m/z* calculated for $C_{22}H_{16}FNO_2$: 345.37, found – 344.3 (M-1).

4.1.3.9. N-(3-(3-(4-methoxyphenyl)acryloyl)phenyl)benzamide ***(31)***. Off white solid, yield- 91%, M.P.- 125–126 °C, ^{1}H NMR (500 MHz, DMSO-d_6) δ 10.48 (s, 1H, amide NH), 8.45 (s, 1H, phenyl C_2), 8.14 (dd, *J* = 8 Hz,1.5 Hz, 1H, β = CH), 8.02 (s,1H, benzamide C_2), 8.01 (s, 1H, benzamide C_6), 7.93 (d, *J* = 8 Hz, 1H, α = CH), 7.86 (d, *J* = 8.5 Hz, 2H, methoxyphenyl C_2, C_6), 7.75 (d, *J* = 2 Hz, 2H, phenyl C_4, C_5), 7.63–7.54 (m, 4H, benzamide C_3,C_6,C_4, Phenyl C_6), 7.04 (d, *J* = 9 Hz, 2H, methoxyphenyl C_3, C_5), 3.83 (s, 3H, -OMe). ^{13}C NMR (125 MHz, DMSO-d_6) δ 189.44 (-C═O, acryloyl), 166.19 (-C═O, amide), 161.91 (methoxyphenyl C_4), 144.65 (β = CH), 140.11 (phenyl C_3), 138.81 (phenyl C_1), 135.10 (benzamide C_1), 132.23 (phenyl C_5), 131.23 (benzamide C_4), 129.56 (benzamide C_3, C_5), 128.91 (methoxyphenyl C_2, C_6), 128.18 (benzamide C_2, C_6), 127.73(methoxyphenyl C_1), 125.12 (phenyl C_6), 124.34 (phenyl C_4), 120.49 (α = CH), 120.07 (phenyl C_2), 114.94 (methoxyphenyl C_3, C_5), 55.87 (-OMe); MS (ESI +): *m/z* calculated for $C_{23}H_{19}NO_3$: 357.41, found – 358.1 (M + 1), 359.2 (M + 2).

4.1.3.10. N-(3-(3-(3-methoxyphenyl)acryloyl)phenyl)benzamide ***(32)***. White solid, yield − 93%, M.P.- 127–128 °C, ^{1}H NMR (500 MHz, DMSO-d_6) δ 10.48 (s, 1H, amide NH), 8.47 (t, J = 2 Hz, 1H, phenyl C_2), 8.16–8.14 (m, J = 8 Hz, 1.5 Hz, 1H, phenyl C_6), 8.02 (m, 2H, benzamide C_2, C_6), 7.97–7.96 (dt, 1H, benzamide C_4), 7.90–7.87 (d, J = 15.5 Hz, 1H, β = CH), 7.77–7.74 (d, J = 16 Hz, α = CH), 7.64–7.54 (m, 4H, benzamide C_3, C_5, phenyl C_4, C_5) 7.48–7.37 (m, 2H, methoxyphenyl C_2,C_6), 7.40 (t, J = 8 Hz, methoxyphenyl C_5), 7.06–7.04 (m, J = 1H, methoxyphenyl C_4), 3.84 (s, 3H, -OMe). ^{13}C NMR (125 MHz, DMSO-d_6) δ 189.68 (-C═O, acryloyl), 166.21 (-C═O, amide), 160.16 (methoxyphenyl C_3), 144.62 β = CH), 140.17 (phenyl C_3), 138.51 (phenyl C_1), 136.53 (methoxyphenyl C_1), 135.09 (benzamide C_1), 132.23 (phenyl C_5), 130.46 (benzamide C_4), 129.61 (methoxyphenyl C_5), 128.91 (benzamide C_3, C_5), 128.18 (benzamide C_2, C_6), 125.38 (phenyl C_6), 124.54 (phenyl C_4), 122.95 (α = CH), 121.97 (methoxyphenyl C_6), 120.57 (phenyl C_2), 117.16 (methoxyphenyl C_4), 114.02 (methoxyphenyl C_2), 55.79 (-OMe); MS (ESI +): m/z calculated for $C_{23}H_{19}NO_3$: 357.41, found – 358.4 (M + 1) 359.2 (M + 2).

4.1.3.11. N-(3-(3-(3,4-dimethoxyphenyl)acryloyl)phenyl)benzamide ***(33)***. Off white solid, yield − 95%, M.P.- 122–123 °C, ^{1}H NMR (500 MHz, DMSO-d_6) δ 10.48 (s, 1H, amide NH), 8.43 (t, J = 2 Hz, 1H, phenyl C_2), 8.14–8.12 (dd, J = 8 Hz, 1.5 Hz, 1H, phenyl C_6), 8.02 (d, J = 7 Hz, 2H, benzamide C_2, C_6), 7.96 (d, J = 8 Hz, 1H, β = CH), 7.80 – 7.72 (m, 2H,α = CH, benzamide C_4), 7.64–7.54 (m, 5H, benzamide C_3, C_5, phenyl C_4, C_5, dimethoxyphenyl C_2), 7.42–7.40 (dd, J = 8.5 Hz, 2 Hz, dimethoxyphenyl C_5), 7.05 (d, J = 8.5 Hz, 1Hdimethoxyphenyl C_6), 3.87 (s, 3H, -OMe C_3), 3.83 (s, 3H, -OMe C_4). ^{13}C NMR (125 MHz, DMSO-d_6) δ 189.54 (-C═O, acryloyl), 166.20 (-C═O, amide), 151.82 (dimethoxyphenyl C_3), 149.50 (dimethoxyphenyl C_4), 145.21 (β = CH), 140.10 (phenyl C_3), 138.87 (phenyl C_1), 135.09 (benzamide C_1), 132.24 (phenyl C_5), 129.52 (benzamide C_4), 128.91 (benzamide C_3, C_5), 128.18 (benzamide C_2, C_6), 127.93 (phenyl C_6), 125.17 (dimethoxyphenyl C_1), 124.47 (phenyl C_4), 124.32 (dimethoxyphenyl C_6), 120.46 (α = CH), 120.23 (phenyl C_2), 112.08 (dimethoxyphenyl C_5), 111.36 (dimethoxyphenyl C_2), 56.22 (-OMe), 56.09 (-OMe); MS (ESI +): m/z calculated for $C_{24}H_{21}NO_4$: 387.44, found – 388.08 (M + 1).

4.1.3.12. N-(3-(3-(4-(trifluoromethyl)phenyl)acryloyl)phenyl)benzamide ***(34)***. White Solid, yield − 97%, M.P.- 144–145 °C, ^{1}H NMR (500 MHz, DMSO-d_6) δ 10.50 (s, 1H, amide NH), 8.49 (s, 1H, phenyl C_2), 8.16 (d, J = 8 Hz, 1H, phenyl C_6), 8.12 (d, J = 8 Hz, 2H, benzamide C_2, C_6), 8.03–7.98 (m, 4H, benzamide C_4, β = CH, phenyl C_4, phenyl C_5), 7.84–7.81 (m, 3H, α = CH, (trifluoromethyl)phenyl C_2, C_6), 7.63–7.54 (m, 4H, (trifluoromethyl)phenyl C_3, C_5, benzamide C_3, C_5). ^{13}C NMR (125 MHz, DMSO-d_6) δ 189.53 (-C═O, acryloyl), 166.23 (-C═O, amide), 142.56 (β = CH), 140.21 (phenyl C_3), 139.13 ((trifluoromethyl)phenyl C_1), 138.20 (phenyl C_1), 135.05 (benzamide C_1), 132.25 (phenyl C_5), 130.70 (benzamide C_4), 130.45 ((trifluoromethyl)phenyl C_4), 129.86 (-CF_3,), 129.67 (phenyl C_6), 128.91 (benzamide C_3, C_5), 128.18 (benzamide C_2, C_6), 126.21 ((trifluoromethyl)phenyl C_2), 126.18 ((trifluoromethyl)phenyl C_6), 125.62 ((trifluoromethyl)phenyl C_5), 125.26 ((trifluoromethyl)phenyl C_3), 124.67 (phenyl C_4), 123.43 (α = CH), 120.60 (phenyl C_2); MS (ESI +): m/z calculated for $C_{23}H_{16}F_3NO_2$: 395.38, found – 396.2 (M + 1).

4.1.3.13. N-(3-(3-(3-(trifluoromethyl)phenyl)acryloyl)phenyl)benzamide ***(35)***. White solid, yield − 96%, M.P.- 141–142 °C, ^{1}H NMR (500 MHz, DMSO-d_6) δ 10.50 (s, 1H, amide NH), 8.48 (s, 1H, phenyl C_2), 8.32 (s, 1H, phenyl C_6), 8.19–8.15 (dd, J = 14 Hz, 8 Hz, 2H, benzamide C_2, C_6), 8.08 (d, J = 16 Hz, 1H, β = CH), 8.02 (d, J = 7.5 Hz, 3H, benzamide C_3, C_5, phenyl C_5), 7.87 (d, J = 16 Hz, 1H, α = CH), 7.81 (d, J = 7.5 Hz, 1H, phenyl C_4), 7.71 (t, J = 8 Hz, 1H, (trifluoromethyl) phenyl) C_5), 7.63–7.54 (m, 4H, benzamide C_4, (trifluoromethyl)phenyl C_2, C4, C6). ^{13}C NMR (125 MHz, DMSO-d_6) δ 189.55 (-C═O, acryloyl), 166.23 (-C═O, amide), 142.75 (β = CH), 140.18 (phenyl C_3), 138.27 (phenyl C_1), 136.30 ((trifluoromethyl)phenyl) C_1), 135.06 (benzamide C_1), 133.21 (phenyl C_5), 132.25 (benzamide C_4), 130.44 ((trifluoromethyl)phenyl) C_6), 130.21 ((trifluoromethyl)phenyl) C_3), 129.62 (phenyl C_6), 128.91 (benzamide C_3, C_5, (trifluoromethyl) phenyl) C_2), 128.18 (benzamide C_2, C_6), 127.19 (-CF_3), 125.63 ((trifluoromethyl)phenyl) C_4), 124.78 (phenyl C_4), 124.57 ((trifluoromethyl)phenyl) C_2), 123.44 (α = CH), 120.60 (phenyl C_2); MS (ESI +): m/z calculated for $C_{23}H_{16}F_3NO_2$: 395.38, found – 396.5 (M + 1).

4.1.3.14. N-(3-(3-(4-(trifluoromethoxy)phenyl)acryloyl)phenyl) benzamide ***(36)***. White solid, yield − 92%, M.P.- 136–137 °C, ^{1}H NMR (500 MHz, DMSO-d_6) δ 10.49 (s, 1H, amide NH), 8.48 – 8.47 (t, J = 2 Hz, 1H, phenyl C_2), 8.15–8.14 (dd, J = 1, 1.5 Hz, 1H, phenyl C_6), 8.06–8.00 (m, 4H, benzamide C_2, C_6, phenyl C_4, phenyl C_5), 7.98–7.96 (d, J = 8 Hz, 1H, benzamide C_4), 7.94–7.91 (d, J = 16 Hz, 1H, β = CH), 7.81–7.78 (d, J = 15.5 Hz, 1H, α = CH), 7.64–7.54 (m, 4H, (trifluoromethoxy)phenyl C_2, C_3, C_5, C_6), 7.48–7.46 (d, J = 8 Hz, 2H, benzamide C_3, C_5). ^{13}C NMR (125 MHz, DMSO-d_6) δ 194.28 (-C═O, acryloyl), 170.95 (-C═O, amide), 154.83 ((trifluoromethoxy)phenyl C_4), 147.56 (β = CH), 144.96 ((trifluoromethoxy)phenyl C_3), 143.10 ((trifluoromethoxy)phenyl C_5), 139.82 (phenyl C_3), 139.22 (phenyl C_1), 137.00 (benzamide C_4), 136.06 (benzamide C_1), 134.37 (phenyl C_5), 133.66 ((trifluoromethoxy)phenyl C_2), 132.94 ((trifluoromethoxy)phenyl C_6), 130.27 (-OCF_3), 129.34 (phenyl C_6), 128.57 (α = CH), 126.59 (benzamide C_5), 126.52 (benzamide C_3), 126.25 (phenyl C_2), 125.36 (benzamide C_2), 125.25 (benzamide C_6), 124.21 (phenyl C_4); MS (ESI +): m/z calculated for $C_{23}H_{16}F_3NO_3$: 411.38, found – 412.2 (M + 1).

4.1.3.15. N-(3-(3-(4-cyanophenyl)acryloyl)phenyl)benzamide ***(37)***. Off white solid, yield − 92%, M.P.- 122–123 °C, ^{1}H NMR (500 MHz, DMSO-d_6) δ 10.48 (s, 1H, amide NH), 8.47 (t, J = 1.5 Hz, 1H, phenyl C_2), 8.15–8.13 (dd, J = 8 Hz, 1.5 Hz, 1H, phenyl C_6), 8.09 (d, J = 8 Hz, 2H, benzamide C_2, C_6), 8.04–7.97 (m, 4H, β = CH, benzamide C_4, cyanophenyl C_3, C_5), 7.94 (d, J = 8.5 Hz, 2H, benzamide C_3, C_5), 7.81 (d, J = 16 Hz, 1H, α = CH), 7.63–7.53 (m, 4H, phenyl C_4, C_5, cyanophenyl C_2, C_6). ^{13}C NMR (125 MHz, DMSO-d_6) δ 189.03 (C═O, acryloyl), 165.74 (-C═O, amide), 141.83 (β = CH), 139.73 (cyanophenyl C_1), 139.20 (phenyl C_3), 137.68 (phenyl C_1), 134.56 (benzamide C_1), 132.73 (cyanophenyl C_3,C_5), 131.76 (phenyl C_5), 129.38 (benzamide C_3, C_5), 129.19 (benzamide C_4), 128.42 (cyanophenyl C_2,C_6), 127.69 (benzamide C_2, C_6), 125.43 (phenyl C_6), 125.20 (phenyl C_4), 124.22(α = CH), 120.14 (phenyl C_2), 118.60 (–CN), 112.35 (cyanophenyl C_4); MS (ESI +): m/z calculated for $C_{23}H_{16}N_2O_2$: 352.39, found – 353.0 (M + 1).

4.1.3.16. N-(3-(3-(3-cyanophenyl)acryloyl)phenyl)benzamide ***(38)***. Off white solid, yield − 93%, M.P.- 115–116 °C, ^{1}H NMR (500 MHz, DMSO-d_6) δ 10.49 (s, 1H, amide NH), 8.48 (t, J = 2 Hz, 2H, phenyl C_2, cyanophenyl C_2), 8.20 (d, J = 8 Hz, 1H, cyanophenyl C_4), 8.16–8.14 (dd, J = 8 Hz, 1 Hz, 1H, phenyl C_6), 8.07 (d, J = 16 Hz, 1H, β = CH), 8.02–8.01 (m, 3H, benzamide C_2, C_6, cyanophenyl C_6), 7.91–7.89 (dt, 1H, benzamide C_4), 7.80 (d, J = 16 Hz, 1H,α = CH), 7.69 (t, J = 8 Hz, 1H, phenyl C_5), 7.64–7.54 (m, 4H, benzamide C_3, C_5, cyanophenyl C_5, phenyl C_4). ^{13}C NMR (125 MHz, DMSO-d_6) δ 189.43 (-C═O, acryloyl), 166.21 (-C═O, amide), 142.09 (β = CH), 140.21 (phenyl C_3), 138.23 (phenyl C_1), 136.45 (cyanophenyl C_1), 135.05 (benzamide C_1), 134.04 (phenyl C_5), 134.00 (cyanophenyl C_6), 132.41 (benzamide C_4), 132.25 (cyanophenyl C_4), 130.60 (cyanophenyl C_2), 129.63 (cyanophenyl C_5), 128.91 (benzamide C_3, C_5), 128.18 (benzamide C_2, C_6), 125.70 (phenyl C_6), 124.89 (phenyl C_4), 124.75 (α = CH), 120.62 (phenyl C_2), 118.93 (–CN), 112.65 (cyanophenyl C_3); MS (ESI +): m/z calculated for $C_{23}H_{16}N_2O_2$: 352.39, found – 353.5 (M + 1).

*4.1.3.17. N-(3-(3-(p-tolyl)acryloyl)phenyl)benzamide**(39)***. White solid, yield − 89%, M.P.- 118–119 °C, ^{1}H NMR (500 MHz, DMSO-d_6) δ 10.47 (s, 1H, amide NH), 8.46 (t, J = 2 Hz, 1H, phenyl C_2), 8.15–8.13 (dd, J = 8 Hz, 1.5 Hz, 1H, phenyl C_6), 8.02 (d, J = 7 Hz, 2H, benzamide C_2, C_6), 7.94 (d, J = 7.5 Hz, 1H,benzamide C_4), 7.84–7.74 (m, 4H, β = CH, phenyl C4, C_5, α = CH), 7.63–7.54 (m, 4H, benzamide C_3, C_5, *p*-tolyl C_2, C_6), 7.30 (d, J = 8 Hz, 2H, *p*-tolyl C_3, C_5), 2.36 (–CH_3). ^{13}C NMR (125 MHz, DMSO-d_6) δ 189.57 (-C═O, acryloyl), 166.21 (-C═O, amide), 144.71 (β = CH), 141.28 (phenyl C_3), 140.15 (*p*-tolyl C_4), 138.64 (phenyl C_1), 135.10 (benzamide C_1), 132.39 (phenyl C_5), 132.23 (*p*-tolyl C_1), 130.07 (benzamide C_3, C_5), 129.60 (benzamide C_4), 129.33 (*p*-tolyl C_3, C_5), 128.91 (*p*-tolyl C_2, C_6), 128.18 (benzamide C_2, C_6), 125.26 (phenyl C_6), 124.40 (phenyl C_4), 121.55 (α = CH), 120.54 (phenyl C_2), 21.57 (–CH_3); MS (ESI +): *m/z* calculated for $C_{23}H_{19}NO_2$: 341.41, found – 342.5 (M + 1).

*4.1.3.18. N-(3-(3-(o-tolyl)acryloyl)phenyl)benzamide**(40)***. White solid, yield − 91%, M.P.- 132–133 °C, ^{1}H NMR (500 MHz, DMSO-d_6) δ 10.48 (s, 1H, amide NH), 8.48 (t, J = 2 Hz, phenyl C_2), 8.16–8.14 (dd, J = 8 Hz, 1 Hz, 1H, phenyl C_6), 8.03–8.00 (m, 3H, benzamide C_2, C_6, β = CH), 7.97 (d, J = 7.5 Hz, benzamide C_4), 7.94 (d, J = 8 Hz, phenyl C_5), 7.76 (d, J = 15.5 Hz, α = CH), 7.64–7.54 (m, 4H, *o*-tolyl C_5, C_6, benzamide C_3, C_5), 7.38–7.35 (m, 1H, phenyl C_4), 7.32–7.30 (m, 2H, *o*-tolyl C_3, C_4), 2.46 (s, 3H, –CH_3). ^{13}C NMR (125 MHz, DMSO-d_6) δ 189.66 (-C═O, acryloyl), 166.24 (-C═O, amide), 141.73 (β = CH), 140.18 (phenyl C_3), 138.52 (phenyl C_1), 135.11 (benzamide C_1), 133.76 (*o*-tolyl C_1), 132.23 (*o*-tolyl C_2), 131.32 (phenyl C_5), 130.92 (benzamide C_4), 129.65 (*o*-tolyl C_4, C_6), 128.91 (benzamide C_3, C_5), 128.18 (benzamide C_2, C_6), 127.25 (phenyl C_6), 126.90 (*o*-tolyl C_3), 125.31 (*o*-tolyl C_5), 124.42 (phenyl C_4), 123.58 (α = CH), 120.60 (phenyl C_2), 19.82 (–CH_3); MS (ESI +): *m/z* calculated for $C_{23}H_{19}NO_2$: 341.41,found – 342.5 (M + 1).

*4.1.3.19. N-(3-(3-(4-isopropylphenyl)acryloyl)phenyl)benzamide **(41)***. Pale yellow solid, yield − 98%, M.P.- 134–135 °C, ^{1}H NMR (500 MHz, DMSO-d_6) δ 10.49 (s, 1H, amide NH), 8.47 (s, 1H, phenyl C_2), 8.15 (d, J = 7.5 Hz, 1H, phenyl C_6), 8.02 (d, J = 7.5 Hz, 2H, benzamide C_2, C_6), 7.94 (d, J = 8 Hz, 1H, β = CH), 7.83–7.74 (m, 4H, benzamide C_3, C_4, C_5, phenyl C_4), 7.63–7.54 (m, 4H, Phenyl C_5, α = CH, , isopropylphenyl C_2, C_6), 7.34 (d, J = 7.5 Hz, isopropylphenyl C_3, C_5), 2.95–2.90 (m, 1H, isopropyl CH), 1.22 (d, J = 6.5 Hz, 6H, isopropyl –CH_3). ^{13}C NMR (125 MHz, DMSO-d_6) δ 189.61 (-C═O, acryloyl), 166.22 (-C═O, amide), 152.03 (isopropylphenyl C_4), 144.73 (β = CH), 140.15 (phenyl C_3), 138.63 (phenyl C_1), 135.08 (benzamide C_1), 132.79 (phenyl C_5), 132.24 (benzamide C_4), 129.61 (isopropylphenyl C_1), 129.46 (benzamide C_3, C_5), 128.91 (isopropylphenyl C_2, C_6), 128.18 (benzamide C_2, C_6), 127.43 (isopropylphenyl C_3, C_5), 125.26 (phenyl C_6), 124.40 (phenyl C_4), 121.65 (α = CH), 120.53 (phenyl C_2), 33.90 (isopropyl CH), 24.07 (isopropyl –CH_3); MS (ESI +): *m/z* calculated for $C_{22}H_{23}NO_2$: 369.46, found –370.6 (M + 1).

*4.1.3.20. N-(3-(3-(naphthalen-1-yl)acryloyl)phenyl)benzamide **(42)***. White solid, yield − 95%, M.P.- 121–122 °C, ^{1}H NMR (500 MHz, DMSO-d_6) δ 10.52 (s, 1H, amide NH), 8.61 (d, J = 15.5 Hz, 1H, β = CH), 8.55 (s, 1H, phenyl C_2), 8.33 (d, J = 8 Hz, 1H, naphthalen-1-yl C_4), 8.24 (d, J = 7.5 Hz, 1H, naphthalen-1-yl C_5), 8.19 (d, J = 8 Hz, 1H, naphthalen-1-yl C_8), 8.09 (d, J = 8 Hz, 1H, naphthalen-1-yl C_2), 8.03–7.93 (m, 5H, benzamide C_2, C_6, phenyl C_6, C_4,α = CH, phenyl C_6), 7.68–7.55 (m, 7H, benzamide C_3, C_4, C_5, naphthalen-1-yl C_7, C_3, C_6, phenyl C_4). ^{13}C NMR (125 MHz, DMSO-d_6) δ 189.53 (-C═O, acryloyl), 166.24 (-C═O, amide), 140.62 (phenyl C_3), 140.22 (phenyl C_1), 138.47 (β = CH), 135.10 (benzamide C_1), 133.86 (phenyl C_5), 132.25 (naphthalen-1-yl C_1), 131.86 (naphthalen-1-yl C_{10}), 131.67 (naphthalen-1-yl C_9), 131.39 (benzamide C_4), 129.70 (naphthalen-1-yl C_5), 129.28 (naphthalen-1-yl C_4), 128.92 (benzamide C_3, C_5), 128.20 (benzamide C_2, C_6), 127.77(phenyl C_6), 126.84 (naphthalen-1-yl C_3), 126.19 (naphthalen-1-yl C_6), 126.12 (naphthalen-1-yl C_7), 125.37 (naphthalen-1-yl C_8), 125.22 (naphthalen-1-yl C_2), 124.51 (phenyl C_4), 123.56 (α = CH), 120.65 (phenyl C_2); MS (ESI +): *m/z* calculated for $C_{26}H_{19}NO_2$: 377.44, found – 378.3 (M + 1).

4.1.4. General procedure for the synthesis of compounds 43–62

To a stirred solution of compounds **(23–42)** in ethanol (10 ml), hydrazine hydrate was added. The reaction mixture was refluxed for 2 h in oil bath and progress was monitored by TLC. After the completion of the reaction, solvent was evaporated and dried under reduced pressure. To this, DMSO and catalytic amount of iodine was added and heated up to 110 °C for 1 h. Then, cool the reaction mixture to room temperature and add ice cold saturated sodium thiosulphate solution to afford solid precipitate. The formed precipitate was filtered, washed with cold water and dried under vacuum pump to get corresponding product **43–62**.

*4.1.4.1. N-(3-(3-phenyl-1H-pyrazol-5-yl)phenyl)benzamide**(43)***. Pale brown solid, yield- 84%, M.P.- 194–195 °C, ^{1}H NMR (500 MHz, DMSO-d_6) δ 13.39 (s, 1H, pyrazole NH), 10.36 (s, 1H, amide NH), 8.30 (s, 1H, phenyl C_2), 8.01 (d, J = 10 Hz, 2H, phenyl C_2, C_6), 7.85 (s, 2H, benzamide C_2, C_6), 7.75 (s, 1H,benzamide C_4), 7.62–7.55 (m, 4H, benzamide C_3, C_5, phenyl C_3, C_5) 7.47 (m, 3H, phenyl C_4, C_5, C_6), 7.36 (s, 1H, phenyl C_4), 7.12 (s, 1H, pyrazole C_4). ^{13}C NMR (125 MHz, DMSO-d_6) δ 164.34 (-C═O, amide), 141.52 (pyrazole C_3, C_5), 135.24 (phenyl$_{(pyrazole\ C5)}$$C_1$), 132.05 (benzamide C_1,C_4), 131.52 (phenyl$_{(pyrazole\ C3)}$ C_1, phenyl$_{(pyrazole\ C5)}$ C_3), 129.27 (phenyl $_{(pyrazole\ C5)}$ C_5), 128.87 (benzamide C_3, C_5, Phenyl$_{(pyrazole\ C3)}$ C_4), 128.57 (Phenyl$_{(pyrazole\ C3)}$ C_3,C_6), 128.04 (benzamide C_2, C_6, phenyl$_{(pyrazole\ C3)}$$C_2$, C_6), 121.82 (phenyl$_{(pyrazole\ C5)}$ C_4, C_6), 117.98 (phenyl $_{(pyrazole\ C5)}$ C_2), 100.12 (pyrazole C_4); MS (ESI +): *m/z* calculated for $C_{22}H_{17}N_3O$: 339.40, found 340.45 (M + 1).

*4.1.4.2. N-(3-(3-(4-chlorophenyl)-1H-pyrazol-5-yl)phenyl)benzamide **(44)***. White solid, yield- 90%, M.P.- 236–237 °C, ^{1}H NMR (500 MHz, DMSO-d_6) δ 13.46 (s, 1H, pyrazole NH), 10.37 (s, 1H, amide NH), 8.33–8.25 (d, J = 41 Hz, 1H, phenyl C_2), 8.01 (d, J = 7 Hz, 2H, benzamide C_2, C_6), 7.88 (bs, 2H, chlorophenyl C_2, C_6), 7.73 (bs, 1H, chlorophenyl C_3), 7.63–7.52 (m, 7H, benzamide C_3, C_4, & C_5 phenyl C_4, C_5, C_6, chlorophenyl C_5), 7.16 (s, 1H, pyrazole C_4). ^{13}C NMR (125 MHz, DMSO-d_6) δ 166.06 (-C═O, amide), 140.11 (pyrazole C_3, C_5), 135.29 (phenyl C_1), 132.12 (benzamide C_1), 129.50 (phenyl C_3), 128.90 (benzamide C_3, C_5, phenyl C_5), 128.15 (benzamide C_4, chlorophenyl C_1, C_3, C_5), 127.30 (benzamide C_2, C_6, chlorophenyl C_2, C_6), 121.18 (chlorophenyl C_4, phenyl C_4), 118.31 (Phenyl C_6), 117.73 (Phenyl C_2), 100.37 (pyrazole C_4); MS (ESI +): *m/z* calculated for $C_{22}H_{16}ClN_3O$: 373.84, found –374.0 (M +), 375.9 (M + 2).

*4.1.4.3. N-(3-(3-(2-chlorophenyl)-1H-pyrazol-5-yl)phenyl)benzamide **(45)***. Off white Solid, yield- 70%, M.P.- 191–192 °C, ^{1}H NMR (500 MHz, DMSO-d_6) δ 13.47 (d, J = 125.0 Hz, 1H, pyrazole NH), 10.36 (s, 1H, amide NH), 8.26 (s, 1H, phenyl C_2), 8.01 (d, J = 10 Hz, 2H, benzamide C_2, C_6), 7.81 (d, J = 10 Hz, 2H, benzamide C_3, C_5), 7.63–7.54 (m, 5H, chlorophenyl C_6 phenyl C_4, C_5, C_6, benzamide C_4), 7.45 (m, 3H, chlorophenyl C_3, C_4, C_5), 7.08 (s, 1H, pyrazole C_4). ^{13}C NMR (126 MHz, DMSO) δ 166.10 (-C═O, amide), 140.12 (pyrazole C_3, C_5), 135.32 (phenyl C_1), 132.11 (benzamide C_1), 131.48 (phenyl C_3), 130.86 (chlorophenyl C_2, C_3), 129.61 (chlorophenyl C_1), 128.88 (benzamide C_3, C_5, C4, chlorophenyl C_6), 128.15 (benzamide C_2, C_6, chlorophenyl C_4, C_5), 127.92 (Phenyl C_5), 121.08 (phenyl C_4, C_6), 117.92 (Phenyl C_2), 103.64 (pyrazole-C_4); MS (ESI +): *m/z* calculated for $C_{22}H_{16}ClN_3O$: 373.84, found – 374.1067 (M +), 376.1049 (M + 2).

*4.1.4.4. N-(3-(3-(2,4-dichlorophenyl)-1H-pyrazol-5-yl)phenyl)benzamide **(46)***. Off white solid, yield- 78%, M.P.- 195–196 °C, ^{1}H NMR

(500 MHz, DMSO-d_6) δ 13.69 (s, 1H, pyrazole NH), 10.36 (s, 1H, amide NH), 8.23 (s, 1H, phenyl C_2), 8.01–7.99 (m, 2H, benzamide C_2, C_6), 7.91–7.75 (m, 3H, phenyl C_4, C6, 2,4-dichlorophenyl C_6), 7.63–7.46 (m, 6H, benzamide C_3, C_4, C_5, 2,4-dichlorophenyl C_3, C_5, phenyl C_5), 7.10 (s, 1H, pyrazole C_4). ^{13}C NMR (125 MHz, DMSO-d_6) δ 166.12 (-C═O, amide), 140.14 (pyrazole C_3, C_5), 135.27 (phenyl C_1), 132.33 (2,4-dichlorophenyl C_4), 132.14 (benzamide C_1, 2,4-dichlorophenyl C_2), 131.98 (benzamide C_4, phenyl C_3), 130.21 (2,4-dichlorophenyl C_6), 128.89 (benzamide C_3, C_5, 2,4-dichlorophenyl C_3, phenyl C_5), 128.13 (benzamide C_2, C_6, 2,4-dichlorophenyl C_1, C_5), 121.10 (phenyl C_4, C_6) , 118.04 (phenyl C_2), 103.70 (pyrazole-C_4); MS (ESI +): *m/z* calculated for $C_{22}H_{15}Cl_2N_3O$: 408.28, found − 408.0 (M +), 409.9 (M + 2).

4.1.4.5. N-(3-(3-(4-bromophenyl)-1H-pyrazol-5-yl)phenyl)benzamide ***(47)***. Pale brown solid, yield- 84%, M.P.- 261–261 °C, ^{1}H NMR (500 MHz, DMSO-d_6) δ 13.46 (s, 1H, pyrazole NH), 10.38 (s, 1H, amide NH), 8.34 (s, 1H, phenyl C_2), 8.02 (d, J = 7 Hz, 2H, benzamide C_2, C_6), 7.84 (m, 2H, bromophenyl C_2, C_6), 7.69–7.54 (m, 7H, benzamide C_3, C_4, & C_5 phenyl C_4, C_5, C_6 & bromophenyl C_5), 7.46 (m, 1H, bromophenyl C_3), 7.17 (s, 1H, pyrazole C_4). ^{13}C NMR (125 MHz, DMSO-d_6) δ 166.07 (-C═O, amide), 140.02 (pyrazole C_3, C_5), 135.29 (phenyl C_1), 132.11 (benzamide C_1), 129.82 (phenyl C_3), 128.90 (benzamide C_3, C_5 & phenyl C_5), 128.14 (benzamide C_4 & bromophenyl C_1, C_3, C_5), 127.60 (benzamide C_2, C_6 & bromophenyl C_2, C_6), 121.18 (bromophenyl C_4 & phenyl C_4), 118.33 (Phenyl C_6), 117.74 (Phenyl C_2), 100.37 (pyrazole-C_4); MS (ESI +): *m/z* calculated for $C_{22}H_{16}BrN_3O$: 418.29, found − 417.9 (M +), 419.9 (M + 2).

4.1.4.6. N-(3-(3-(3-bromophenyl)-1H-pyrazol-5-yl)phenyl)benzamide ***(48)***. Pale brown solid, yield- 88%, M.P.- 249–250 °C, ^{1}H NMR (500 MHz, DMSO-d_6) δ 13.51 (d, J = 16.5 Hz, 1H, pyrazole NH), 10.38 (d, J = 22.5 Hz, 1H, amide NH), 8.35 (d, 1H, J = 50 Hz, phenyl C_2), 8.09 (s, 1H, bromophenyl C_2), 8.02 (d, J = 7 Hz, 2H, benzamide C_2, C_6), 7.89 (d, J = 17 Hz, 1H, bromophenyl C_6), 7.76 (d, J = 23.5 Hz, 1H, bromophenyl C_4), 7.63–7.43 (m, 7H, benzamide C_3, C_4, & C_5 phenyl C_4, C_5, C_6 & bromophenyl C_5), 7.25 (d, J = 26.5 Hz, 1H, pyrazole C_4). ^{13}C NMR (125 MHz, DMSO-d_6) δ 166.06 (-C═O, amide), 140.12 (pyrazole C_3, C_5) 135.30 (phenyl C_1), 132.13 (benzamide C_1), 131.38 (phenyl C_3), 128.90 (benzamide C_3, C_5 & bromophenyl C_1), 128.14 (benzamide C_4 & bromophenyl C_2, C_4, C_5 & phenyl C_5), 128.05 (benzamide C_2, C_6 & bromophenyl C_6), 124.55 (bromophenyl C_3, phenyl C_4), 121.22 (phenyl C_6), 118.38 (phenyl C_2), 100.93 (pyrazole-C_4); MS (ESI +): *m/z* calculated for $C_{22}H_{16}BrN_3O$: 418.29, found − 417.8 (M +), 419.9 (M + 2).

4.1.4.7. N-(3-(3-(4-fluorophenyl)-1H-pyrazol-5-yl)phenyl)benzamide ***(49)***. White solid, yield- 79%, M.P.- 192–193 °C, ^{1}H NMR (500 MHz, DMSO-d_6) δ 13.37 (s, 1H, pyrazole NH), 10.35 (s, 1H, amide NH), 8.31 (m, 1H, phenyl C_2), 8.02 (d, J = 7 Hz, 2H, benzamide C_2, C_6), 7.90 (bs, 2H, fluorophenyl C_2, C_6), 7.74 (bs, 1H, phenyl C_5), 7.63–7.54 (m, 4H, benzamide C_3,C_5, phenyl C_4, C_6), 7.44 (bs, 1H, benzamide C_4), 7.30 (bs, 2H, fluorophenyl C_3, C_5), 7.10 (s, 1H, pyrazole C_4). ^{13}C NMR (125 MHz, DMSO-d_6) δ 166.07 (C═O, amide), 161.29 (fluorophenyl C_4), 140.04 (pyrazole C_3, C_5), 135.32 (phenyl C_1), 132.10 (benzamide C_1), 128.89 (benzamide C_3, C_4 C_5,), 128.14 (benzamide C_2, C_6,fluorophenyl C_5), 127.64 (fluorophenyl C_1), 121.19 (phenyl C_4), 116.36 (phenyl C_2), 100.09 (pyrazole-C_4); MS (ESI +): *m/z* calculated for $C_{22}H_{16}FN_3O$: 357.39, found – 356.3 (M + 1).

4.1.4.8. N-(3-(3-(3-fluorophenyl)-1H-pyrazol-5-yl)phenyl)benzamide ***(50)***. White solid, yield- 75%, M.P.- 240–241 °C, ^{1}H NMR (500 MHz, DMSO-d_6) δ 13.49 (s, 1H, pyrazole NH), 10.37 (s, 1H, amide NH), 8.30 (s, 1H, phenyl C_2), 8.03(d, J = 7 Hz, 2H, benzamide C_2, C_6), 7.74–7.69 (m, 3H, phenyl C_4, C_5, C_6), 7.63–7.46 (m, 6H, benzamide C_4, C_3, C_5, fluorophenyl C_2, C_5, C_6), 7.20 (bs, 2H, pyrazole C_4, fluorophenyl C_4). ^{13}C NMR (125 MHz, DMSO-d_6) δ 166.09 (C═O, amide), 164.06 (fluorophenyl C_3), 162.13 (fluorophenyl C_1), 140.08 (pyrazole C_3, C_5), 135.31 (phenyl C_1), 132.11 (benzamide C_1, phenyl C_3), 129.57 (phenyl C_5), 128.89 (benzamide C_3, C_4 C_5,), 128.14 (benzamide C_2, C_6, fluorophenyl C_5), 121.68 (phenyl C_4, fluorophenyl C_6), 121.23 (phenyl C_2, C_6), 112.28 (fluorophenyl C_2), 112.11 (fluorophenyl C_4), 100.74 (pyrazole-C_4); MS (ESI +):*m/z* calculated for $C_{22}H_{16}FN_3O$: 357.39, found – 356.3 (M + 1).

4.1.4.9. N-(3-(3-(4-methoxyphenyl)-1H-pyrazol-5-yl)phenyl)benzamide ***(51)***. Pale yellow, yield- 89%, M.P.- 207–208 °C, ^{1}H NMR (500 MHz, DMSO-d_6) δ 13.20 (s, 1H, pyrazole NH), 10.34 (s, 1H, amide NH), 8.29 (s, 1H, phenyl C_2), 8.01 (d, J = 8.5 Hz, 2H, benzamide C_2, C_6), 7.79 (m, 3H, phenyl C_4, C_5, C_6), 7.63–7.54 (m, 4H, benzamide C_3, C_5 & methoxyphenyl C_2, C_6), 7.44 (t, 1H, J = 7.5 Hz, benzamide C_4), 7.04 (d, J = 9 Hz, 2H, methoxy phenyl C_3, C_5), 7.01 (s, 1H, pyrazoleC_4), 3.81 (s, 3H, -OMe). ^{13}C NMR (125 MHz, DMSO-d_6) δ 166.03 (-C═O, amide), 160.86 (methoxyphenyl C_4), 140.00 (pyrazole C_3, C_5), 135.35 (phenyl C_1), 132.08 (benzamide C_1), 128.87 (benzamide C_3, C_5 & methoxyphenyl C_2, C_6), 128.14 (benzamide C_2, C_6), 126.97 (methoxyphenyl C_1 & Phenyl C_4, C_6), 121.15 (Phenyl C_2), 114.76 (methoxyphenyl C_3, C_5), 99.28 (pyrazole-C_4), 55.66 (-OMe); HRMS (ESI +): *m/z* calculated for $C_{23}H_{19}N_3O_2$: 369.42, found 370.1552 (M + 1), 371.1604 (M + 2).

4.1.4.10. N-(3-(3-(3-methoxyphenyl)-1H-pyrazol-5-yl)phenyl)benzamide ***(52)***. Pale yellow solid, yield- 93%, M.P.- 215–216 °C, ^{1}H NMR (500 MHz, DMSO-d_6) δ 13.38 (s, 1H, pyrazole NH), 10.35 (s, 1H, amide NH), 8.32 (s, 1H, phenyl C_2), 8.02 (d, J = 7 Hz, 2H, benzamide C_2, C_6), 7.76 (s, 1H, methoxyphenyl C_2), 7.63–7.55 (m, 4H, phenyl C_4, C_5, C_6 & benzamide C_4), 7.43 (m, 4H, benzamide C_3, C_5 & methoxyphenyl C_5, C_6), 7.15 (s, 1H, methoxyphenyl C_4), 6.93 (s, 1H, pyrazole C_4), 3.84 (s, 3H, -OMe). ^{13}C NMR (125 MHz, DMSO-d_6) δ 166.04 (-C═O, amide), 160.14 (methoxyphenyl C_3), 140.00 (pyrazole C_3, C_5), 135.34 (phenyl C_1), 132.09 (benzamide C_1), 128.88 (benzamide C_3, C_5 & methoxyphenyl C_5), 128.14 (Phenyl C_4, C_6 & benzamide C_2, C_6), 121.19 (Phenyl C_2 & methoxyphenyl C_6), 117.97 (methoxyphenyl C_4), 110.89 (methoxyphenyl C_2), 100.33 (pyrazole-C_4), 55.65 (-OMe); MS (ESI +): *m/z* calculated for $C_{23}H_{19}N_3O_2$: 369.42, found- 370.15 (M + 1).

*4.1.4.11. N-(3-(3-(3,4-dimethoxyphenyl)-1H-pyrazol-5-yl)phenyl) benzamide****(53)***. Pale yellow solid, yield- 70%, M.P.- 105–106 °C, ^{1}H NMR (500 MHz, DMSO-d_6) δ 13.22 (s, 1H, pyrazole NH), 10.33 (s, 1H, amide NH), 8.30 (s, 1H, phenyl C_2), 8.02 (d, J = 7.5 Hz, 2H, benzamide C_2, C_6), 7.75 (s, 1H, phenyl C_5), 7.63–7.54 (m, 4H, benzamide C_3, C_5, phenyl C_4, C_6), 7.44–7.38 (m, 3H, benzamide C_4, 3,4-dimethoxyphenyl C_2, C_6), 7.06 (s, 2H, pyrazole C_4, 3,4-dimethoxyphenyl C_5), 3.86 (s, 3H, methoxyphenyl C_3 -Me), 3.80 (s, 3H, methoxyphenyl C_4 -Me). ^{13}C NMR (125 MHz, DMSO-d_6) δ 166.04 (-C═O, amide), 149.51 (3,4-dimethoxyphenyl C_3, C_4), 139.98 (pyrazole C_3, C_5), 135.34 (phenyl C_1), 132.09 (benzamide C1, phenyl C_3), 128.88 (benzamide C_3, C_5, phenyl C_5), 128.13 (benzamide C_2, C_6, 3,4-dimethoxyphenyl C_1), 121.17 (phenyl C_4, C_6), 118.10 (phenyl C_2, 3,4-dimethoxyphenyl C_6), 112.60 (3,4-dimethoxyphenyl C_5), 109.54 (3,4-dimethoxyphenyl C_2), 99.45 (pyrazole C_4), 56.07 (-OMe); MS (ESI +): *m/z* calculated for $C_{24}H_{21}N_3O_3$: 399.45 found – 400.0 (M + 1).

*4.1.4.12. N-(3-(3-(4-(trifluoromethyl)phenyl)-1H-pyrazol-5-yl)phenyl) benzamide****(54)***. Off white solid, yield- 83%, M.P.- 210–211 °C, ^{1}H NMR (500 MHz, DMSO-d_6) δ 13.91 (d, J = 149 Hz, 1H, pyrazole NH), 10.46 (d, J = 41.5 Hz, 1H, amide NH), 8.31 (s, 1H, phenyl C_2), 8.09–7.99 (m, 4H, benzamide C_2, C_6 (trifluoromethyl)phenyl) C_3, C_5), 7.88–7.74 (m, 3H, phenyl C_4, C_5, C_6), 7.63–7.47 (m, 5H, benzamide C_4, (trifluoromethyl)phenyl) C_2, C_6, benzamide C_4, C_3, C_5), 7.27 (s, 1H, pyrazole C_4). ^{13}C NMR (125 MHz, DMSO-d_6) δ 166.11 (C═O, amide), 140.10 (pyrazole C_3, C_5), 135.25 (phenyl C_1, (trifluoromethyl)phenyl

C_1), 132.16 (benzamide C_1, phenyl C_3), 128.92 ((trifluoromethyl) phenyl C_2, C_6, benzamide C_4), 128.18 (phenyl C_5), 128.14 (benzamide C_3, C_5,), 126.26 (-CF_3), 126.12 ((trifluoromethyl)phenyl C_3,C_5, benzamide C_2, C_6), 121.22 (phenyl C_6, C_4), 120.63 (phenyl C_2), 101.14 (pyrazole-C_4); MS (ESI +): *m/z* calculated for $C_{23}H_{16}F_3N_3O$: 407.40, found – 408.52 (M + 1).

*4.1.4.13. N-(3-(3-(3-(trifluoromethyl)phenyl)-1H-pyrazol-5-yl)phenyl) benzamide**(55)***. Off white solid, yield- 81%, M.P.- 215–217 °C, ^{1}H NMR (500 MHz, DMSO-d_6) δ 13.89–13.57 (d, J = 160 Hz, pyrazole NH), 10.50 – 10.39 (d, J = 53.5 Hz, amide NH), 8.34–8.16 (m, 3H, (trifluoromethyl)phenyl C_2, C_6 phenyl C_2), 8.02–7.98 (m, 2H, benzamide C_2, C_6), 7.88–7.42 (m, 8H, benzamide C_4, C_3, C_5 phenyl C_4, C_5, C_6, (trifluoromethyl)phenyl C_4, C_5), 7.31(s, 1H, pyrazole C_4). ^{13}C NMR (125 MHz, DMSO-d_6) δ 166.07 (C═O, amide), 140.09 (pyrazole C_3, C_5), 135.28 (phenyl C_1), 132.16 (benzamide C_1), 130.05 (benzamide C_4) 129.43 ((trifluoromethyl)phenyl C_1, phenyl C_3), 128.91 (benzamide C_3, C_5, (trifluoromethyl)phenyl C_3,C_5), 128.18 (phenyl C_5, (trifluoromethyl)phenyl C_6), 128.14 (benzamide C_2, C_6, (trifluoromethyl)phenyl C_2, C_4), 121.89 (phenyl C_6), 121.22 (phenyl C_4), 120.64 (phenyl C_2), 100.86 (pyrazole-C_4); MS (ESI +): *m/z* calculated for $C_{23}H_{16}F_3N_3O$: 407.40, found – 408.53 (M + 1).

*4.1.4.14. N-(3-(3-(4-(trifluoromethoxy)phenyl)-1H-pyrazol-5-yl)phenyl) benzamide**(56)***. White solid, yield- 84%, M.P.- 210–211 °C, ^{1}H NMR (500 MHz, DMSO-d_6) δ 13.51 (s, 1H, pyrazole NH), 10.41 (d, J = 24.5 Hz, 1H, amide NH), 8.36 (d, J = 49.5 Hz, 1H, phenyl C_2), 8.02–7.97 (m, 4H, benzamide C_2, C_6, (trifluoromethyl)phenyl) C_3, C_5), 7.77 (d, J = 19.5 Hz, 1H, phenyl C_5), 7.63–7.44 (m, 7H, benzamide C_3, C_4, C_5, (trifluoromethyl)phenyl) C_2, C_6, phenyl C_4, C_6), 7.19 (d, J = 20 Hz, 1H, pyrazole C_4). ^{13}C NMR (125 MHz, DMSO-d_6) δ 166.09 (C═O, amide), 150.48 ((trifluoromethyl)phenyl) C_4), 140.16 (pyrazole C_3, C_5), 135.24 (phenyl C_1), 132.12 (benzamide C_1, phenyl C_3), 129.79 (phenyl C_5), 128.89 (benzamide C_3, C_4, C_5), 128.15 ((trifluoromethyl) phenyl) C_2, C_6 benzamide C_2, C_6), 127.39 ((trifluoromethyl)phenyl) C_3, C_5), 122.14 ((trifluoromethyl)phenyl) C_1), 121.18 (phenyl C_6, C_4), 119.57 (phenyl C_2), 100.40 (pyrazole-C_4); MS (ESI +): *m/z* calculated for $C_{23}H_{16}F_3N_3O_2$: 423.40, found – 424.1 (M + 1).

*4.1.4.15. N-(3-(3-(4-cyanophenyl)-1H-pyrazol-5-yl)phenyl)benzamide **(57)***. Pale yellow solid, yield- 79%, M.P.- 225–226 °C, ^{1}H NMR (500 MHz, DMSO-d_6) δ 13.67 (s, 1H, pyrazole NH), 10.41 (s, 1H, amide NH), 8.37 (d, J = 51.5 Hz, 1H, phenyl C_2), 8.09–7.90 (m, 6H, benzamide C_2, C_6, cyanophenyl C_2, C_3, C_5, C_6), 7.77 (m, 1H,benzamide C_4), 7.63–7.44 (m, 5H, phenyl C_4, C_5, C_6 benzamide C_3, C_5), 7.35 (d, J = 41.5 Hz, 1H, pyrazole C_4). ^{13}C NMR (125 MHz, DMSO-d_6) δ 166.11 (-C═O, amide), 144.50 (pyrazole C_3), 140.20 (pyrazole C_5), 138.51 (cyanophenyl C_1), 135.22 (phenyl C_1), 133.53 (benzamide C_1), 133.22 (phenyl C_3), 132.15 (benzamide C_4), 129.82 (phenyl C_5), 128.91 (phenyl C4, cyanophenyl C_3, C_5), 128.14 (benzamide C_3, C_5, C_2, C_6), 126.17 (phenyl C_6, cyanophenyl C_2, C_6), 121.23 (phenyl C_2), 118.37 (-CN), 110.19 (cyanophenyl C_4), 101.19 (pyrazole-C_4); HRMS (ESI +): *m/z* calculated for $C_{23}H_{16}N_4O$: 364.41, found − 365.1405 (M + 1), 366.1430 (M + 2).

*4.1.4.16. N-(3-(3-(3-cyanophenyl)-1H-pyrazol-5-yl)phenyl)benzamide **(58)***. yellow solid, yield- 85%, M.P.- 215–216 °C, ^{1}H NMR (500 MHz, DMSO-d_6) δ 13.53 (s, 1H, pyrazole NH), 10.43 (s, 1H, amide NH), 8.32 (s, 1H, phenyl C_2), 8.22 (d, J = 7.5 Hz, 2H, benzamide C_2, C_6), 8.05–7.98 (m, 3H, phenyl C_4, C_5, C_6), 7.81 (d, J = 7 Hz, 1H, cyanophenyl C_4), 7.73–7.43 (m, 7H, benzamide C_4, C_3, C_5, cyanophenyl C_2, C_5, C_6), 7.30 (s, 1H, pyrazole C_4). ^{13}C NMR (125 MHz, DMSO-d_6) δ 166.11 (-C═O, amide), 140.10 (pyrazole C_3, C_5), 135.26 (phenyl C_1), 132.20 (benzamide C_1), 131.70 (cyanophenyl C_1), 130.61 (benzamide C_4), 130.04 (cyanophenyl C_4), 129.66 (phenyl C_3), 129.34 (cyanophenyl C_6), 128.97 (cyanophenyl C_2), 128.91 (cyanophenyl C_5), 128.90 (phenyl C_5), 128.16 (benzamide C_3, C_5), 128.13 (benzamide C_2, C_6), 124.90 (phenyl C_4), 121.20 (phenyl C_6), 119.18 (phenyl C_2), 118.12 (-CN), 112.49 (cyanophenyl C_3), 100.99 (pyrazole-C_4); MS (ESI +): *m/z* calculated for $C_{23}H_{16}N_4O$ 364.41, found – 365.52 (M + 1).

*4.1.4.17. N-(3-(3-(p-tolyl)-1H-pyrazol-5-yl)phenyl)benzamide**(59)***. Pale yellow solid, yield- 70%, M.P.- 182–183 °C, ^{1}H NMR (500 MHz, DMSO-d_6) δ 13.32 (s, 1H, pyrazole NH), 10.35 (s, 1H, amide NH), 8.32 (s, 1H, phenyl C_2), 8.02 (d, J = 7 Hz, 2H, benzamide C_2, C_6), 7.74 (s, 3H, phenyl C_4,C_5 C_6,), 7.63–7.54 (m, 4H, tolyl C_2, C_6 & benzamide C_3, C_5), 7.43 (s, 1H, benzamide C_4), 7.28 (s, 2H, tolyl C_3, C_5), 7.06 (s, 1H, pyrazole C_4), 2.34 (s, 3H, -Me). ^{13}C NMR (125 MHz, DMSO-d_6) δ 166.05 (-C═O, amide), 140.00 (pyrazole C_3, C_5), 135.35 (phenyl C_1), 132.09 (benzamide C_1), 129.93 (phenyl C_3), 128.88 (benzamide C_3, C_5, tolyl C_1, C_4), 128.14 (tolyl C_3, C_5, phenyl C_5, benzamide C_4), 125.53 (benzamide C_2 C_6, tolyl C_2, C_6), 121.18 (phenyl C_4, C_6), 117.69 (phenyl C_2), 99.70 (pyrazole-C_4), 21.30 (-Me); HRMS (ESI +): *m/z* calculated for $C_{23}H_{19}N_3O$:353.43, found − 354.1600 (M + 1), 355.1632 (M + 2).

*4.1.4.18. N-(3-(3-(o-tolyl)-1H-pyrazol-5-yl)phenyl)benzamide**(60)***. Off white, yield- 75%, M.P.- 174–175 °C, ^{1}H NMR (500 MHz, DMSO-d_6) δ 13.11 (s, 1H, pyrazole NH), 10.34 (s, 1H, amide NH), 8.27 (s, 1H, phenyl C_2), 8.01 (d, J = 7 Hz, 2H, benzamide C_2, C_6), 7.79 (d, J = 8 Hz, 1H, tolyl C_6), 7.62–7.59 (m, 2H, phenyl C_4, C_6), 7.57–7.54 (m, 3H, phenyl C_5, tolyl C_3, C_4), 7.45 (t, J = 8 Hz, 1H, benzamide C_4), 7.31 (m, 3H, benzamide C_3, C_5 & tolyl C_5), 6.86 (s, 1H, pyrazole C_4), 2.47(s, 3H, -Me). ^{13}C NMR (125 MHz, DMSO-d_6) δ 166.08 (-C═O, amide), 139.99 (pyrazole C_3, C_5), 135.84 (phenyl C_1), 135.35 (tolyl C_2), 132.09 (benzamide C_1), 131.31 (benzamide C_4, tolyl C_1), 129.19 (phenyl C3, tolyl C_6), 128.88 (benzamide C_3, C_5, tolyl C_4), 128.16 (tolyl C_3), 128.14 (benzamide C_2, C_6, tolyl C_5), 126.46 (Phenyl C_5), 121.22 (phenyl C_4), 120.39 (phenyl C_6), 117.90 (phenyl C_2), 102.89 (pyrazole C_4), 21.22 (-Me); MS (ESI +): *m/z* calculated for $C_{23}H_{19}N_3O$-353.43, found –354.16 (M + 1), 355.17 (M + 2).

*4.1.4.19. N-(3-(3-(4-isopropylphenyl)-1H-pyrazol-5-yl)phenyl)benzamide **(61)***. Off white solid, yield- 73%, M.P.- 207–208 °C, ^{1}H NMR (500 MHz, DMSO-d_6) δ 13.32 (s, 1H, pyrazole NH), 10.34 (s, 1H, amide NH), 8.31 (s, 1H, phenyl C_2), 8.03 (d, J = 7 Hz, 2H, benzamide C_2, C_6), 7.76 (bs, 3H, phenyl C_4, C_5, C_6), 7.63–7.54 (m, 4H, benzamide C_3, C_5, isopropylphenyl C_2, C_6), 7.43 (bs, 1H, benzamide C_4), 7.34 (bs, 2H, isopropylphenyl C_3, C_5), 7.05 (s, 1H, pyrazole C_4), 2.95–2.90 (m, 1H –CH), 1.24 (s, 3H, –CH_3), 1.23 (s, 3H, -CH_3). ^{13}C NMR (125 MHz, DMSO-d_6) δ 166.06 (C═O, amide), 140.01 (pyrazole C_3, C_5), 135.36 (phenyl C_1), 132.08 (benzamide C_1, C_4), 129.43 (phenyl C_3), 128.88 (benzamide C_3, C_5 phenyl C_5), 128.14 (isopropylphenyl C_3, C_5 benzamide C_2, C_6), 127.31 (isopropylphenyl C_1), 125.65 (isopropylphenyl C_2, C_6), 121.17 (phenyl C_4, C_6), 117.79 (phenyl C_2), 99.72 (pyrazole C_4), 33.68 (isopropyl –CH), 24.24 (isopropyl –CH_3); MS (ESI +): *m/z* calculated for $C_{25}H_{23}N_3O$: 381.48, found – 382.5 (M + 1).

*4.1.4.20. N-(3-(3-(naphthalen-1-yl)-1H-pyrazol-5-yl)phenyl)benzamide **(62)***. Pale yellow solid, yield- 90%, M.P.- 141–142 °C, ^{1}H NMR (500 MHz, DMSO-d_6) δ 13.60 (s, 1H, pyrazole NH), 10.37 (s, 1H, amide NH), 8.03–8.01 (m, 4H, phenyl C_2, naphthalene C_2 C_4, C_5), 7.80–7.46 (m, 12H, benzamide C_2, C_3, C_4, C_5, C_6, phenyl C_4, C_5, C_6, naphthalene C_3, C_6, C_7, C_8), 7.02 (s, 1H, pyrazole C_4). ^{13}C NMR (125 MHz, DMSO-d_6) δ 166.09 (C═O, amide), 140.06 (pyrazole C_3, C_5), 135.35 (phenyl C_1), 133.98 (naphthalene C_1), 132.10 (benzamide C_1), 131.02 (benzamide C_4), 128.89 (benzamide C_2, C_6, C_3, C_5), 128.18 (naphthalene C_2), 128.15 (naphthalene C4, C_{4a}, C_{8a}, phenyl C_5), 127.43 (naphthalene C_5, C_8), 125.99 (naphthalene C_3, C_6, C_7), 121.29 (phenyl C_4, C_6), 120.47 (phenyl C_2), 103.69 (pyrazole-C_4); MS (ESI +): *m/z* calculated for $C_{26}H_{19}N_3O$: 389.46, found – 390.51 (M + 1).

4.1.5. General procedure for the synthesis of compounds 63, 64 and 65

Compounds **63, 64, 65** were synthesized according to a previously described method and compared with proton NMR data [38].

4.1.6. General procedure for the synthesis of compounds 66–85

To a stirred solution of chalcone derivatives (**23–42**, 0.5 eq) in 1,4-Dioxane (5 ml), cyclohexanone tosylhydrazone (**65**, 1.0 eq) and dry Cs_2CO_3 (1.0 eq) was added. The reaction mixture was refluxed for 2 h in oil bath under nitrogen atmosphere and progress was monitored by TLC. After the completion of the reaction, it was cooled to room temperature, and water (10 ml) and ethyl acetate (20 ml) were added. The two layers were separated, and the aqueous phase was extracted with ethyl acetate (2 × 10 ml). The combined organic extracts were washed with brine solution, dried over anhydrous sodium sulfate, filtered, and evaporated under reduced pressure. The residue was purified by column chromatography on silica gel (60–120 mesh) to afford the desired spiropyrazoline **(66–85)**.

*4.1.6.1. N-(3-(4-phenyl-1,2-diazaspiro[4.5]dec-2-ene-3-carbonyl)phenyl) benzamide**(66)***. Brown solid, yield- 72%, M.P.- 190–191 °C, ^{1}H NMR (500 MHz, DMSO-d_6) δ 8.20 (s, 1H, phenyl C_2), 8.08–8.05 (m, 2H, amide NH, phenyl' C_5), 7.89–7.85 (m, 3H, phenyl' C_2, C_3, C_6), 7.55–7.52 (t, J = 7.5 Hz, 1H, benzamide C_4), 7.48–7.41 (m, 3H, phenyl C_4, C_5, C_6), 7.26 (d, J = 6 Hz, 2H, benzamide C_3, C_5), 7.22–7.19 (m, 1H, phenyl' C_4), 7.13 (d, J = 7 Hz, 2H, benzamide C_2, C_6), 6.60 (s, 1H, pyrazole NH), 4.21(s, 1H, pyrazole C_4), 1.74–1.26 (m, 10*H*, cyclohexane). ^{13}C NMR (125 MHz, $CDCl_3$) δ 186.78 (C═O, carbonyl), 165.89 (C═O, amide), 152.70 (pyrazole C_3), 138.18 (phenyl C_3), 137.81 (phenyl C_1), 136.05 (phenyl' C_1), 134.79 (benzamide C_1), 131.95 (benzamide C_4), 128.88 (phenyl' C_4), 128.80 (phenyl' C_3, C_5), 128.60 (phenyl C_5), 128.47 (phenyl' C_2, C_6), 127.17 (benzamide C_3, C_5), 127.11 (benzamide C_2, C_6), 126.03 (phenyl C_6), 124.04 (phenyl C_4), 121.44 (phenyl C_2), 69.55 (pyrazole C_5), 57.65 (pyrazole C_4), 37.37, 31.63, 25.14, 23.33, 22.38 (cyclohexane ring); HRMS (ESI +): m/z calculated for $C_{28}H_{27}N_3O_2$: 437.54, found –438.2181 (M + 1), 439.2226 (M + 2).

*4.1.6.2. N-(3-(4-(4-chlorophenyl)-1,2-diazaspiro[4.5]dec-2-ene-3-carbonyl)phenyl)benzamide**(67)***. Yellow solid, yield- 80%, M.P.- 210–211 °C, ^{1}H NMR (500 MHz, $CDCl_3$) δ 8.27 (s, 1H, 4-chlorophenyl C_5), 8.13 (s, 1H, amide NH), 8.06 (d, J = 7.5 Hz, 1H, 4-chlorophenyl C_6), 7.90–7.87 (m, 3H, phenyl C_2, 4-chlorophenyl C_3, C_2), 7.57–7.55 (m, 1H, benzamide C_4), 7.49–7.43 (m, 3H, phenyl C_4, C_5, C_6), 7.26 (d, J = 7.5 Hz, 2H, benzamide C_2, C_6), 7.08 (bs, 2H, benzamide C_3, C_5), 6.65 (s, 1H, pyrazole NH), 4.19 (s, 1H, pyrazole C_4), 1.67–1.28 (m, 10*H*, cyclohexane). ^{13}C NMR (125 MHz, $CDCl_3$) δ 186.62 (C═O, carbonyl), 165.92 (C═O, amide), 152.24 (pyrazole C_3), 138.02 (phenyl C_3), 137.86 (phenyl C_1), 134.74 (benzamide C_1), 134.72 (phenyl C_5), 132.94 (chlorophenyl C_1), 131.99 (benzamide C_4), 129.92 (chlorophenyl C_4), 128.91 (chlorophenyl C_2, C_6), 128.81 (chlorophenyl C_3, C_5), 128.69 (benzamide C_3, C_5), 127.11(benzamide C_2, C_6), 125.98 (phenyl C_6), 124.11 (phenyl C_4), 121.47 (phenyl C_2), 69.54 (pyrazole C_5), 56.93 (pyrazole C_4), 37.22, 31.56, 25.08, 23.33, 22.33 (cyclohexane ring); HRMS (ESI +): m/z calculated for $C_{28}H_{26}ClN_3O_2$: 471.99, found – 472.1797 (M + 1), 474.1788 (M + 3).

*4.1.6.3. N-(3-(4-(2-chlorophenyl)-1,2-diazaspiro[4.5]dec-2-ene-3-carbonyl)phenyl)benzamide**(68)***. Pale yellow solid, yield- 205–206 °C, M.P.- 75%, ^{1}H NMR (500 MHz, $CDCl_3$) δ 8.27 (s, 1H, 2-chlorophenyl C_5), 8.08 (s, 1H, amide NH), 8.05 (d, J = 7.5 Hz, 1H, 2-chlorophenyl C_6), 7.91 (d, J = 7.5 Hz, 1H, 2-chlorophenyl C_3), 7.87–7.85 (m, 2H, phenyl C_2, 2-chlorophenyl C_4), 7.54–7.52 (m, 1H, benzamide C_4), 7.48–7.38 (m, 4H, phenyl C_4, C_5, C_6, benzamide C_3), 7.13 (bs, 2H, benzamide C_2, C_6), 6.92 (bs, 1H, benzamide C_5), 6.73 (s, 1H, pyrazole NH), 4.82 (s, 1H, pyrazole C_4), 1.75–1.35 (m, 10*H*, cyclohexane). ^{13}C NMR (125 MHz, $CDCl_3$) δ 186.21 (C═O, carbonyl), 165.90 (C═O, amide), 152.12 (pyrazole C_3), 138.05 (phenyl C_3), 137.83 (phenyl C_1), 134.77 (benzamide C_1), 134.20 (2-chlorophenyl C_1), 134.18 (phenyl C_5), 131.96 (benzamide C_4), 129.86 (2-chlorophenyl C_2), 129.13 (2-chlorophenyl C_6), 128.91 (2-chlorophenyl C_3), 128.81 (benzamide C_3, C_5), 128.35 (2-chlorophenyl C_4), 127.10 (benzamide C_2, C_6), 126.99(2-chlorophenyl C_5), 125.98 (phenyl C_6), 124.07 (phenyl C_4), 121.50 (phenyl C_2), 69.61 (pyrazole C_5), 53.64 (pyrazole C_4), 37.21, 31.40, 25.07, 23.22, 22.44 (cyclohexane ring); MS (ESI +): m/z calculated for $C_{28}H_{26}ClN_3O_2$: 471.99, found – 472.1692 (M + 1), 474.1658 (M + 3).

*4.1.6.4. N-(3-(4-(2,4-dichlorophenyl)-1,2-diazaspiro[4.5]dec-2-ene-3-carbonyl)phenyl)benzamide**(69)***. Pale yellow solid, yield- 82%, M.P.- 202–203 °C, ^{1}H NMR (500 MHz, $CDCl_3$) δ 8.33 (s, 1H, 2,4-dichlorophenyl C_2), 8.05 (m, 2H, amide NH, 2,4-dichlorophenyl C_5), 7.93–7.88 (m, 3H, 2,4-dichlorophenyl C_6, phenyl C_2, benzamide C_5), 7.57–7.56 (m, 1H, benzamide C_4), 7.51–7.43 (m, 4H, phenyl C_4, C_5, C_6, benzamide C_3), 7.14 (d, J = 8 Hz,1H, benzamide C_2), 6.87 (d, J = 8 Hz, 1H, benzamide C_6), 6.74 (s, 1H, pyrazole NH), 4.78 (s, 1H, pyrazole C_4), 1.76–1.28 (m, 10*H*, cyclohexane). ^{13}C NMR (125 MHz, $CDCl_3$) δ 186.04 (C═O, carbonyl), 165.88 (C═O, amide), 151.79 (pyrazole C_3), 137.89 (phenyl C_3), 137.84 (phenyl C_1), 134.76 (benzamide C_1), 133.32 (2,4-dichlorophenyl C_1), 132.98 (2,4-dichlorophenyl C_2), 132.01 (phenyl C_5, benzamide C_4), 130.00 (2,4-dichlorophenyl C_4), 129.66 (2,4-dichlorophenyl C_6), 128.96 (2,4-dichlorophenyl C_3), 128.84 (benzamide C_3, C_5), 127.37 (2,4-dichlorophenyl C_5), 127.08 (benzamide C_2, C_6), 125.96 (phenyl C_6), 124.11 (phenyl C_4), 121.47 (phenyl C_2), 69.60 (pyrazole C_5), 53.13 (pyrazole C_4), 37.14, 31.40, 25.03, 23.22, 22.42 (cyclohexane ring); HRMS (ESI +): m/z calculated for $C_{28}H_{25}Cl_2N_3O_2$: 506.43, found – 506.1408 (M +), 508.1379 (M + 2), 509.1419 (M + 3).

*4.1.6.5. N-(3-(4-(4-bromophenyl)-1,2-diazaspiro[4.5]dec-2-ene-3-carbonyl)phenyl)benzamide**(70)***. Pale brown solid, yield- 77%, M.P.- 265–266 °C, ^{1}H NMR (500 MHz, $CDCl_3$) δ 8.26 (s, 1H, 4-bromophenyl C_5), 8.08 (m, 2H, amide NH, 4-bromophenyl C_3), 7.91–7.88 (m, 3H, phenyl C_2, 4-bromophenyl C_6, C_2), 7.58–7.55 (m, 1H, benzamide C_4), 7.50–7.40 (m, 5H, phenyl C_4, C_5, C_6, benzamide C_2, C_6), 7.03 (d, J = 7 Hz, 2H, benzamide C_3, C_5), 6.62 (s, 1H, pyrazole NH), 4.19 (s, 1H, pyrazole C_4), 1.68–1.28 (m, 10*H*, cyclohexane). ^{13}C NMR (125 MHz, $CDCl_3$) δ 186.56 (C═O, carbonyl), 165.87 (C═O, amide), 152.23 (pyrazole C_3), 138.01 (phenyl C_3), 137.85 (phenyl C_1), 135.25 (benzamide C_1), 134.77 (4-bromophenyl C_1), 131.99 (phenyl C_5), 131.64 (4-bromophenyl C_3, C_5), 130.29 (benzamide C_4), 128.92 (4-bromophenyl C_2, C_6), 128.82 (benzamide C_3, C_5), 127.09 (benzamide C_2, C_6), 125.99 (phenyl C_6), 124.09 (phenyl C_4), 121.43 (phenyl C_2), 121.10 (4-bromophenyl C_4), 69.49 (pyrazole C_5), 57.03 (pyrazole C_4), 37.24, 31.58, 25.09, 23.35, 22.34 (cyclohexane ring); HRMS (ESI +): m/z calculated for $C_{28}H_{26}BrN_3O_2$: 516.44, found – 516.8124 (M +), 518.5471 (M + 2).

*4.1.6.6. N-(3-(4-(3-bromophenyl)-1,2-diazaspiro[4.5]dec-2-ene-3-carbonyl)phenyl)benzamide**(71)***. Pale brown solid, yield- 78%, M.P.- 262–263 °C, ^{1}H NMR (500 MHz, $CDCl_3$) δ 8.22 (s, 1H, 3-bromophenylC_2), 8.08–8.04 (m, 2H, amide NH, 3-bromophenyl C_5), 7.90–7.86 (m, 3H, phenyl C_2, 3-bromophenyl C_6, C_4), 7.54–7.53 (m, 1H, benzamide C_4), 7.49–7.43 (m, 3H, phenyl C_4, C_5, C_6), 7.35 (d, J = 7.5 Hz, 1H, benzamide C_6), 7.27 (d, J = 6.5 Hz, 1H, benzamide C_3), 7.15–7.12 (t, J = 7 Hz, 1H, benzamide C_5), 7.05 (bs, 1H, benzamide C_2), 6.63 (s, 1H, pyrazole NH), 4.15 (s, 1H, pyrazole C_4), 1.68–1.28 (m, 10*H*, cyclohexane). ^{13}C NMR (125 MHz, $CDCl_3$) δ 186.47 (C═O, carbonyl), 165.87 (C═O, amide), 152.03 (pyrazole C_3), 138.55 (phenyl C_3), 137.97 (3-bromophenyl C_1), 137.86 (phenyl C_1), 134.77 (benzamide C_1), 131.98 (phenyl C_5), 130.36 (3-bromophenyl C_2), 130.04 (benzamide C_4), 128.94 (3-bromophenyl C_6), 128.82 (3-bromophenyl C_4, benzamide C_3, C_5), 127.10 (3-bromophenyl C_5, benzamide C_2, C_6), 126.03 (phenyl C_6), 124.13 (phenyl C_4), 122.64

(3-bromophenyl C_3), 121.44 (phenyl C_2), 69.65 (pyrazole C_5), 57.28 (pyrazole C_4), 37.25, 31.57, 25.06, 23.33, 22.34 (cyclohexane ring); HRMS (ESI +): *m/z* calculated for $C_{28}H_{26}BrN_3O_2$: 516.44, found – 516.1281 (M +), 517.1330 (M + 2), 518.1270 (M + 3) and 519.1301 (M + 4).

*4.1.6.7. N-(3-(4-(4-fluorophenyl)-1,2-diazaspiro[4.5]dec-2-ene-3-carbonyl)phenyl)benzamide**(72)***. Off white solid, yield- 78%, M.P.- 244–245 °C, ^{1}H NMR (500 MHz, $CDCl_3$) δ 8.23 (s, 1H, 4-fluorophenyl C_5), 8.04 (bs, 2H, amide NH, 4-fluorophenyl C_3), 7.89–7.86 (m, 3H, phenyl C_2, 4-fluorophenyl C_2, C_6), 7.54–7.53 (m, 1H, benzamide C_4), 7.48–7.42 (m, 3H, phenyl C_4, C_5, C_6), 7.08 (bs, 2H, benzamide C_3, C_5), 6.97–6.94 (m , 2H, benzamide C_2, C_6), 6.58 (s, 1H, pyrazole NH), 4.20 (s, 1H, pyrazole C_4), 1.66–1.26 (m, 10*H*, cyclohexane). ^{13}C NMR (125 MHz, $CDCl_3$) δ 186.65 (C═O, carbonyl), 165.86 (C═O, amide), 162.95, 161.00 (4-fluorophenyl C_4), 152.59 (pyrazole C_3), 138.09 (phenyl C_3), 137.84 (phenyl C_1), 134.78 (benzamide C_1), 131.98 (phenyl C_5), 131.89, 131.87 (4-fluorophenyl C_1), 130.10, 130.07 (4-fluorophenyl C_2, C_6), 128.92 (benzamide C_4), 128.82 (benzamide C_3, C_5), 127.09 (benzamide C_2, C_6), 126.00 (phenyl C_6), 124.05 (phenyl C_4), 121.42 (phenyl C_2), 115.48 (4-fluorophenyl C_5), 115.31 (4-fluorophenyl C_3), 69.43 (pyrazole C_5), 56.79 (pyrazole C_4), 37.22, 31.57, 25.11, 23.34, 22.36 (cyclohexane ring); HRMS (ESI +): *m/z* calculated for $C_{28}H_{26}FN_3O_2$: 455.53, found – 456.2154 (M + 1), 457.2163 (M + 2).

*4.1.6.8. N-(3-(4-(3-fluorophenyl)-1,2-diazaspiro[4.5]dec-2-ene-3-carbonyl)phenyl)benzamide**(73)***. Pale yellow solid, yield- 89%, M.P.- 260–261 °C, ^{1}H NMR (500 MHz, $CDCl_3$) δ 8.22 (s, 1H, 3-fluorophenyl C_2), 8.08 (m, 2H, amide NH, 3-fluorophenyl C_5), 7.90–7.86 (m, 3H, phenyl C_2, 3-fluorophenyl C_6, C_4,), 7.54–7.53 (m, 1H, benzamide C_4), 7.48–7.42 (m, 3H, phenyl C_4, C_5, C_6),7.23 (d, *J* = 7 Hz, 1H, benzamide C_3), 6.92 (d, *J* = 8 Hz, 2H, benzamide C_2, C_6), 6.84 (d, *J* = 8.5 Hz, 1H, benzamide C_5), 6.62 (s, 1H, pyrazole NH), 4.19 (s, 1H, pyrazole C_4), 1.67–1.28 (m, 10*H*, cyclohexane). ^{13}C NMR (125 MHz, $CDCl_3$) δ 186.54 (C═O, carbonyl), 165.86 (C═O, amide), 163.91, 161.95 (3-fluorophenyl C_3), 152.14 (pyrazole C_3), 138.72, 138.67 (3-fluorophenyl C_1), 138.01 (phenyl C_3), 137.85 (phenyl C_1), 134.78 (benzamide C_1), 131.97 (phenyl C_5), 129.95, 129.88 (3-fluorophenyl C_5), 128.93 (benzamide C_4), 128.81 (benzamide C_3, C_5), 127.09 (benzamide C_2, C_6), 126.01 (phenyl C_6), 124.33 (3-fluorophenyl C_6), 124.11 (phenyl C_4), 121.42 (phenyl C_2), 114.26 (3-fluorophenyl C_2), 114.09 (3-fluorophenyl C_4), 69.66 (pyrazole C_5), 57.34 (pyrazole C_4), 37.28, 31.49, 25.08, 23.34, 22.35 (cyclohexane ring); HRMS (ESI +): *m/z* calculated for $C_{28}H_{26}FN_3O_2$: 455.53, found – 456.2085 (M + 1), 457.2122 (M + 2).

*4.1.6.9. N-(3-(4-(4-methoxyphenyl)-1,2-diazaspiro[4.5]dec-2-ene-3-carbonyl)phenyl)benzamide**(74)***. Yellow Solid, yield- 66%, M.P.- 258–259 °C, ^{1}H NMR (500 MHz, $CDCl_3$) δ 8.27 (s, 1H, 4-methoxyphenyl C_5), 8.23 (s, 1H, amide NH), 8.10 (d, *J* = 7.5 Hz, 1H, 4-methoxyphenyl C_6), 7.88–7.87 (m, 3H, phenyl C_2, 4-methoxyphenyl C_2, C_3), 7.55–7.52(m, 1H, benzamide C_4), 7.46–7.41 (m, 3H, phenyl C_4, C_5, C_6), 7.05 (d, *J* = 7 Hz, 2H, benzamide C_2, C_6), 6.80 (d, *J* = 8 Hz, 2H, benzamide C_3, C_5), 4.18 (s, 1H, pyrazole C_4), 3.75 (s, 3H, OCH_3), 1.66–1.28 (m, 10*H*, cyclohexane). ^{13}C NMR (125 MHz, $CDCl_3$) δ 186.95 (C═O, carbonyl), 165.98 (C═O, amide), 158.63 (4-methoxyphenyl C_4), 152.95 (pyrazole C_3), 138.17 (phenyl C_3), 137.91 (phenyl C_1), 134.74 (benzamide C_1), 131.90 (benzamide C_4), 129.60 (phenyl C_5), 128.84 (4-methoxyphenyl C_1), 128.74 (4-methoxyphenyl C_2, C_6), 128.06 (benzamide C_2), 127.87 (benzamide C_6), 127.17 (benzamide C_3, C_5), 125.94 (phenyl C_6), 124.10 (phenyl C_4), 121.56 (phenyl C_2), 113.88 (4-methoxyphenyl C_3, C_5), 69.40 (pyrazole C_5), 56.82 (pyrazole C_4), 55.15 (–OCH_3), 37.20, 31.56, 25.15, 23.34, 22.36 (cyclohexane ring); HRMS (ESI +): *m/z* calculated for $C_{29}H_{29}N_3O_3$: 467.57, found – 468.2502 (M + 1), 469.2343 (M + 2).

*4.1.6.10. N-(3-(4-(3-methoxyphenyl)-1,2-diazaspiro[4.5]dec-2-ene-3-carbonyl)phenyl)benzamide**(75)***. Pale yellow solid, yield- 75%, M.P.- 262–263 °C, ^{1}H NMR (500 MHz, $CDCl_3$) δ 8.18 (s, 1H, 3-methoxyphenyl C_5), 8.09 (d, *J* = 8 Hz, 1H, 3-methoxyphenyl C_6), 8.01 (s, 1H, amide NH), 7.90–7.86 (m, 3H, 3-methoxyphenyl C_2, C_4, phenyl C_2), 7.56–7.53 (m, 1H, benzamide C_4), 7.49–7.42 (m, 3H, phenyl C_4, C_5, C_6), 7.20–7.17 (t, *J* = 8 Hz, 1H, benzamide C_6), 6.76 (d, *J* = 8.5 Hz, 2H, benzamide C_3, C_5), 6.68 (s, 1H, benzamide C_2), 6.56 (s, 1H, pyrazole NH), 4.18 (s, 1H, pyrazole C_4), 3.76 (s, 3H, OCH_3), 1.68–1.29 (m, 10*H*, cyclohexane). ^{13}C NMR (125 MHz, $CDCl_3$) δ 186.72 (C═O, carbonyl), 165.80 (C═O, amide), 159.65 (3-methoxyphenyl C_3), 152.55 (pyrazole C_3), 138.19 (phenyl C_3), 137.81 (3-methoxyphenyl C_1), 137.60 (phenyl C_1), 134.82 (benzamide C_1), 131.95 (phenyl C_5), 129.41 (benzamide C_4), 128.90 (3-methoxyphenyl C_5), 128.82 (3-methoxyphenyl C_6, benzamide C_3, C_5), 127.09 (benzamide C_2, C_6), 126.03 (phenyl C_6), 123.99 (phenyl C_4), 121.36 (phenyl C_2), 112.22 (3-methoxyphenyl C_2, C_4), 69.55 (pyrazole C_5), 57.72 (pyrazole C_4), 55.17 (–OCH_3), 37.42, 31.52, 25.14, 23.41, 22.41 (cyclohexane ring); HRMS (ESI +): *m/z* calculated for $C_{29}H_{29}N_3O_3$: 467.57, found – 468.2283 (M + 1), 469.2323 (M + 2).

*4.1.6.11. N-(3-(4-(3,4-dimethoxyphenyl)-1,2-diazaspiro[4.5]dec-2-ene-3-carbonyl)phenyl)benzamide**(76)***. Yellow solid, yield- 85%, M.P.- 260–261 °C, ^{1}H NMR (500 MHz, $CDCl_3$) δ 8.25 (s, 1H, 3,4-dimethoxyphenyl C_3), 8.05 (m, 2H, amide NH, 3,4-dimethoxyphenyl C_6), 7.89–7.86 (m, 3H, phenyl C_2, 3,4-dimethoxyphenyl C_5, benzamide C_5), 7.54 (m, 1H, benzamide C_4), 7.48–7.42 (m, 3H, phenyl C_4, C_5, C_6), 6.77 (d, *J* = 8 Hz, 1H, benzamide C_3), 6.69 (m, 2H, benzamide C_2, C_6) 6.55 (s, 1H, pyrazole NH), 4.16 (s, 1H, pyrazole C_4), 3.82 (s, 6H, –OCH_3 *2), 1.67–1.26 (m, 10*H*, cyclohexane). ^{13}C NMR (125 MHz, $CDCl_3$) δ 186.92 (C═O, carbonyl), 165.83 (C═O, amide),152.84 (pyrazole C_3), 148.89 (3,4-dimethoxyphenyl C_3), 148.12 (3,4-dimethoxyphenyl C_4), 138.27 (phenyl C_3), 137.86 (phenyl C_1), 134.80 (benzamide C_1), 131.96 (phenyl C_5), 128.88 (3,4-dimethoxyphenyl C_1, C_6), 128.81 (benzamide C_3, C_5), 128.55 (benzamide C_4), 127.08 (benzamide C_2, C_6), 125.98 (phenyl C_6), 123.94 (phenyl C_4), 121.37 (phenyl C_2), 111.11 (3,4-dimethoxyphenyl C_2, C_5), 69.43 (pyrazole C_5), 57.25 (pyrazole C_4), 55.92 (–OCH_3), 55.77 (–OCH_3), 37.28, 31.49, 25.18, 23.49, 22.42 (cyclohexane ring); HRMS (ESI +): *m/z* calculated for $C_{30}H_{31}N_3O_4$: 497.60, found – 498.5027 (M + 1), 499.3421 (M + 2).

*4.1.6.12. N-(3-(4-(4-(trifluoromethyl)phenyl)-1,2-diazaspiro[4.5]dec-2-ene-3-carbonyl)phenyl)benzamide**(77)***. White solid, yield- 75%, M.P.- 229–230 °C, ^{1}H NMR (500 MHz, $CDCl_3$) δ 8.30 (s, 1H, 4-(trifluoromethyl)phenyl C_5), 8.11 (s, 1H, amide NH), 8.05 (d, *J* = 7.5 Hz, 1H, 4-(trifluoromethyl)phenyl C_6), 7.91–7.88 (m, 3H, 4-(trifluoromethyl)phenyl C_2, C_3, phenyl C_2,), 7.55–7.54 (m, 3H, phenyl C_4, C_5, C_6), 7.50–7.44 (m, 3H, benzamide C_3, C_4. C_5), 7.27 (d, *J* = 6.5 Hz, 2H, benzamide C_2, C_6), 6.73 (bs, 1H, pyrazole NH), 4.28 (s, 1H, pyrazole C_4), 1.72–1.28 (m, 10*H*, cyclohexane). ^{13}C NMR (125 MHz, $CDCl_3$) δ 186.52 (C═O, carbonyl), 165.95 (C═O, amide), 151.94 (pyrazole C_3), 140.38 (4-(trifluoromethyl)phenyl C_1), 137.91 (phenyl C_3), 137.86 (phenyl C_1), 134.71 (benzamide C_1), 132.01 (phenyl C_5), 129.51 (4-(trifluoromethyl)phenyl C_2), 129.26 (4-(trifluoromethyl)phenyl C_6), 128.94 (benzamide C_4), 128.82 (benzamide C_3, C_5), 127.10 (benzamide C_2, C_6), 125.99 (phenyl C_6), 125.48 (4-(trifluoromethyl)phenyl C_3), 125.45 (4-(trifluoromethyl) phenyl C_5), 125.22 (-CF_3), 124.17 (phenyl C_4), 123.06 (4-(trifluoromethyl)phenyl C_4), 121.51 (phenyl C_2), 69.77 (pyrazole C_5), 57.40 (pyrazole C_4), 37.27, 31.60, 25.04, 23.30, 22.33 (cyclohexane ring); HRMS (ESI +): *m/z* calculated for $C_{29}H_{26}F_3N_3O_2$: 505.54, found – 506.2035 (M + 1), 507.2121 (M + 2).

*4.1.6.13. N-(3-(4-(3-(trifluoromethyl)phenyl)-1,2-diazaspiro[4.5]dec-2-ene-3-carbonyl)phenyl)benzamide**(78)***. White solid, yield- 70%, M.P.- 230–231 °C, ^{1}H NMR (500 MHz, $CDCl_3$) δ 8.26 (s, 1H, 3-

(trifluoromethyl)phenyl C_2), 8.09–8.04 (m, 2H, amide NH, 3-(trifluoromethyl)phenyl C_4), 7.92–7.88 (m, 3H, 3-(trifluoromethyl) phenyl C_6, C_5, phenyl C_2), 7.58–7.56 (m, 1H, benzamide C_4), 7.51–7.42 (m, 6H, phenyl C_4, C_5, C_6, benzamide C_3, C_2, C_6), 7.32 (s, 1H, benzamide C_5), 6.68 (s, 1H, pyrazole NH), 4.28 (s, 1H, pyrazole C_4), 1.73–1.23 (m, 10*H*, cyclohexane). ^{13}C NMR (125 MHz, $CDCl_3$) δ 186.48 (C═O, carbonyl), 165.85 (C═O, amide), 152.07 (pyrazole C_3), 137.95 (3-(trifluoromethyl)phenyl C_1), 137.87 (phenyl C_3), 137.28 (phenyl C_1), 134.76 (benzamide C_1), 131.99 (phenyl C_5), 130.94 (3-(trifluoromethyl)phenyl C_6), 130.68 (3-(trifluoromethyl)phenyl C_5), 128.98 (3-(trifluoromethyl)phenyl C_3, benzamide C_4), 128.97 (3-(trifluoromethyl)phenyl C_4), 128.83 (benzamide C_3, C_5), 127.08 (benzamide C_2, C_6), 125.99 (phenyl C_6), 125.17 (3-(trifluoromethyl) phenyl C_2), 124.14 (phenyl C_4),123.01 (-CF_3), 121.37 (phenyl C_2), 69.68 (pyrazole C_5), 57.41 (pyrazole C_4), 37.22, 31.61, 25.03, 23.30, 22.33 (cyclohexane ring); HRMS (ESI +): *m/z* calculated for $C_{29}H_{26}F_3N_3O_2$: 505.54, found – 506.2057 (M + 1), 507.2077 (M + 2).

*4.1.6.14. N-(3-(4-(4-(trifluoromethoxy)phenyl)-1,2-diazaspiro[4.5]dec-2-ene-3-carbonyl)phenyl)benzamide**(79)***. Off white solid, yield- 75%, M.P.- 245–246 °C, ^{1}H NMR (500 MHz, $CDCl_3$) δ 8.29 (s, 1H, 4-(trifluoromethoxy)phenyl C_5), 8.06 (bs, 2H, amide NH, phenyl C_2), 7.92–7.88 (m, 3H, 4-(trifluoromethoxy)phenyl C_3, C_2, C_6), 7.58–7.56 (m, 1H, benzamide C_4), 7.51–7.45 (m, 3H, phenyl C_4, C_5, C_6), 7.16–7.12 (m, 4H, benzamide C_2, C_6, C_3, C_5), 6.65 (bs, 1H, pyrazole NH), 4.24 (s, 1H, pyrazole C_4), 1.70–1.28 (m, 10*H*, cyclohexane). ^{13}C NMR (125 MHz, $CDCl_3$) δ 186.54 (C═O, carbonyl), 165.87 (C═O, amide), 152.34 (pyrazole C_3), 148.31 (4-(trifluoromethoxy)phenyl C_4), 138.00 (phenyl C_3), 137.86 (phenyl C_1), 134.85(4-(trifluoromethoxy) phenyl C_2, C_6), 134.76 (benzamide C_1), 132.00 (phenyl C_5), 129.88 (-OCF_3), 128.94 (benzamide C_4), 128.83 (benzamide C_3, C_5, 4-(trifluoromethoxy)phenyl C_1), 127.08 (benzamide C_2, C_6), 126.01 (phenyl C_6), 124.10 (phenyl C_4), 121.44 (phenyl C_2), 120.88 (4-(trifluoromethoxy)phenyl C_3, C_5), 69.57 (pyrazole C_5), 56.91 (pyrazole C_4), 37.21, 31.57, 25.07, 23.33, 22.35 (cyclohexane ring); HRMS (ESI +): *m/z* calculated for $C_{29}H_{26}F_3N_3O_3$: 521.54, found – 522.4601 (M + 1), 523.2424 (M + 2).

*4.1.6.15. N-(3-(4-(4-cyanophenyl)-1,2-diazaspiro[4.5]dec-2-ene-3-carbonyl)phenyl)benzamide**(80)***. Pale yellow solid, yield- 80%, M.P.- 256–257 °C, ^{1}H NMR (500 MHz, $CDCl_3$) δ 8.33 (s, 1H, 4-cyanophenyl C_5), 8.13 (s, 1H, amide NH), 8.02 (d, J = 7.5 Hz, 1H, 4-cyanophenyl C_6), 7.91–7.88 (m, 3H, 4-cyanophenyl C_2, C_3, phenyl C_2), 7.58–7.56 (m, 3H, benzamide C_2, C_6, C_4), 7.50–7.44 (m, 3H, phenyl C_4, C_5, C_6), 7.25 (d, J = 6.5 Hz, 2H, benzamide C_3, C_5), 6.73 (s, 1H, pyrazole NH), 4.24 (s, 1H, pyrazole C_4), 1.71–1.28 (m, 10*H*, cyclohexane). ^{13}C NMR (125 MHz, $CDCl_3$) δ 186.38 (C═O, carbonyl), 165.92 (C═O, amide), 151.55 (pyrazole C_3), 141.98 (4-cyanophenyl C_1), 137.92 (phenyl C_3), 137.78 (phenyl C_1), 134.70 (benzamide C_1), 132.32 (4-cyanophenyl C_3, C_5), 132.04 (phenyl C_5), 129.38 (benzamide C_4), 128.95 (4-cyanophenyl C_2, C_6), 128.83 (benzamide C_3, C_5), 127.10 (benzamide C_2, C_5), 125.96 (phenyl C_6), 124.21 (phenyl C_4), 121.51 (phenyl C_2), 118.80 (–CN), 111.07 (4-cyanophenyl C_4), 69.91 (pyrazole C_5), 57.63 (pyrazole C_4), 37.24, 31.59, 24.99, 23.29, 22.30 (cyclohexane ring); HRMS (ESI +): *m/z* calculated for $C_{29}H_{26}N_4O_2$: 462.55, found – 463.0271 (M + 1), 464.1430 (M + 2).

*4.1.6.16. N-(3-(4-(3-cyanophenyl)-1,2-diazaspiro[4.5]dec-2-ene-3-carbonyl)phenyl)benzamide**(81)***. Pale yellow solid, yield- 75%, M.P.- 256–257 °C, ^{1}H NMR (500 MHz, $CDCl_3$) δ 8.30 (s, 1H, 3-cyanophenyl C_2), 8.08–8.06 (m, 2H, amide NH, 3-cyanophenyl C_6), 7.91–7.89 (m, 3H, 3-cyanophenyl C_5, C_4, phenyl C_2,), 7.57–7.39 (m, 8H, benzamide C_4, phenyl C_4, C_5, C_6, benzamide C_3, C_5, C_2, C_6), 6.72 (s, 1H, pyrazole NH), 4.24 (s, 1H, pyrazole C_4), 1.72–1.28 (m, 10*H*, cyclohexane). ^{13}C NMR (125 MHz, $CDCl_3$) δ 186.30 (C═O, carbonyl), 165.90 (C═O, amide), 151.70 (pyrazole C_3), 137.98 (3-cyanophenyl C_1), 137.89 (phenyl C_3), 137.74 (phenyl C_1), 134.72 (benzamide C_1), 132.03 (phenyl C_5, 3-cyanophenyl C_6), 130.97 (3-cyanophenyl C_2, benzamide C_4), 129.35 (3-cyanophenyl C_4), 128.99 (3-cyanophenyl C_5), 128.84 (benzamide C_3, C_5), 127.10 (benzamide C_2, C_6), 125.98 (phenyl C_6), 124.26 (phenyl C_4), 121.51 (phenyl C_2), 118.82 (–CN), 112.64 (3-cyanophenyl C_3), 69.70 (pyrazole C_5), 57.12 (pyrazole C_4), 37.14, 31.62, 24.99, 23.31, 22.29 (cyclohexane ring); HRMS (ESI +): *m/z* calculated for $C_{29}H_{26}N_4O_2$: 462.55, found – 463.3405 (M + 1), 464.2121 (M + 2).

*4.1.6.17. N-(3-(4-(p-tolyl)-1,2-diazaspiro[4.5]dec-2-ene-3-carbonyl) phenyl)benzamide**(82)***. Pale yellow, yield- 75%, M.P.- 255–256 °C, ^{1}H NMR (500 MHz, $CDCl_3$) δ 8.21 (s, 1H, *p*-tolyl C_5), 8.12 – 8.09 (m, 2H, amide NH, *p*-tolyl C_6), 7.90–7.87 (m, 3H, *p*-tolyl C_2, C_3, phenyl C_2), 7.57–7.54 (m, 1H, benzamide C_4), 7.49–7.42 (m, 3H, phenyl C_4, C_5, C_6), 7.09–7.01 (m, 4H, benzamide C_2, C_6, C_3, C_5), 6.59 (s, 1H, pyrazole NH), 4.20 (s, 1H, pyrazole C_4), 2.29 (s, 3H, –CH_3), 1.67–1.28 (m, 10*H*, cyclohexane). ^{13}C NMR (125 MHz, $CDCl_3$) δ 186.83 (C═O, carbonyl), 165.88 (C═O, amide), 152.84 (pyrazole C_3), 138.23 (phenyl C_3), 137.82 (phenyl C_1), 136.70 (*p*-tolyl C_4), 134.80 (benzamide C_1), 132.94 (phenyl C_5), 131.92 (benzamide C_4), 129.20 (*p*-tolyl C_3, C_5), 128.85 (*p*-tolyl C_1), 128.78 (benzamide C_3, C_5), 128.46 (*p*-tolyl C_2, C_6), 127.12 (benzamide C_2, C_6), 126.01 (phenyl C_6), 124.00 (phenyl C_4), 121.43 (phenyl C_2), 69.42 (pyrazole C_5), 57.27 (pyrazole C_4), 37.33, 31.63, 25.16, 23.36, 22.39 (cyclohexane ring), 21.13 (–CH_3); HRMS (ESI +): *m/z* calculated for $C_{29}H_{29}N_3O_2$: 451.57, found – 452.2333 (M + 1), 453.2377 (M + 2).

*4.1.6.18. N-(3-(4-(o-tolyl)-1,2-diazaspiro[4.5]dec-2-ene-3-carbonyl) phenyl)benzamide**(83)***. Yellow solid, yield- 78%, M.P.- 190–191 °C, ^{1}H NMR (500 MHz, $CDCl_3$) δ 8.24 (s, 1H, *o*-tolyl C_5), 8.08 (bs, 2H, amide NH, *o*-tolyl C_6), 7.91–7.87 (m, 3H, *o*-tolyl C_3, C_4, phenyl C_2), 7.57–7.55 (m, 1H, benzamide C_4), 7.50–7.43 (m, 3H, phenyl C_4, C_5, C_6), 7.19 (d, J = 6.5 Hz, 1H,benzamide C_3), 7.12–7.07 (m, 2H, benzamide C_2, C_6), 6.94 (d, J = 7 Hz, 1H, benzamide C_5), 6.65 (s, 1H, pyrazole NH), 4.50 (s, 1H, pyrazole C_4), 2.53 (s, 3H, –CH_3), 1.76–1.28 (m, 10*H*, cyclohexane). ^{13}C NMR (125 MHz, $CDCl_3$) δ 186.59 (C═O, carbonyl), 165.86 (C═O, amide), 153.81 (pyrazole C_3), 138.15 (*o*-tolyl C_2), 137.80 (phenyl C_3), 136.07 (*o*-tolyl C_1), 134.81 (phenyl C_1), 134.64 (benzamide C_1), 131.93 (phenyl C_5), 130.63 (benzamide C_4), 128.90 (*o*-tolyl C_3), 128.80 (benzamide C_3, C_5), 127.81 (*o*-tolyl C_4), 127.09 (benzamide C_2, C_6), 126.96 (*o*-tolyl C_5), 126.14 (o-tolyl C_6), 125.95 (phenyl C_6), 124.01 (phenyl C_4), 121.43 (phenyl C_2), 69.33 (pyrazole C_5), 52.94 (pyrazole C_4), 37.64, 31.48, 25.15, 23.37, 22.58 (cyclohexane ring), 20.28 (–CH_3); HRMS (ESI +): *m/z* calculated for $C_{29}H_{29}N_3O_2$: 451.57, found – 452.2315 (M + 1), 453.2358 (M + 2).

*4.1.6.19. N-(3-(4-(4-isopropylphenyl)-1,2-diazaspiro[4.5]dec-2-ene-3-carbonyl)phenyl)benzamide**(84)***. Yellow solid, yield- 80%, M.P.- 240–241 °C, ^{1}H NMR (500 MHz, $CDCl_3$) δ 8.18 (s, 1H, 4-isopropylphenyl C_5), 8.09–8.05 (m, 2H, amide NH , 4-isopropylphenyl C_6), 7.89–7.85 (m, 3H, 4-isopropylphenyl C_2, C_3, phenyl C_2,), 7.54–7.52 (m, 1H, benzamide C_4), 7.48–7.41 (m, 3H, phenyl C_4, C_5, C_6), 7.11 (d, J = 7.5 Hz, 2H, benzamide C_3, C_5), 7.03 (d, J = 7 Hz, 2H, benzamide C_2, C_6), 6.58 (s, 1H, pyrazole NH), 4.19 (s, 1H, pyrazole C_4), 2.87 – 2.79 (m, 1H, -CH_{tert}), 1.69–1.26 (m, 10*H*, cyclohexane), 1.20 (s, 3H, -CH_{3b}), 1.18 (s, 3H, -CH_{3a}). ^{13}C NMR (125 MHz, $CDCl_3$) δ 186.83 (C═O, carbonyl), 165.85 (C═O, amide), 152.95 (pyrazole C_3), 147.53 (4-isopropylphenyl C_4), 138.24 (phenyl C_3), 137.81 (phenyl C_1), 134.80 (benzamide C_1), 133.12 (4-isopropylphenyl C_1), 131.94 (phenyl C_5), 128.89 (benzamide C_4), 128.80 (benzamide C_3, C_5), 128.40 (4-isopropylphenyl C_2, C_6), 127.11 (benzamide C_2, C_6), 126.51 (4-isopropylphenyl C_3, C_5), 126.04 (phenyl C_6), 124.00 (phenyl C_4), 121.41 (phenyl C_2), 69.51 (pyrazole C_5), 57.31 (pyrazole C_4), 37.33 (cyclohexane ring), 33.66 (-CH_{tert}), 31.63 (cyclohexane ring), 29.71, 29.67 (-CH_{3b}), 25.18

(cyclohexane ring), 23.95, 23.90 (-CH_{3a}), 23.38, 22.42 (cyclohexane ring); HRMS (ESI +): *m/z* calculated for $C_{31}H_{33}N_3O_2$: 479.62, found – 479.3470 (M +), 481.3417 (M + 2).

*4.1.6.20. N-(3-(4-(naphthalen-1-yl)-1,2-diazaspiro[4.5]dec-2-ene-3-carbonyl)phenyl)benzamide(**85**)*. Pale yellow solid, yield- 70%, M.P.- 254–255 °C, ^{1}H NMR (500 MHz, $CDCl_3$) δ 8.27 (s, 1H, naphthalen-1-yl C_5), 8.17 (d, J = 8.5 Hz, 1H, naphthalen-1-yl C_8), 8.07 (bs, 2H, phenyl C_2, amide NH), 7.95 (d, J = 7.5 Hz, 1H, naphthalen-1-yl C_4), 7.86 (d, J = 7 Hz, 3H, phenyl C_4, C_5, C_6), 7.72 (d, J = 8 Hz, 1H, benzamide C_4), 7.58–7.44 (m, 6H, benzamide C_3, C_5, C_2, C_6, naphthalen-1-yl C_3,C_6), 7.35–7.32 (t, J = 7.5 Hz, 1H, naphthalen-1-yl C_7), 7.07 (d, J = 7 Hz, 1H, naphthalen-1-yl C_2), 6.81 (s, 1H, pyrazole NH), 5.11 (s, 1H, pyrazole C_4), 1.76–1.25 (m, 10*H*, cyclohexane). ^{13}C NMR (125 MHz, $CDCl_3$) δ 186.52 (C═O, carbonyl), 165.87 (C═O, amide), 153.15 (pyrazole C_3), 138.14 (phenyl C_3), 137.86 (phenyl C_1), 134.78 (naphthalen-1-yl C_1), 134.15 (benzamide C_1), 132.36 (phenyl C_5), 132.09 (naphthalen-1-yl C_{4a}), 131.94 (naphthalen-1-yl C_{8a}), 129.03 (naphthalen-1-yl C_5), 128.93 (benzamide C_4), 128.79 (benzamide C_3, C_5), 127.76 (naphthalen-1-yl C_3), 127.10 (benzamide C_2, C_6), 126.41 (naphthalen-1-yl C_4), 126.04 (phenyl C_6), 125.50 (naphthalen-1-yl C_6), 125.36 (naphthalen-1-yl C_7), 125.35 (naphthalen-1-yl C_2), 124.08 (naphthalen-1-yl C_8), 123.45 (phenyl C_4), 121.49 (phenyl C_2), 69.58 (pyrazole C_5), 52.60 (pyrazole C_4), 37.34, 31.35, 25.00, 23.28, 22.68 (cyclohexane ring); HRMS (ESI +): *m/z* calculated for $C_{32}H_{29}N_3O_2$: 487.60, found – 488.6501 (M + 1), 489.1351 (M + 2).

4.2. Biological evaluation

4.2.1. In-vitro enzyme inhibition studies (Inhibitory activity against cholinesterases)

The inhibitory potencies of all synthesized derivatives (**43–62 and 66–85**) against AChE and BuChE were determined by earlier reported protocol with minor modifications [14]. Briefly, stock solutions (1 mg/ml) of test compounds were prepared in DMSO. The percentage inhibitions were determined at 100 μM and 50 μM for the selection of concentration range of IC_{50} assays. Six different concentrations of 0.01 μM, 0.1 μM, 1 μM, 10 μM, 50 μM, and 100 μM of test compounds were used to determine IC_{50}. 2 μL of test or standard compounds and 100 μL of DTNB (0.0005 M) were incubated in 96 well plate for 10 min. 50 μL of AChE (0.5 U mL^{-1}) or 50 μL of BuChE (0.5 U mL^{-1}) was added and incubated for 30 min. The substrate i.e. ATCI (for AChE, 0.00375 M, 20 μL) or BTCI (for BuChE, 0.00375 M, 20 μL) was added into it. Formation of yellow 5-thio-2-nitrobenzoate anion as a result of the reaction of DTNB with thiocholines was monitored for 1 min as change in absorbance at 415 nm for 20 min, on Synergy HTX multi-mode reader (BioTek, USA) against blank reading containing 2 μL DMSO instead of test compound. Donepezil (0.01–100 μM) was used as the positive control. IC_{50} values were calculated using absorbance obtained from test and standard compounds. All the assays were performed in triplicate and in three independent runs.

Enzyme (AChE) kinetics study was performed to ascertain the mechanism of enzyme inhibition of compounds **44** and **67**. Seven different substrate concentrations in range of 0.25–5 mM were used in the study. Compounds **44** and **67** were used in three separate concentration range of 1, 2, and 4 μM. Each concentration of test compounds was used with seven different concentrations of the substrate. The activity was measured for 10 min at an interval of 2 min in absence and presence of test compounds. The product formed during the time frame of 10 min was calculated by Beer-Lambert law. The velocity of the enzyme reaction was obtained by plotting product formed during 10 min and V_{max}, K_m was computed by Michaelis-Menten nonlinear regression graph and Lineweaver-Burk reciprocal linear regression plots were used to determine the mechanism of enzyme inhibition by GraphPad Prism version 5.01. Ki value was determined by Dixon method in which slope of the lines from the double reciprocal Lineweaver-Burk plot was plotted as a function of test compound [39]. The enzyme kinetic assay was performed in triplicate.

4.2.2. In-vitro blood-brain barrier permeation assay

To determine the blood–brain barrier penetration potential of compounds (**43–62** and **66–85**), parallel artificial membrane permeation assay (PAMPA-BBB) was executed [31]. Porcine brain lipid (PBL) was procured from Avanti polar lipids, Alabaster and dodecane was acquired from Avra Synthesis, Hyderabad. Acceptor microplates with PVDF membrane (pore size 0.45 μm) and donor microplates were purchased from Merck Millipore. The assay was carried out by following previously reported procedure with minor modifications for BBB permeability determination [14]. Concisely, the acceptor plate was impregnated with 4 μL of 20 mg/ml PBL in dodecane and filled with 200 μL of buffer (pH 7.4). The acceptor plate was incubated overnight to get saturated. Compounds **43–62** and **66–85** (5 mg each), were dissolved in 1 ml of DMSO and 5 μL of the solution of compounds were taken and were further diluted with 70% DMSO and buffer of pH 7.5 to get a final concentration of 25 μg/ml. 200 μL of 25 μg/ml compounds were added to donor well plate in triplicate. The acceptor plate was placed carefully over the donor plate like a sandwich and incubated for 18 h. After incubation, plates were carefully separated and absorbance spectra of blank (buffer, pH 7.5), donor, acceptor, and reference wells were measured with a microplate reader (HTX multi-mode reader, BioTek, USA). Each of the samples was scanned for at least five different wavelengths and in three independent runs. PAMPA model was validated with 9 commercial drugs (Verapamil HCl, Diazepam, Progesterone, Atenolol, Dopamine, Lomefloxacin, Alprazolam, Chlorpromazine and Oxazepam) whose BBB permeability has been reported earlier. *Pe* was calculated using the following equation:

$$P_e = \left(\frac{(V_D \times V_A)}{(V_D + V_A)a \times t}\right) \times In\left(1 - \frac{[Drug]_{acceptor}}{[Drug]_{equilibrium}}\right)$$

where V_D and V_A are volumes of donor and acceptor compartments respectively. a is the total filter area, t is the penetration time. $[drug]_{acceptor}$ and $[drug]_{equilibrium}$ are the absorbance of test compound at acceptor well and theoretical equilibrium absorbance respectively.

4.2.3. Propidium iodide displacement assay

To demonstrate the binding of compounds **44** and **67** to the peripheral anionic site (PAS) of AChE, propidium iodide displacement assay was performed [40]. The assay mixture includes AChE (5U) and with or without test compounds (final concentrations 10 μM and 50 μM, 150 μL), was incubated for 6 h at 25 °C. After incubation, 50 μL of propidium iodide (1 mM concentration) was added to make the total volume of 200 μL. Fluorescence intensity was measured after 10 min, at excitation and emission wavelength of 535 nm and 595 nm, respectively using microplate reader (HTX multi-mode reader, BioTek, USA). The percentage inhibition was calculated by following equation:

$$100 - \left(\frac{IF_i}{IF_o} \times 100\right)$$

where IF_i and IF_o are the fluorescence intensities with and without inhibitor respectively. Each assay was performed as three indipendent experiments.

4.2.4. Inhibition assay of $A\beta_{1\text{-}42}$ aggregation

Metal dyshomeostasis has been suggested as a strong neurotoxic condition to induce changes in Aβ aggregation. Metal ions bind to amyloid beta peptide (Aβ) and are involved in the production of reactive oxygen species (ROS), leading to neuronal death [41]. Thioflavin T (ThT) assay was carried out to ascertain the inhibitory potential of compounds **44** and **67** against Fe^{+2} induced $A\beta_{1\text{-}42}$ aggregation [42]. $A\beta_{1\text{-}42}$ (Sigma) was dissolved in phosphate buffer (PBS, 10 mM, pH 7.5), compounds **44** and **67** were dissolved in DMSO. Different proportions

(1:0.5, 1:1, 1:2) of the $A\beta_{1-42}$: Inhibitor was used in the ThT assay. The final concentration of $A\beta_{1-42}$, compounds **44** and **67** and Fe^{+2} was 10 μM (2 μL), 0.5, 10, 20 μM (2 μL) and 10 μM (16 μL) respectively. The mixtures were incubated at room temperature for 48 h under dark. After the incubation period, 178 μL of 20 μM ThT was added and fluorescence intensities were measured at an excitation and emission wavelengths of 485 and 528 nm respectively.

Confocal Fluorescence Imaging: The assay mentioned in Section 4.2.4 was further used for the confocal fluorescence imaging after 10 days of incubation. Fluorescence dye ThT; $A\beta_{1-42}$; $A\beta_{1-42}$ and ThT; $A\beta_{1-42}$ and Fe^{+2}; $A\beta_{1-42}$, Fe^{+2} and ThT; $A\beta_{1-42}$, Fe^{+2}, test compound **44** or **67** and ThT; test compound **44** or **67** and ThT; test compound **44** or **67** alone were incubated and mounted on glass slide using 1,4-diazabicyclo[2.2.2]octane (DABCO; Sigma) as fixing agent. The images were taken at 40X using FITC fluorescence filter cube at excitation and emission wavelengths of 494 nm and 518 nm respectively. Experiments containing 10 μM of test compounds **44** and **67** were used for confocal imaging.

4.2.5. MC65 neuroprotection assay

MC65 cell lines were obtained from Dr. George M. Martin of University of Washington [43,44]. The cell growth and assay was performed exactly as described previously [14]. Briefly, MC65 cells were grown in MEM, 5×10^4 cells/well were placed in well plates and incubated with TC + and TC- in CO_2 incubator. The incubated cells were further used for experiments. In the test group (50–1 μM) TC was absent (TC−). The response was expressed in percentage cell viability relative to TC+ as a control. The assay was performed in triplicate and in three independent runs.

4.2.6. Scopolamine induced amnesia model

4.2.6.1. Materials. Scopolamine hydrobromide, donepezil (DNZ), and sodium carboxy methyl cellulose (SCMC) were purchased from Sigma-Aldrich. All other chemicals used in the present study were of analytic grade.

4.2.6.2. Animals and housing. Adult female Swiss Albino mice, weighing 20–25 g were used in the study. The animals were housed on a 12 h light/dark cycle under controlled temperature (25 ± 2 °C) and humidity (50 ± 10%). They were allowed to acclimatize for 1 week with free access of food and water *ad libitum*. The food was withheld 1 h before the behavioral study. All the experimental protocols were approved by the Institutional Animal Ethics Committee of the university (Banaras Hindu University, Varanasi, India) (Dean/2017/CAEC/265)

4.2.6.3. Experimental design

4.2.6.3.1. Experimental protocol and drug administration. Animals were divided into ten groups containing 6 animals in each group i.e. (i) vehicle (1 ml) (ii) scopolamine (3 mg/kg), (iii) scopolamine plus DNZ (3 mg/kg), (iv) scopolamine plus compound **44** (1.5 mg/kg), (v) scopolamine plus compound **44** (3 mg/kg), (vi) scopolamine plus compound **44** (6 mg/kg), (vii) scopolamine plus compound **67** (1.5 mg/kg), (viii) scopolamine plus compound **67** (3 mg/kg), (ix) scopolamine plus compound **67** (6 mg/kg), (x) control. The doses of compounds were fixed on the basis of their LD_{50}. DNZ and scopolamine hydrobromide were freshly dissolved in distilled water and test compounds in 0.5% SCMC before dosing. The route of drug administration was intraperitoneal injection (i.p) for scopolamine and oral route (p.o) for DNZ and test compounds. DNZ and compounds **44** and **67** were administered once daily in different groups for seven days. All the group animals except vehicle and control were administered with scopolamine on the seventh day to induce amnesia. The behavioral experiments were performed 5 min after scopolamine injection [45].

4.2.6.3.2. LD_{50} determination. Compounds **44** and **67** were tested for LD_{50} determination according to specified protocols of OECD test guidelines for chemicals at fixed dosages of 5, 50 and 300 mg/kg. Three female Wistar rats were used for each dose. The three groups of animals containing three female rats were dosed with 5, 50, 300 mg/kg and monitored for 72 h (Supporting information-S5). As per the guidelines LD_{50} of compounds **44** and **67** were calculated.

4.2.6.4. Y-maze test. The test was performed to evaluate the immediate working memory of all the groups. The Y-maze apparatus was of wooden made and consisted of three identical arms (labelled as A, B, and C) separated apart by an angle of 120°. Compounds **44** and **67** were evaluated at 1.5, 3 and 6 mg/kg doses. The test was carried out on seventh day (last day) of the treatment. During the experimentation, a training session of 15 min. was performed after dosing in which animals were placed in Y-maze with novel arm closed. After 5 h of training session, main test was executed after 5 min. of scopolamine hydrobromide i.p. injection. In this session, each animal was placed at the center of arm and allowed to move freely through the maze. The experiment was performed for 15 min. and series of arm entry of mice in each of the arms was recorded with a prefixed video camera. The repeated arm entry was considered as an index of memory impairment. Spontaneous alternations with three different arms in three consecutive entries (ABC, BCA, CAB not BAB) and novel arm entry were considered as the memory improvement [14,35,46]. The memory improvement score was calculated using the equation:

$$\%\ Spontaneous\ Alternation = \frac{Number\ of\ alternations}{(total\ arm\ entries) - 2)} \times 100$$

4.2.7. Neurochemical analysis

After the behavioral study, all animals were sacrificed and whole brain was isolated for neurochemical analysis. The brain was homogenized in 10 mM phosphate buffer (pH 7.4) and centrifuged for 15 min at 4350 g force at 4 °C, the supernatants were further used for the determination of AChE and catalase (CAT) levels.

AChE level was estimated in the brain of an animal by previously described methods [14,47]. Briefly, 100 μL of the supernatant was incubated with 15 mM of freshly prepared ATCI (100 μL) in presence of 2.7 ml of PBS for 5 min. The absorbance was recorded at 415 nm after addition of 100 μL of 1.5 mM DTNB.

CAT is an enzyme, which catalyzes the decomposition of toxic insult H_2O_2 produced in the body to form oxygen and water. CAT activity was determined by mixing 100 μL of supernatant with 150 μL of 0.01 M PBS. The reaction was started by the addition of 250 μL of 0.16 M H_2O_2 followed by incubation for 1 min. at 37 °C. 1 ml of dichromate/acetic acid solution (5% $K_2Cr_2O_7$/glacial acetic acid; 1:3 v/v) was used to stop the reaction at the end. The reaction mixture was kept on boiling water for 15 min, once the green color appears, absorbance was measured spectrophotometrically at 570 nm wavelength. All the experiments were performed in triplicate.

4.2.8. In-vivo pharmacokinetics and brain penetration study

Pharmacokinetics and brain penetration studies were performed using albino mice, weighing 25–30 g. All animals were housed under constant environmental conditions (22 ± 1 °C room temperature; 55 ± 10% relative humidity; 12 h light/dark cycle) and were allowed food and water *ad libitum*. Animals were fasted overnight (12 h) before dosing and continued on fasting until 4 h post administration of formulation. Thereafter, mice feed was provided *ad libitum*. Animals were randomly divided in two groups with five animals in each time interval. For each group, there were six time intervals (15 min, 30 min, 1, 2, 4, and 8 h). The first group of mice received single oral dose (30 mg/kg body weight) of compound **44** (dissolved in 0.5% SCMC pre mix) and the second group animals received single oral dose (30 mg/kg body weight) of compound **67** (dissolved in 0.5% SCMC pre mix).

The blood samples (orbital-sinus puncture) and brain samples were collected at earlier mentioned time intervals. Blood samples were

centrifuged immediately after collection at 894 g force for 10 min at 4 °C. Plasma samples were stored at −70 °C until further analysis. Brain samples were homogenized with milli Q water. All the collected plasma and brain samples were extracted by using HPLC grade methanol and stored for further analysis [48,49].

4.2.8.1. Pharmacokinetic and brain penetration analysis. Plasma and brain data were subjected to non-compartmental pharmacokinetic analysis using PK solver. The observed maximum plasma concentration (C_{max}) and the time to reach the maximum plasma concentration (T_{max}) were obtained by visual inspection of the experimental data. The area under the plasma concentration time curve (AUC) was calculated using linear trapezoidal method. The elimination constant (k_{el}) was estimated by linear regression of the plasma concentrations in the log-linear terminal phase. The apparent elimination half-life ($t_{1/2}$) was calculated as $0.693/k_{el}$ and systemic total body clearance (Cl/F) following oral dosing was calculated as $Dose/AUC_{0-\infty}$. The degree of drug uptake from plasma into brain tissue was estimated from the ratio of exposure in brain over the plasma exposure (AUC_{brain}/AUC_{plasma}).

Declaration of Competing Interest

All authors declare no conflict of interests.

Acknowledgment

Authors acknowledge the research support from Department of Biotechnology (DBT), New Delhi, India (File No. BT/PR9624/MED/30/1253/2013 dated-29/11/2014). GG, PP, and AG are thankful to Indian Institute of Technology (Banaras Hindu University), Varanasi for providing Teaching Assistantship to them. We would also like to thank Dr. George M. Martin of University of Washington, Seattle for generously providing the MC65 cells and Dr. Sureshbabu Popuri of Department of Chemistry, Indian Institute of Technology (Banaras Hindu University), Varanasi for helping in X-ray crystal structure data analysis.

Appendix A. Supplementary material

Supplementary data to this article can be found online at https://doi.org/10.1016/j.bioorg.2019.103080.

References

[1] C.L. Masters, R. Bateman, K. Blennow, C.C. Rowe, R.A. Sperling, J.L. Cummings, Alzheimer's disease, Nat. Rev. Dis. Primers 1 (2015) 15056.
[2] W.V. Graham, A. Bonito-Oliva, T.P. Sakmar, Update on Alzheimer's disease therapy and prevention strategies, Ann. Rev. Med. 68 (2017) 413–430.
[3] Q.-F. Zhao, L. Tan, H.-F. Wang, T. Jiang, M.-S. Tan, L. Tan, W. Xu, J.-Q. Li, J. Wang, T.-J. Lai, The prevalence of neuropsychiatric symptoms in Alzheimer's disease: systematic review and meta-analysis, J. Affect. Disord. 190 (2016) 264–271.
[4] D. Kumar, A. Ganeshpurkar, D. Kumar, G. Modi, S.K. Gupta, S.K. Singh, Secretase inhibitors for the treatment of Alzheimer's disease: long road ahead, Eur. J. Med. Chem. 148 (2018) 436–452.
[5] D. Kumar, S.K. Gupta, A. Ganeshpurkar, R. Singh, D. Kumar, N. Das, S. Krishnamurthy, S.K. Singh, Biological profiling of piperazinediones for the management of anxiety, Pharmacol. Biochem. Behav. 176 (2019) 63–71.
[6] S.N.A. Bukhari, I. Jantan, Synthetic curcumin analogs as inhibitors of β -amyloid peptide aggregation: potential therapeutic and diagnostic agents for Alzheimer's disease, Mini Rev. Med. Chem. 15 (13) (2015) 1110–1121.
[7] S.N.A. Bukhari, I. Jantan, V.H. Masand, D.T. Mahajan, M. Sher, M. Naeem-ul-Hassan, M.W. Amjad, Synthesis of α, β-unsaturated carbonyl based compounds as acetylcholinesterase and butyrylcholinesterase inhibitors: characterization, molecular modelling, QSAR studies and effect against amyloid β-induced cytotoxicity, Eur. J. Med. Chem. 83 (2014) 355–365.
[8] G.-F. Zha, C.-P. Zhang, H.-L. Qin, I. Jantan, M. Sher, M.W. Amjad, M.A. Hussain, Z. Hussain, S.N.A. Bukhari, Biological evaluation of synthetic α, β-unsaturated carbonyl based cyclohexanone derivatives as neuroprotective novel inhibitors of acetylcholinesterase, butyrylcholinesterase and amyloid-β aggregation, Bioorg. Med. Chem. 24 (10) (2016) 2352–2359.
[9] L. Jalili-Baleh, H. Nadri, A. Moradi, S.N.A. Bukhari, M. Shakibaie, M. Jafari, M. Golshani, F.H. Moghadam, L. Firoozpour, A. Asadipour, New racemic annulated pyrazolo [1, 2-b] phthalazines as tacrine-like AChE inhibitors with potential use in Alzheimer's disease, Eur. J. Med. Chem. 139 (2017) 280–289.
[10] P. Sharma, A. Tripathi, P.N. Tripathi, S.K. Prajapati, A. Seth, M.K. Tripathi, P. Srivastava, V. Tiwari, S. Krishnamurthy, S.K. Shrivastava, Design and development of multitarget-directed N-benzylpiperidine analogs as potential candidates for the treatment of Alzheimer's disease, Eur. J. Med. Chem. 167 (2019) 510–524.
[11] I.E. Orhan, Nature: a substantial source of auspicious substances with acetylcholinesterase inhibitory action, Curr. Neuropharmacol. 11 (4) (2013) 379–387.
[12] X. Zhang, K. Rakesh, S. Bukhari, M. Balakrishna, H. Manukumar, H.-L. Qin, Multitargetable chalcone analogs to treat deadly Alzheimer's disease: current view and upcoming advice, Bioorg. Chem. 80 (2018) 86–93.
[13] L. Jalili-Baleh, E. Babaei, S. Abdpour, S.N.A. Bukhari, A. Foroumadi, A. Ramazani, M. Sharifzadeh, M. Abdollahi, M. Khoobi, A review on flavonoid-based scaffolds as multi-target-directed ligands (MTDLs) for Alzheimer's disease, Eur. J. Med. Chem. 152 (2018) 570–589.
[14] D. Kumar, S.K. Gupta, A. Ganeshpurkar, G. Gutti, S. Krishnamurthy, G. Modi, S.K. Singh, Development of piperazinediones as dual inhibitor for treatment of Alzheimer's disease, Eur. J. Med. Chem. 150 (2018) 87–101.
[15] M.F. Khan, M.M. Alam, G. Verma, W. Akhtar, M. Akhter, M. Shaquiquzzaman, The therapeutic voyage of pyrazole and its analogs: a review, Eur. J. Med. Chem. 120 (2016) 170–201.
[16] A. Kling, K. Jantos, H. Mack, W. Hornberger, K. Drescher, V. Nimmrich, A. Relo, K. Wicke, C.W. Hutchins, Y. Lao, Discovery of novel and highly selective inhibitors of calpain for the treatment of Alzheimer's disease: 2-(3-phenyl-1 H-pyrazol-1-yl)-nicotinamides, J. Med. Chem. 60 (16) (2017) 7123–7138.
[17] N. Ahsan, S. Mishra, M.K. Jain, A. Surolia, S. Gupta, Curcumin pyrazole and its derivative (N-(3-nitrophenylpyrazole) curcumin inhibit aggregation, disrupt fibrils and modulate toxicity of wild type and mutant α-synuclein, Sci. Rep. 5 (2015) 9862.
[18] A.A. Estrada, B.K. Chan, C. Baker-Glenn, A. Beresford, D.J. Burdick, M. Chambers, H. Chen, S.L. Dominguez, J. Dotson, J. Drummond, Discovery of highly potent, selective, and brain-penetrant aminopyrazole leucine-rich repeat kinase 2 (LRRK2) small molecule inhibitors, J. Med. Chem. 57 (3) (2014) 921–936.
[19] H.R. Hoveyda, M.-O. Roy, S. Blanc, S. Noël, J.M. Salvino, M.A. Ator, G. Fraser, Discovery of 3-aryl-5-acylpiperazinyl-pyrazoles as antagonists to the NK 3 receptor, Bioorg. Med. Chem. Lett. 21 (7) (2011) 1991–1996.
[20] R. Neelarapu, D.L. Holzle, S. Velaparthi, H. Bai, M. Brunsteiner, S.Y. Blond, P.A. Petukhov, Design, synthesis, docking, and biological evaluation of novel diazide-containing isoxazole-and pyrazole-based histone deacetylase probes, J. Med. Chem. 54 (13) (2011) 4350–4364.
[21] T. Wang, D. Banerjee, T. Bohnert, J. Chao, I. Enyedy, J. Fontenot, K. Guertin, H. Jones, E.Y. Lin, D. Marcotte, Discovery of novel pyrazole-containing benzamides as potent RORγ inverse agonists, Bioorg. Med. Chem. Lett. 25 (15) (2015) 2985–2990.
[22] X. Liang, J. Zang, M. Zhu, Q. Gao, B. Wang, W. Xu, Y. Zhang, Design, synthesis, and antitumor evaluation of 4-amino-(1 H)-pyrazole derivatives as JAKs inhibitors, ACS Med. Chem. Lett. 7 (10) (2016) 950–955.
[23] N. Nayak, J. Ramprasad, U. Dalimba, P. Yogeeswari, D. Sriram, H.S. Kumar, S. Peethambar, R. Achur, Synthesis of new pyrazole-triazole hybrids by click reaction using a green solvent and evaluation of their antitubercular and antibacterial activity, Res. Chem. Intermed. 42 (4) (2016) 3721–3741.
[24] M.J. Wasko, K.A. Pellegrene, J.D. Madura, C.K. Surratt, A role for fragment-based drug design in developing novel lead compounds for central nervous system targets, Front. Neurol. 6 (2015) 197.
[25] E. Shang, Y. Yuan, X. Chen, Y. Liu, J. Pei, L. Lai, De novo design of multitarget ligands with an iterative fragment-growing strategy, J. Chem. Inf. Model. 54 (4) (2014) 1235–1241.
[26] D. Kumar, G. Kaur, A. Negi, S. Kumar, S. Singh, R. Kumar, Synthesis and xanthine oxidase inhibitory activity of 5, 6-dihydropyrazolo/pyrazolo [1, 5-c] quinazoline derivatives, Bioorg. Chem. 57 (2014) 57–64.
[27] H. Liu, H. Jia, B. Wang, Y. Xiao, H. Guo, Synthesis of spirobidihydropyrazole through double 1, 3-dipolar cycloaddition of nitrilimines with allenoates, Org. Lett. 19 (18) (2017) 4714–4717.
[28] D. Verma, S. Mobin, I.N. Namboothiri, Highly selective synthesis of pyrazole and spiropyrazoline phosphonates via base-assisted reaction of the bestmann–ohira reagent with enones, J. Organ. Chem. 76 (11) (2011) 4764–4770.
[29] Q.-X. Wu, H.-J. Li, H.-S. Wang, Z.-G. Zhang, C.-C. Wang, Y.-C. Wu, Catalyst-free synthesis of spiropyrazolines from chalcones and cyclic ketone N-tosylhydrazones, Synlett 26 (02) (2015) 243–249.
[30] D. Silva, M. Chioua, A. Samadi, P. Agostinho, P. Garção, R. Lajarín-Cuesta, C. de los Ríos, I. Iriepa, I. Moraleda, L. Gonzalez-Lafuente, Synthesis, pharmacological assessment, and molecular modeling of acetylcholinesterase/butyrylcholinesterase inhibitors: effect against amyloid-β-Induced neurotoxicity, ACS Chem. Neurosci. 4 (4) (2013) 547–565.
[31] L. Di, E.H. Kerns, K. Fan, O.J. McConnell, G.T. Carter, High throughput artificial membrane permeability assay for blood–brain barrier, Eur. J. Med. Chem. 38 (3) (2003) 223–232.
[32] N.A. Vyas, S.B. Singh, A.S. Kumbhar, D.S. Ranade, G.R. Walke, P.P. Kulkarni, V. Jani, U.B. Sonavane, R.R. Joshi, S. Rapole, Acetylcholinesterase and Aβ aggregation inhibition by heterometallic ruthenium (II)–platinum (II) polypyridyl complexes, Inorg. Chem. (2018).
[33] D.D. Allen, R. Caviedes, A.M. Cárdenas, T. Shimahara, J. Segura-Aguilar, P.A. Caviedes, Cell lines as in vitro models for drug screening and toxicity studies, Drug Dev. Ind. Pharm. 31 (8) (2005) 757–768.
[34] P. Shastry, A. Basu, M.S. Rajadhyaksha, Neuroblastoma cell lines-A versatile in vztro model in neurobiology, Int. J. Neurosci. 108 (1–2) (2001) 109–126.

[35] C.J. Miedel, J.M. Patton, A.N. Miedel, E.S. Miedel, J.M. Levenson, Assessment of spontaneous alternation, novel object recognition and limb clasping in transgenic mouse models of amyloid-β and tau neuropathology, J. Visual. Exp.: JoVE 123 (2017).
[36] X. Liu, C. Chen, B.J. Smith, Progress in brain penetration evaluation in drug discovery and development, J. Pharmacol. Exp. Ther. 325 (2) (2008) 349–356.
[37] S. Ueda, H. Nagasawa, Copper-catalyzed synthesis of benzoxazoles via a regioselective C− H functionalization/C− O bond formation under an air atmosphere, J. Organ. Chem. 74 (11) (2009) 4272–4277.
[38] A.K. Jha, N. Jain, The microwave-assisted ortho-alkylation of azine N-oxides with N-tosylhydrazones catalyzed by copper (i) iodide, Chem. Commun. 52 (9) (2016) 1831–1834.
[39] R.A. Copeland, J. Retey, Enzymes: a practical introduction to structure, mechanism, and data analysis, VCH Publishers, New York, 1996.
[40] L. Peauger, R. Azzouz, V. Gembus, M.-L. Tintas, J. Sopková-de Oliveira Santos, P. Bohn, C. Papamicaël, V. Levacher, Donepezil-based central acetylcholinesterase inhibitors by means of a “bio-oxidizable” prodrug strategy: design, synthesis, and in vitro biological evaluation, J. Med. Chem. 60 (13) (2017) 5909–5926.
[41] M.A. Greenough, J. Camakaris, A.I. Bush, Metal dyshomeostasis and oxidative stress in Alzheimer’s disease, Neurochem. Int. 62 (5) (2013) 540–555.
[42] A. Jan, D.M. Hartley, H.A. Lashuel, Preparation and characterization of toxic Aβ aggregates for structural and functional studies in Alzheimer's disease research, Nat. Protoc. 5 (6) (2010) 1186.
[43] P.F. Copenhaver, T.S. Anekonda, D. Musashe, K.M. Robinson, J.M. Ramaker, T.L. Swanson, T.L. Wadsworth, D. Kretzschmar, R.L. Woltjer, J.F. Quinn, A translational continuum of model systems for evaluating treatment strategies in Alzheimer’s disease: isradipine as a candidate drug, Dis. Models Mechan. (2011) 634–648.
[44] L.-W. Jin, D.H. Hua, F.-S. Shie, I. Maezawa, B. Sopher, G.M. Martin, Novel tricyclic pyrone compounds prevent intracellular APP C99-induced cell death, J. Mol. Neurosci. 19 (1–2) (2002) 57–61.
[45] G. Saxena, S.P. Singh, R. Pal, S. Singh, R. Pratap, C. Nath, Gugulipid, an extract of Commiphora whighitii with lipid-lowering properties, has protective effects against streptozotocin-induced memory deficits in mice, Pharmacol. Biochem. Behav. 86 (4) (2007) 797–805.
[46] T. Mamiya, M. Ukai, [Gly14]-Humanin improved the learning and memory impairment induced by scopolamine in vivo, Br. J. Pharmacol. 134 (8) (2001) 1597–1599.
[47] G.L. Ellman, K.D. Courtney, V. Andres, R.M. Featherstone, A new and rapid colorimetric determination of acetylcholinesterase activity, Biochem. Pharmacol. 7 (2) (1961) 88–95.
[48] G. Kumar, P. Paliwal, S. Mukherjee, N. Patnaik, S. Krishnamurthy, R. Patnaik, Pharmacokinetics and brain penetration study of chlorogenic acid in rats, Xenobiotica (2018) 1–7.
[49] B. Kumar, M. Modi, B. Saikia, B. Medhi, Evaluation of brain pharmacokinetic and neuropharmacodynamic attributes of an antiepileptic drug, lacosamide, in hepatic and renal impairment: preclinical evidence, ACS Chem. Neurosci. 8 (7) (2017) 1589–1597.